University of São Paulo
"Luiz de Queiroz" College of Agriculture

Long-term water stress and fertilization on *Eucalyptus grandis* trees: implications for growth, recovery and wood properties

Roger Chambi Legoas

Thesis presented to obtain the degree of Doctor in Science. Area: Forest Resources. Option in: Silviculture and Forest Management

Piracicaba
2022

Roger Chambi Legoas
Ingeniero Forestal y Medio Ambiente

Long-term water stress and fertilization on *Eucalyptus grandis* trees: implications for growth, recovery and wood properties

versão revisada de acordo com a resolução CoPGr 6018 de 2011

Advisor:
Prof. Dr. **MARIO TOMMASIELLO FILHO**

Co-advisor:
Dr. **GILLES CHRISTOPHE CHAIX**

Thesis presented to obtain the degree of Doctor in Science. Area: Forest Resources. Option in: Silviculture and Forest Management

Piracicaba
2022

Dados Internacionais de Catalogação na Publicação
DIVISÃO DE BIBLIOTECA – DIBD/ESALQ/USP

Chambi Legoas, Roger

Long-term water stress and fertilization on *Eucalyptus grandis* trees: implications for growth, recovery and wood properties / Roger Chambi Legoas. - - versão revisada de acordo com a resolução CoPGr 6018 de 2011. - - Piracicaba, 2022.

108 p.

Tese (Doutorado) - - USP / Escola Superior de Agricultura “Luiz de Queiroz”.

1. Mudanças climáticas 2. Nutrição florestal 3. Plasticidade do xilema 4. Seca 5. Resiliência das árvores 6. NIRS I. Título

DEDICATION

I dedicate this thesis to the memory of my parents ***Etelvina Legoas Armas*** *and* ***Victor Gregorio Chambi Quispe****, whom I miss every day. This work is the result of their effort, sacrifices, and dedication to me. And although they are not present at this time and place to share this achievement and happiness with me, I feel that their energy surrounds me and comforts me. They still live in my memories and dreams, and there are even days that I feel them next to me talking to me. This is for them.*

ACKNOWLEDGMENTS

I am very grateful to my advisors Dr. Gilles Chaix and Prof. Dr. Mario Tommasiello Filho for their guidance during the development of my thesis, but above all, for the great friendship forged more than 7 years ago.

To my friends, colleagues and researchers at the Laboratory of Anatomy, Densitometry and Dendrochronology (LAIM) of the Escola Superior de Agricultura Luiz de Queiroz (ESALQ): Leif Armando Portal Cahuana, Ricardo Ortega Rodriguez, Manolo Trindade Quintilhan, Júlia Lôbo Ribeiro Anciotti Gil, Guilherme Roquette, Francisco de Marques de Figueiredo, Luiz Santini Junior, Bruna Hornink, Gabriel de Assis Pereira, Cláudia Fontana, and Claudio Roberto Anholetto Júnior, for the scientific discussions about our projects, pleasant conversations during free time, lunch and coffee, and for friendship.

I also make a special acknowledgement to the researchers and workers of the Plateforme d'histocytologie et d'imagerie cellulaire végétale (PHIV) of the Centre de coopération internationale en recherche agronomique pour le développement (CIRAD), specially to Christelle Baptiste, Jean-Luc Verdeil and Frederic Gatineau, for guiding me in the sample preparation and acquisition of high-resolution images of wood anatomy. Also, to all my friends I met in France with whom I had a good time.

To Rildo M. Moreira and the Itatinga Research Station (ESALQ/USP) staff for authorization to conduct the experiment and for their technical support in sample collection and dendrometer data readings.

To Eder Araujo da Silva (http://www.floragroapoio.com.br) for technical support in installing the 80% throughfall exclusion device and growth monitoring.

To Dr. Juan Sinforiano Delgado Rojas for support in installing, maintaining, and reading the automatic dendrometers and for sharing meteorological data of the experimental plantation

To Dr. Jean-Paul Laclau for sharing the soil water content and sap flow data of the experimental plantation.

To Aparecido Candido Siqueira for their excellent support in the preparation of wood samples for X-ray densitometry analysis.

My doctoral studies were funded by a scholarship from Fondo Nacional de Desarrollo Científico, Tecnológico y de Innovación Tecnológica (FONDECYT-CONCYTEC, Perú) (Award Number 239-2018) during 28 months, and by a scholarship from Conselho Nacional de Desenvolvimento Científico e Tecnológico (CNPq) (Processes 170461/2017-3 and 140166/2019-0) during 21 months. I am very grateful to these institutions for making it possible to complete my doctorate.

I also thank the CIRAD for providing me grants for yearly stays in Montpellier, France, to develop my thesis analysis in the PHIV-CIRAD. My co-advisor, Dr. Gilles Chaix, deserves special thanks for his support in obtaining these grants.

The set-up and monitoring of the experiments were funded partially by the Agropolis Foundation under reference ID1203-003 through the «*Investissements d'avenir*» program (LabexAgro/ANR-10-LABX-0001-01), CNPq (170461/2017-3, 140166/2019-0, 444793/2014-3, and 014/2012), Fundação de Amparo à Pesquisa do Estado de São Paulo (FAPESP) (2013/25642-5), and FONDECYT-CONCYTEC (Award Number 239-2018).

SUMMARY

RESUMO……7
ABSTRACT……8
1. GENERAL INTRODUCTION 9
References 12
2. INTER-ANNUAL EFFECTS OF POTASSIUM FERTILIZATION ON GROWTH AND XYLEM PLASTICITY OF *Eucalyptus grandis* TREES UNDER CHANGING ENVIRONMENTAL CONDITIONS 17
Abstract 17
2.1. Introduction 17
2.2. Material and Methods 19
2.3. Results 22
2.4. Discussions 31
2.5. Conclusions 34
References 34
3. HIGH GROWTH RECOVERY ABILITY OF *Eucalyptus grandis* TREES FOLLOWING A 3-YEAR PERIOD OF 80% THROUGHFALL REDUCTION 39
Abstract 39
3.1. Introduction 39
3.2. Material and Methods 41
3.3. Results 46
3.4. Discussion 54
3.5. Conclusions 56
References 58
Appendix 62
4. INTER-ANNUAL EFFECTS OF POTASSIUM/SODIUM FERTILIZATION AND WATER DEFICIT ON WOOD QUALITY OF *Eucalyptus grandis* TREES OVER A FULL ROTATION 65
Abstract 65
4.1. Introduction 66
4.2. Material and Methods 67

4.3. Results 71
4.4. Discussion 77
4.5. Conclusions 80
References 81
5. WOOD DENSITY PREDICTION USING NEAR-INFRARED HYPERSPECTRAL IMAGING: AN APPLICATION TO EARLY SELECTION OF *Eucalyptus grandis* TREES 87
Abstract 87
5.1. Introduction 87
5.2. Material and Methods 89
5.4. Discussion 101
5.5. Conclusions 102
References 102
6. FINAL CONSIDERATIONS 107
References 107

RESUMO

Longo estresse hídrico e fertilização em árvores de *Eucalyptus grandis*: implicações para o crescimento, recuperação e propriedades da madeira

As plantações de eucalipto já estão estabelecidas ou se estão expandindo para regiões com deficiência hídrica com alto risco de seca severa. Em climas futuros mais secos, incluindo eventos extremos, as respostas de crescimento e a plasticidade do xilema das árvores às secas e a capacidade de recuperação do crescimento após secas severas emergem como fatores cruciais para a sustentabilidade das plantações florestais. Além disso, uma vez que fertilizantes como o potássio (K) são usados intensivamente para alcançar alta produtividade do *Eucalyptus grandis* nessas regiões, é importante conhecer os efeitos interativos da fertilização com K e da disponibilidade de água ao longo de uma rotação completa, não apenas na produtividade, mas também nas propriedades da madeira, pois são determinantes da qualidade e do rendimento dos produtos. Para atender a essas preocupações, dois plantações experimentais de *E. grandis* foram instalados em Itatinga, São Paulo, Brasil. (i) Um experimento de 6 anos envolvendo dois níveis de regime hídrico: 37% de redução da precipitação e precipitação não perturbada, e dois níveis de fertilização: adição de K e não adição de K; e (ii) outro experimento de 6 anos envolvendo dois níveis de regime hídrico: 80% de redução de precipitação e precipitação não perturbada. No primeiro experimento, os objetivos principais foram avaliar os efeitos interativos da fertilização com K, disponibilidade de água e idade, no incremento em área basal (BAI) e na qualidade da madeira, mesmo como testar se a fertilização com K aumenta a plasticidade do xilema em resposta à seca. O objetivo principal do segundo experimento foi avaliar a capacidade de recuperação do crescimento após uma redução de 80% na precipitação. O estudo se concentrou nas mudanças na área basal, raio do tronco e altura total, medida por dendrômetros de alta resolução temporal e censos das árvores. As características do xilema medidas foram a densidade da madeira (WD), fração da parede celular (CWF), densidade de células (CDen), condutividade hidráulica específica teórica do xilema (Kst), diâmetro do vaso (VD), densidade de vasos (VDen), área ocupada por vasos (VA), e índice de vulnerabilidade (VI). As propriedades da madeira compreenderam a proporção do cerne, o tamanho das fibras e a densidade da madeira. Os resultados mostram que a fertilização com K aumentou a taxa de crescimento ao longo da rotação completa. No entanto, esses efeitos eram altamente dependentes da disponibilidade de água, aumentando o BAI em 3 vezes em estações chuvosas, mas interrompendo o crescimento em períodos de seca sazonal severa. A redução de 37% da precipitação afetou o crescimento apenas em árvores fertilizadas com K até 2,5 anos após o plantio. A fertilização com K aumentou a plasticidade das características do xilema. A redução de 80% na precipitação ao longo de 3 anos reduziu significativamente as taxas de crescimento das árvores em 73% na área basal e 95% na altura total. No entanto, sob a disponibilidade normal de água após o fim da redução da precipitação, a taxa de crescimento da área basal das árvores foi 97% maior do que a das árvores de controle, enquanto a taxa de crescimento da altura total foi apenas 8% maior. Apesar do severo estresse hídrico, não foi observada mortalidade de árvores. As árvores recuperaram 51% de sua área basal ao longo do período de recuperação de 31 meses. Em contraste, apenas 5% da altura total foi recuperada. Isto demonstra a grande capacidade de recuperação das árvores de *E. grandis* no crescimento da área basal. Em relação à qualidade da madeira, a fertilização com K não promoveu perdas significativas na qualidade da madeira, mesmo sob estresse hídrico ao longo de uma rotação completa.

Palavras-chave: Mudanças climáticas, Nutrição florestal, Plasticidade do xilema, Seca, Resiliência das árvores, NIRS

ABSTRACT

Long-term water stress and fertilization on *Eucalyptus grandis* trees: Implications for growth, recovery and wood properties

Eucalyptus plantations are already planted in - or expanding to - water-limited regions with a high risk of severe drought. In future drier climate including extreme events, the growth responses and xylem plasticity of trees to droughts, and the growth recovery ability following severe droughts emerge as a crucial for the sustainability of forest plantations. Also, since fertilizers such as potassium (K) are intensively used to achieve high productivity for *Eucalyptus grandis* in these regions, it is important to know the interactive effects of K fertilization and water availability over a full rotation, not only in productivity but also in wood properties, since they are determinants of the quality and yield of products. To address these concerns, two experimental plantations of *E. grandis* were set up in Itatinga, São Paulo, Brazil. (i) A 6-year experiment involving two levels of water regime: 37% throughfall reduction and undisturbed throughfall, and two levels of fertilization: K addition and non-K addition; and (ii) another 6-year experiment involving two levels of water regime: 80% throughfall reduction and undisturbed throughfall. In the first experiment, the main objectives were to evaluate the interactive effects of K fertilization, water availability, and age on basal area increment (BAI) and wood quality and test if K fertilization increases xylem plasticity in response to drought. The second experiment's main objective was to evaluate the growth recovery ability following 80% throughfall reduction. The study focused on the changes in basal area, stem radius, and total height measured by high-temporal resolution dendrometers and periodical surveys of trees. Xylem traits measured were wood density (WD), cell wall fraction (CWF), cell density (CDen), theoretical xylem specific hydraulic conductivity (Kst), vessel diameter (VD), vessel density (VDen), vessel area (VA), and vulnerability index (VI). Wood properties comprised heartwood proportion, fibers size, and wood density. The results show that K fertilization increased growth rate over the full rotation. However, these effects were highly dependent of water availability, increasing BAI by 3-fold in well-watered seasons but stopping growth in severe seasonal drought periods. The 37% throughfall reduction affected growth only in K-fertilized trees until 2.5 years after planting. K fertilization increased xylem traits plasticity. The 80% reduction in throughfall over 3 years significantly reduced tree growth rates by 73% in basal area and 95% in total height. However, under normal water availability following throughfall reduction, the basal area growth rate of water-stressed trees was 97% higher than that of the control trees while total height growth rate was only 8% higher. Despite the severe water stress, no tree mortality was observed. Trees recovered 51% of their basal area over the 31-month recovery period. In contrast, only 5% of total height was recovered. It demonstrates a great recovery ability of *E. grandis* trees in basal area growth. Regarding wood quality, K fertilization did not promote significant losses in wood quality, even under water stress over a complete rotation.

Keywords: Climate change, Forest nutrition, Xylem plasticity, Drought, Tree resilience, NIRS

1. GENERAL INTRODUCTION

Eucalyptus is the most widespread genus of commercial forest plantations in tropical, subtropical, and temperate regions, covering about 20 million hectares, representing about 15% of the global forest plantation areas (Carle and Holmgren, 2009; FAO, 2020).

Due to their rapid growth, high wood yield, easy propagation, and wide genetic variation, *Eucalyptus* plantations are expanding worldwide for wood production in various zones (FAO, 2020), many of which are water-limited areas with risk of severe drought (Gonçalves et al., 2017). The Brazilian planted tree industry is based mainly on *Eucalyptus* plantations, covering 77.4% (6.97 million ha) of the total planted area (IBÁ, 2020). Of these, 49% (3.4 million ha) are concentrated in the southeastern region, subject to seasonal dry periods of 3 to 5 months with monthly rainfall less than 50 mm (Gonçalves et al., 2013, 2017; IBÁ, 2020).

Climate change scenarios project a rise in global temperature and changes in the amount and precipitation patterns around the world (IPCC, 2021). In most subtropical regions, a decrease in precipitation and aggravation of the intensity and frequency of dry seasonal periods are expected (IPCC, 2021; Lee et al., 2021). In fact, since 2000, the southeastern region of Brazil has been experienced an increase in frequency and duration of the dry periods, compared to that in 1965-2000 (Nobre et al., 2016). For example, in 2001 and 2014 occurred a prolonged seasonal drought with severe effects on water availability (Coelho et al., 2016; Nobre et al., 2016).

Eucalyptus grandis is one of Brazil's most planted and productive species (Campinhos, Jr., 1999); however, it is also one the most sensitive to water stress (Gonçalves et al., 2013). As the productivity of Eucalyptus plantation in this region is limited strongly by rainfall amount (Stape et al., 2010), the effects of prolonged drought are expected to affect tree growth negatively. Although many studies describe plant responses to water stress in Eucalyptus species, the assessments of impacts on tree growth – xylem traits binomial in prolonged drought field conditions over full rotation are scarce. Even more, growth recovery ability following water stress is rare. In contexts where drought is inevitable, tree resilience to severe water stress is also crucial for the sustainability of forest plantations. In the context of variability and unpredictability of precipitations scenarios, experiments recreating different levels of water deficit by rainfall reduction are needed to elucidate the impacts on forest productivity and wood properties of a wide range of possible scenarios (Wu et al., 2011).

On the other hand, soil fertility improvement is essential for the successful establishment of eucalyptus plantations (Gonçalves and Barros, 1999; Zeng et al., 2013). The applications of nitrogen, phosphorus, and potassium are extended in the silviculture of Eucalyptus for high productivity. Particularly, potassium (K) is the main driver for increasing aboveground biomass and growth rates of Eucalyptus trees (Laclau et al., 2009). In addition, many studies reported an important role of K in Eucalyptus for optimal leaf osmotic adjustment, efficient stomatal regulation, improving water-use efficiency, and increasing fine roots density and distribution to higher soil exploration for water uptake (Asensio et al., 2020; Battie-Laclau et al., 2016, 2014, 2013; Christina et al., 2018), suggesting a great involvement of K in drought-adaptive mechanisms. However, fertilizers also increase tree water demand and reduce water reserves in soils, increasing the risk of death by embolism during severe drought (Battie-Laclau et al., 2014). Thus, the study of the interaction between K fertilization and water deficit on tree development over a full rotation is considered of great importance for Eucalyptus plantations management in water-limited regions with risk of prolonged drought.

Under this framework, we must also worry about the effects of fertilization on wood quality under different water availability conditions. As well as wood productivity, wood quality is also an important factor in

forest management because it influences the transformation process and quality of end-use wood products. Higher wood density, larger fiber size, and higher sapwood/heartwood ratio are desirable attributes for higher yield and quality of pulp and paper products (Gonçalves et al., 2004). The greater the fiber length, the higher the tearing resistance of paper, while the lesser the fiber wall thickness, the higher the burst and tensile strengths but lower the tear resistance (Rana et al., 2011; Shmulsky and Jones, 2011). Heartwood has a higher content of extractives than sapwood, increasing chemical consumption and decreasing pulp yield and pulp brightness (Lourenço et al., 2011; Morais and Pereira, 2007). Environmental conditions, including silvicultural practices, affect tree growth rate, which can lead to changes in xylem traits, mainly in wood anatomy and density and its variation across age (Gonçalves et al., 2004; Pillai et al., 2013; Thomas et al., 2007; Zobel and van Buijtenen, 1989). Thus, applying silvicultural techniques in highly changing environmental conditions must consider the potential impacts on wood quality.

To address these concerns, two experiments of throughfall reduction recreating different levels of drought were established in Itatinga, São Paulo State, Brazil, aiming to study the interaction between fertilization and water deficit, as well as the tree recovery capacity after drought, on growth and wood properties on *E. grandis*.

(i) ***37% throughfall reduction experiment*****:** Six treatments consisting of a factorial combination of throughfall exclusion (37% throughfall exclusion vs. undisturbed throughfall) and fertilization (K supply, Na supply, and non-K or Na supply). The experiment assesses the interactions between fertilization and a moderate water deficit on basal area growth rate and xylem traits.

(ii) ***80% throughfall reduction experiment*****:** The experiment comprised the assessments of tree growth (basal area and total height) prior, during and after a prolonged 80% throughfall reduction, to understand the effects of extreme water deficit on tree development, as well as the recovery ability following water stress. A control group without throughfall exclusion was also monitored. Treatments had the same fertilization regime (NPK+micronutrients).

The first studies in the 37% throughfall exclusion experiment reported that K supply could be increased from 3 to 4-fold the stem volume and biomass of *E. grandis* trees and also increase water use efficiency (Almeida et al., 2010; Battie-Laclau et al., 2016; Chambi-Legoas et al., 2020). However, there is a concern about whether the current K fertilization regimes applied could detrimentally affect forest productivity under prolonged droughts. Even more, assessments of growth patterns and xylem traits over the full rotation (6 years) have not been addressed yet. The interactive effects of fertilization and water availability across age are still unknown. Knowing at what stage trees are more vulnerable or more resilient, or if the effects of fertilization and the water deficit affect trees only during the first or last years, or if they are maintained throughout the rotation, are critical to making silvicultural corrections and preventing actions in order to reduce losses in wood production.

On the other hand, the original experiment involving 80% throughfall reduction was conducted to reproduce severe drought conditions to gain insight into *E. grandis* trees' responses to prolonged (3-year) extreme water deficit and the ability of this species to recover following water stress. Drought recovery capacity has been described in other species, including Scots pine and black pine, both of which showed limited resiliency capacity to drought, were unable to recover their previous growth rates, and were susceptible to death (Guada et al., 2016). The depletion in carbon reserves resulting from reduced photosynthetic tissue led to tree mortality. In surviving trees, severe drought leads to delayed recovery (Galiano et al., 2011).

In contrast, *Eucalyptus globulus* clone seedlings growing in plastic containers subjected to water limitation revealed high recovery ability when water again became available, overcompensation of CO2, and greater growth (Correia et al., 2014). However, to date, no studies have measured the resilience of *Eucalyptus* trees in field conditions,

and responses may differ considerably due to increased physiological activity or to the exposure of the xylem hydraulic system to cavitation. In contexts where drought is inevitable, tree resilience to severe water stress is crucial for the sustainability of forest plantations.

In addition, since plant growth is linked to the environment, the environmental conditions directly influence physiological processes. Therefore, understanding how the growth of plants responds to these changes at short and long scale is fundamental for simulating ecosystem dynamics under future climate

To detect these changes appropriately, the high temporal resolution monitoring (either at daily, weekly, or fortnightly scale) of secondary growth is critical (Campoe et al., 2016; Chambi-Legoas et al., 2020; Deslauriers et al., 2007; Mcmahon and Parker, 2015; Wunder et al., 2013). In this matter, band dendrometers and automatic dendrometers have been widely used to monitor changes in stem size (Drew and Downes, 2009) to identify long-term growth patterns as a function of short-term environmental variability. On the other hand, automatic dendrometers measure the fluctuations in stem radius at 30 minutes intervals, which provide the daily patterns of stem variation needed to study cambial activity and tree water status and help identify cell division periods and plant response environmental conditions.

With this work, we intend to answer the following general questions:

- ***a.*** How do the effects of K fertilization on tree growth change with climatic variation and across tree age? Moreover, do these effects interact with 37% of throughfall reduction?
- ***b.*** How do *E. grandis* trees adjust their xylem structure to fit the changing environmental constraints? Is it affected by K fertilization?
- ***c.*** *E. grandis* trees will cope with a long-term 80% water deficit and, if so, to what extent can they recover over time following such a severe water deficit?
- ***d.*** How do additions of K and Na affect tree wood properties? (ii) do wood properties change with 37% throughfall reduction and tree age?
- ***e.*** Is the near-infrared hyperspectral imaging suitable for mapping wood density under different water availability conditions?

Thus, the thesis was structured in four chapters:

1. Inter-annual effects of potassium fertilization on growth and xylem plasticity of *Eucalyptus grandis* trees under changing environmental conditions

This chapter covered the question ***a*** and ***b***. The basal area growth patterns of trees under two fertilization regimes (potassium addition, no potassium addition) and two water regimes (37% throughfall exclusion, no throughfall exclusion) were evaluated over the full rotation (6 years), using fortnightly measurements by dendrometers bands. Xylem traits such as wood density (WD), cell wall fraction (CWF), cell density (CDen), theoretical xylem specific hydraulic conductivity (Kst), vessel diameter (VD), vessel density (VDen), vessel area (VA), and vulnerability index (VI) were measured in 6-months periods (rainy and dry seasons) over 6 years. Meteorological variables, soil water content, and tree transpiration were also monitored on a daily scale. The objectives were: (i) evaluate the interactions between K fertilization, water availability, and age on stem growth and xylem traits change of *E. grandis* trees over a full rotation; (ii) evaluate the relationships between stem growth, xylem traits, and environmental variables, and if these are affected by omission or application of K fertilization.

.

2. High growth recovery ability of *Eucalyptus grandis* trees following a 3-year period of 80% throughfall reduction.

This chapter answers question ***c***. It consists of an original experiment involving an 80% reduction in throughfall set up in Brazil to gain insight into the responses of *Eucalyptus grandis* trees to prolonged (3-year) extreme water deficit and the ability of this species to recover following water stress. The study focused on the changes in basal area, stem radius, and total height measured by high-temporal resolution dendrometers and periodical surveys of trees affected by 80% throughfall reduction (treatment group) and in a control group. The differences in basal area, stem radius, and total height growth rate were compared between groups over (i) 37 months of 80% throughfall reduction and (ii) 31 months following the end of 80% throughfall reduction. The correlations among growth rates, stem radius fluctuations, and meteorological variables in each group were determined to gain insights into the trees' responses to environmental conditions and stem water status.

3. Inter-annual effects of potassium/sodium fertilization and water deficit on wood quality of *Eucalyptus grandis* trees over a full rotation

This chapter address question ***d***. It focuses on the alterations in wood properties due to interactions between K/Na fertilization, water availability, and stand age. Through annual sampling of *E. grandis* trees throughout a complete rotation (6 years) in Brazil, the study evaluated the interactive effects of K/Na fertilization, water availability, and stand age on stem volume, sapwood/heartwood ratio, wood density, fiber, and vessel features. The relationships between growth rate, wood density, and fiber and vessel features were also evaluated. The split-plot experimental design consisted of two water supply regimes (37% throughfall reduction versus undisturbed throughfall) and three fertilization regimes (K, Na, and control).

4. Wood density prediction using near-infrared hyperspectral imaging: an application to early selection of *Eucalyptus grandis* trees

Finally, in this chapter, question ***e*** was developed. The chapter investigated the use of near-infrared hyperspectral imaging (NIR-HSI) combined with X-ray microdensitometry (XRD) to indirectly estimate wood density from relating XRD density values with NIR-HSI spectra, and thus, evaluate the juvenile-mature correlations on wood density for early selection of *E. grandis* trees. The objective was (i) to evaluate the performance of using NIR-HSI to estimate wood density variation across age, (ii) to estimate the juvenile-mature correlations on wood density, and (iii) to examine the effects of water deficit on these correlations. The results provided helpful insights to evaluate the reliability of selecting wood density at early growth stages in *E. grandis* trees growing in different soil water availability conditions using NIR-HSI.

References

Almeida, J.C.R., Laclau, J.P., Gonçalves, J.L. de M., Ranger, J., Saint-André, L., 2010. A positive growth response to NaCl applications in Eucalyptus plantations established on K-deficient soils. For. Ecol. Manage. 259, 1786–1795. https://doi.org/10.1016/j.foreco.2009.08.032

Asensio, V., Domec, J.C., Nouvellon, Y., Laclau, J.P., Bouillet, J.P., Jordan-Meille, L., Lavres, J., Rojas, J.D., Guillemot, J., Abreu-Junior, C.H., 2020. Potassium fertilization increases hydraulic redistribution and water use efficiency for stemwood production in Eucalyptus grandis plantations. Environ. Exp. Bot. 176, 104085. https://doi.org/10.1016/j.envexpbot.2020.104085

Battie-Laclau, P., Delgado-Rojas, J.S., Christina, M., Nouvellon, Y., Bouillet, J.-P., Piccolo, M. de C., Moreira, M.Z., Gonçalves, J.L. de M., Roupsard, O., Laclau, J.-P., 2016. Potassium fertilization increases water-use efficiency for stem biomass production without affecting intrinsic water-use efficiency in Eucalyptus grandis plantations. For. Ecol. Manage. 364, 77–89. https://doi.org/10.1016/j.foreco.2016.01.004

Battie-Laclau, P., Laclau, J.P., Domec, J.C., Christina, M., Bouillet, J.P., de Cassia Piccolo, M., de Moraes Gonçalves, J.L., Moreira, R.M., Krusche, A.V., Bouvet, J.M., Nouvellon, Y., 2014. Effects of potassium and sodium supply on drought-adaptive mechanisms in Eucalyptus grandis plantations. New Phytol. 203, 401–413. https://doi.org/10.1111/nph.12810

Battie-Laclau, P., Laclau, J.P., Piccolo, M. de C., Arenque, B.C., Beri, C., Mietton, L., Muniz, M.R.A., Jordan-Meille, L., Buckeridge, M.S., Nouvellon, Y., Ranger, J., Bouillet, J.P., 2013. Influence of potassium and sodium nutrition on leaf area components in Eucalyptus grandis trees. Plant Soil 371, 19–35. https://doi.org/10.1007/s11104-013-1663-7

Campinhos, Jr., E., 1999. Sustainable plantations of high-yield shape Eucalyptus trees for production of fiber: the Aracruz case. New For. 17, 129–143. https://doi.org/10.1023/A:1006562225915

Campoe, O.C., Munhoz, J.S.B., Alvares, C.A., Carneiro, R.L., de Mattos, E.M., Ferez, A.P.C., Stape, J.L., 2016. Meteorological seasonality affecting individual tree growth in forest plantations in Brazil. For. Ecol. Manage. 380, 149–160. https://doi.org/10.1016/j.foreco.2016.08.048

Carle, J.B., Holmgren, L.P.B., 2009. Wood from planted forests: Global outlook to 2030, in: Evans, J. (Ed.), Planted Forests: Uses, Impacts and Sustainability. CABI, pp. 47–59. https://doi.org/10.1079/9781845935641.0047

Chambi-Legoas, R., Chaix, G., Tomazello-Filho, M., 2020. Effects of potassium/sodium fertilization and throughfall exclusion on growth patterns of Eucalyptus grandis W. Hill ex Maiden during extreme drought periods. New For. 51, 21–40. https://doi.org/10.1007/s11056-019-09716-x

Christina, M., le Maire, G., Nouvellon, Y., Vezy, R., Bordon, B., Battie-Laclau, P., Gonçalves, J.L.M., Delgado-Rojas, J.S., Bouillet, J.P., Laclau, J.P., 2018. Simulating the effects of different potassium and water supply regimes on soil water content and water table depth over a rotation of a tropical Eucalyptus grandis plantation. For. Ecol. Manage. 418, 4–14. https://doi.org/10.1016/j.foreco.2017.12.048

Coelho, C.A.S., de Oliveira, C.P., Ambrizzi, T., Reboita, M.S., Carpenedo, C.B., Campos, J.L.P.S., Tomaziello, A.C.N., Pampuch, L.A., Custódio, M. de S., Dutra, L.M.M., Da Rocha, R.P., Rehbein, A., 2016. The 2014 southeast Brazil austral summer drought: regional scale mechanisms and teleconnections. Clim. Dyn. 46, 3737–3752. https://doi.org/10.1007/s00382-015-2800-1

Correia, B., Pintó-Marijuan, M., Neves, L., Brossa, R., Dias, M.C., Costa, A., Castro, B.B., Araújo, C., Santos, C., Chaves, M.M., Pinto, G., 2014. Water stress and recovery in the performance of two Eucalyptus globulus clones: Physiological and biochemical profiles. Physiol. Plant. 150, 580–592. https://doi.org/10.1111/ppl.12110

Deslauriers, A., Rossi, S., Anfodillo, T., 2007. Dendrometer and intra-annual tree growth: What kind of information can be inferred? Dendrochronologia 25, 113–124. https://doi.org/10.1016/j.dendro.2007.05.003

Drew, D.M., Downes, G.M., 2009. The use of precision dendrometers in research on daily stem size and wood property variation: A review. Dendrochronologia 27, 159–172. https://doi.org/10.1016/j.dendro.2009.06.008

FAO, 2020. Global Forest Resources Assessment 2020 Main report. Rome. https://doi.org/10.4060/ca9825en

Galiano, L., Martínez-Vilalta, J., Lloret, F., 2011. Carbon reserves and canopy defoliation determine the recovery of Scots pine 4 yr after a drought episode. New Phytol. 190, 750–759. https://doi.org/10.1111/J.1469-8137.2010.03628.X

Gonçalves, J.L. de M., Alvares, C.A., Higa, A.R., Silva, L.D., Alfenas, A.C., Stahl, J., Ferraz, S.F. de B., Lima, W. de P., Brancalion, P.H.S., Hubner, A., Bouillet, J.-P.D., Nouvellon, Y., Epron, D., 2013. Integrating genetic and silvicultural strategies to minimize abiotic and biotic constraints in Brazilian eucalypt plantations. For. Ecol. Manage. 301, 6–27. https://doi.org/10.1016/j.foreco.2012.12.030

Gonçalves, J.L. de M., Barros, N.F. de, 1999. Improvement of site productivity for short-rotation plantations in Brazil. Bosque 20, 89–106.

Gonçalves, J.L. de M., Stape, J.L., Laclau, J.-P., Smethurst, P., Gava, J.L., 2004. Silvicultural effects on the productivity and wood quality of eucalypt plantations. For. Ecol. Manage. 193, 45–61. https://doi.org/10.1016/j.foreco.2004.01.022

Gonçalves, J.L.M., Alvares, C.A., Rocha, J.H.T., Brandani, C.B., Hakamada, R., 2017. Eucalypt plantation management in regions with water stress. South. For. 79, 169–183. https://doi.org/10.2989/20702620.2016.1255415

Guada, G., Camarero, J.J., Sánchez-Salguero, R., Cerrillo, R.M.N., 2016. Limited Growth Recovery after Drought-Induced Forest Dieback in Very Defoliated Trees of Two Pine Species. Front. Plant Sci. 7, 418. https://doi.org/10.3389/fpls.2016.00418

IBÁ, 2020. Annual Report 2020. São Paulo.

IPCC, 2021. Climate Change 2021: The Physical Science Basis. Contribution of Working Group I to the Sixth Assessment Report of the Intergovernmental Panel on Climate Change, In Press. ed. Cambridge University Press.

Laclau, J.P., Almeida, J.C.R., Gonalves, J.L.M., Saint-Andr, L., Ventura, M., Ranger, J., Moreira, R.M., Nouvellon, Y., 2009. Influence of nitrogen and potassium fertilization on leaf lifespan and allocation of above-ground growth in Eucalyptus plantations. Tree Physiol. 29, 111–124. https://doi.org/10.1093/treephys/tpn010

Lee, J.Y., Marotzke, J., Bala, G., Cao, L., Corti, S., Dunne, J.P., Engelbrecht, F., Fischer, E., Fyfe, J.C., Jones, C., Maycock, A., Mutemi, J., Ndiaye, O., Panickal, S., Zhou, T., 2021. Future Global Climate: Scenario-Based Projections and Near-Term Information, in: Masson-Delmotte, V., Zhai, P., Pirani, A., Connors, S.L., Péan, C., Berger, S., Caud, N., Chen, Y., Goldfarb, L., Gomis, M.I., Huang, M., Leitzell, K., Lonnoy, E., Matthews, J.B.R., Maycock, T.K., Waterfield, T., Yelekçi, O., Yu, R., Zhou, B. (Eds.), Climate Change 2021: The Physical Science Basis. Contribution of Working Group I to the Sixth Assessment Report of the Intergovernmental Panel on Climate Change. Cambridge University Press, p. 195.

Lourenço, A., Gominho, J., Pereira, H., 2011. Modeling of sapwood and heartwood delignification kinetics of Eucalyptus globulus using consecutive and simultaneous approaches. J. Wood Sci. 57, 20–26. https://doi.org/10.1007/s10086-010-1137-y

Mcmahon, S.M., Parker, G.G., 2015. A general model of intra-annual tree growth using dendrometer bands. Ecol. Evol. 5, 243–254. https://doi.org/10.1002/ece3.1117

Morais, M., Pereira, H., 2007. Heartwood and sapwood variation in Eucalyptus globulus Labill. trees at the end of rotation for pulp wood production. Ann. For. Sci. 64, 665–671. https://doi.org/10.1051/forest:2007045

Nobre, C.A., Marengo, J.A., Seluchi, M.E., Cuartas, A., Alves, L.M., 2016. Some Characteristics and Impacts of the Drought and Water Crisis in Southeastern Brazil during 2014 and 2015 Some Characteristics and Impacts of the Drought and Water Crisis in Southeastern Brazil during 2014 and 2015. J. od Water Resour. Prot. 8, 252–262. https://doi.org/10.4236/jwarp.2016.82022

Pillai, P.K.C., Pandalai, R.C., Dhamodaran, T.K., Sankaran, K. V., 2013. Effect of silvicultural practices on fibre properties of Eucalyptus wood from short-rotation plantations. New For. 44, 521–532. https://doi.org/10.1007/s11056-012-9360-6

Rana, V., Singh, S.P., Gupta, P.K., 2011. Eucalypts in Pulp and Paper Industry, in: Bhojvaid, P.P., Kaushik, S., Singh, Y.P., Kumar, D., Thapliyal, M., Barthwal, S. (Eds.), Eucalypts in India. ENVIS Centre on Forestry, Indian Council of Forestry Research and Education, Dehradun, pp. 470–506.

Shmulsky, R., Jones, P.D., 2011. Forest Products and Wood Science An Introduction: Sixth Edition, Sixth Edit. ed, Forest Products and Wood Science An Introduction: Sixth Edition. Wiley-Blackwell. https://doi.org/10.1002/9780470960035

Stape, J.L., Binkley, D., Ryan, M.G., Fonseca, S., Loos, R.A., Takahashi, E.N., Silva, C.R., Silva, S.R., Hakamada, R.E., Ferreira, J.M. de A., Lima, A.M.N., Gava, J.L., Leite, F.P., Andrade, H.B., Alves, J.M., Silva, G.G.C., Azevedo, M.R., 2010. The Brazil Eucalyptus Potential Productivity Project: Influence of water, nutrients and stand uniformity on wood production. For. Ecol. Manage. 259, 1684–1694. https://doi.org/10.1016/j.foreco.2010.01.012

Thomas, D.S., Montagu, K.D., Conroy, J.P., 2007. Temperature effects on wood anatomy, wood density, photosynthesis and biomass partitioning of Eucalyptus grandis seedlings. Tree Physiol. 27, 251–260. https://doi.org/10.1093/treephys/27.2.251

Wu, Z., Dijkstra, P., Koch, G.W., Peñuelas, J., Hungate, B.A., 2011. Responses of terrestrial ecosystems to temperature and precipitation change: A meta-analysis of experimental manipulation. Glob. Chang. Biol. 17, 927–942. https://doi.org/10.1111/j.1365-2486.2010.02302.x

Wunder, J., Fowler, A.M., Cook, E.R., Pirie, M., McCloskey, S.P.J., 2013. On the influence of tree size on the climate-growth relationship of New Zealand kauri (Agathis australis): Insights from annual, monthly and daily growth patterns. Trees - Struct. Funct. 27, 937–948. https://doi.org/10.1007/s00468-013-0846-4

Zeng, S., Jacobs, D.F., Sloan, J.L., Xue, L., Li, Y., Chu, S., 2013. Split fertilizer application affects growth, biomass allocation, and fertilizer uptake efficiency of hybrid Eucalyptus. New For. 44, 703–718. https://doi.org/10.1007/s11056-013-9371-y

Zobel, B.J., van Buijtenen, J.P., 1989. Variation Within and Among Trees, in: Zobel, B.J., Buijtenen, J.P. van (Eds.), Wood Variation: Its Causes and Control. Springer-Verlag, pp. 72–131. https://doi.org/10.1007/978-3-642-74069-5_3

2. INTER-ANNUAL EFFECTS OF POTASSIUM FERTILIZATION ON GROWTH AND XYLEM PLASTICITY OF *Eucalyptus grandis* TREES UNDER CHANGING ENVIRONMENTAL CONDITIONS

Abstract

In Brazil, most Eucalyptus plantations are located in regions experiencing periods of water shortage, where fertilizers such as potassium (K) are intensively used to achieve high productivity. In a changing environment, the effects of K fertilization on growth rate and xylem plasticity across tree age in function to climate is fundamental to forest management. The objectives of this study were (i) evaluate the interactions between K fertilization, water availability, and age on stem growth and xylem traits change of *E. grandis* trees over a full rotation; (ii) evaluate the relationships between stem growth, xylem traits, and meteorological variables, and if these are affected by omission or application of K fertilization.An experimental plantation of *E. grandis* trees established in São Paulo, Brazil, were monitored over a full rotation (6 years). The experiment consisted of a split-plot design with two water supply regimes (37% throughfall reduction versus undisturbed throughfall) and two fertilization regimes (K supply and K omission). Basal area increment (BAI) was monitored by band dendrometers at 14-day intervals. Xylem traits such as wood density (WD), cell wall fraction (CWF), cell density (CDen), theoretical xylem specific hydraulic conductivity (Kst), vessel diameter (VD), vessel density (VDen), vessel area (VA), and vulnerability index (VI) were measured in 6-months periods (rainy and dry seasons) over 6 years. Meteorological variables, soil water content, and tree transpiration were also monitored on a daily scale. Mixed-effect models were used to test the effects of factors and their interactions on BAI and xylem traits. Stepwise multiple regression and Pearson correlation expressed graphically through correlation network allowed to identify the climatic variables affecting BAI and xylem traits.The effects of K fertilization increasing growth rate were maintained from over the full rotation. K fertilization increased BAI by 3-fold under non-water deficit but stopped tree growth under the severe drought during the 2014 dry season. Reducing 37% throughfall in plots affected growth only in K-fertilized trees and only until 2.5 years after planting. K fertilization also increased xylem plasticity in response to drought. Main changes occurred in vessel traits, declining hydraulic conductivity by 53% in severe drought but recovering after drought. High plasticity also was observed for WD, CWF, CDen, and VI. The growth patterns and high xylem plasticity in response to severe changes in precipitation revealed an additive effect of K to increase resilience during long-term drought periods and recovery ability for growth following drought. Soil water availability and minimum and maximum temperature were the most important environmental variables affecting the xylem traits and growth rate of *E. grandis trees*. K fertilization increased responsiveness to climatic variation.

Keywords: Wood properties, Vessels, Inter-annual wood variation; Climatic variables; Tree resilience

2.1. Introduction

The Forest industry worldwide is increasingly using Eucalyptus plantations as the main source of raw material for wood and non-wood products, leading to a considerable expansion in various zones, many of which are water-limited areas. Particularly, in Brazil, most Eucalyptus plantations areas (49%, 3.4 million ha) are concentrated in the southeastern region (IBÁ, 2020), subject to seasonal dry periods of three to five months during which the monthly rainfall is less than 50 mm (Gonçalves et al., 2013). Since 2000, this region has been experienced an increase in frequency and duration of the dry periods, compared to that in 1965-2000 (Coelho et al., 2016; Nobre et al., 2016). Eucalyptus grandis is one of Brazil's most planted and productive species (Campinhos, Jr., 1999); however, it is also susceptible to water stress (Gonçalves et al., 2013). As the productivity of Eucalyptus plantation in this region is limited strongly by rainfall amount (Stape et al., 2010), the effects of prolonged drought are expected to affect tree growth negatively.

In this context, the revision of management strategies to improve tree tolerance to drought is necessary. Fertilization is maybe the main management practice involved in tree water use. Particularly, potassium (K) is the main driver for an increased growth rate of Eucalyptus trees (Laclau et al., 2009), with high involvement in drought-adaptive mechanisms. Some studies evaluating the effects of K fertilization on *E. grandis* trees have found a great improvement in stomatal regulation, water use efficiency, and capacity of roots for water access at great depths, which led to increased basal area, stem volume, and aboveground biomass by 3-fold (Asensio et al., 2020; Battie-Laclau et al., 2016, 2014, 2013; Christina et al., 2018). However, K fertilization also increases tree water demand and reduces water reserves in soils, aggravating the effects of water stress under prolonged severe droughts (Battie-Laclau et al., 2014).

Nevertheless, the high responsiveness to rainfall with sudden basal area growth (Chambi-Legoas et al., 2020) could suggest a high resistance and recovery ability to drought. The Eucalyptus genus is considered among the most resilient trees globally and is exceptionally well adapted to resist and recover from significant partial tree dieback (Matusick and Fontaine, 2020). In this context, it is necessary to monitor the tree growth over a full rotation (6 years), to test the actual impacts of K fertilization on productivity and wood quality under prolonged severe drought. In addition, since the growth rate can be affected by age and changes in environmental conditions, the effects of fertilization could change over time.

Under changing environmental conditions, trees need continuously adjust their structure to guarantee the fulfilment of future needs, such as safe and efficient water transport and mechanical stability (Deslauriers et al., 2017). The changes in composition and structure of xylem are known as xylem plasticity, which is the main adaptation strategy of trees to the environment. Eucalyptus species have shown great changes in vessels traits and hydraulic architecture in response to water availability variations, as an efficient adaptation to reduce the risk of embolism but maintain high water transport efficiency; whereas changes in fibers size and wall thickness seems to be less responsive (Câmara et al., 2020; Freitas et al., 2015). For example, when a drought begins, more vessels with smaller diameters will form to transport less water and reduce the risk of cavitation. However, if water availability increases, larger but fewer vessels will form to increase water transport. The magnitude of these anatomical changes depends on the duration and intensity of environmental changes.

K fertilization has been associated with an increase in periclinal cell divisions in the cambium in *Picea abies* (Dünisch and Bauch, 1994) and an increase in vessels size in poplar (Langer et al., 2002). K plays an important osmotic role during cambial cell expansion (Wind et al., 2004). This high involvement of K in xylogenesis could suggest an increase in xylem plasticity. However, the effects of K fertilization on xylem plasticity in Eucalyptus species are not documented. Under fluctuating environmental conditions, knowing if fertilization increases xylem plasticity in Eucalyptus is crucial for choosing suitable management practices to increase the resilience of trees to drought.

Even more, age is an important factor controlling tree development. Older trees have a higher root system which confers higher capacity to soil exploration and water uptake; however, older trees also have a higher leaf area index (LAI) and eventually higher transpiration (Battie-Laclau et al., 2014; Christina et al., 2018). Therefore, tree growth rate and xylem plasticity could greatly differ in function to age in highly productive *E. grandis* clones. Knowing at what stage trees are more vulnerable or more resilient, or if the effects of fertilization and the water deficit affect trees only during the first or last years, or if they are maintained throughout the rotation, is critical to making silvicultural corrections and preventing actions in order to reduce losses in wood production in *E. grandis* plantations.

The hypothesis that we questioned is (i) if effects of K fertilization and water deficit on growth will be constant across age during the full rotation, (ii) if K fertilization increase tree resilience for growth under changing environment, and (iii) if K fertilization enhance xylem plasticity in response to drought period.

To evaluate these concerns, an experimental plantation of 37% throughfall reduction was monitored over a full rotation (6 years). Artificially reducing throughfall in plots is helpful to reproduce prolonged water deficit conditions and allows aggravating the dry seasonal periods to understand better the potential impacts of severe droughts on trees (Wu et al., 2011). In addition, the study was performed over inter-annual or seasonal contrasting periods, such as dry and rainy seasons, and over abnormally drought period (as occurred in 2014 in southeastern Brazil) to test the magnitude and limits of changes in xylem plasticity and growth rates.

Thus, the objectives of this study were: (i) evaluate the interactions between K fertilization, water availability, and age on stem growth and xylem traits change of *E. grandis* trees over a full rotation; (ii) evaluate the relationships between stem growth, xylem traits, and environmental variables, and if these are affected by omission or application of K fertilization.

2.2. Material and Methods

2.2.1. Study area

The study was conducted at the Itatinga Experimental Station of the University of São Paulo, São Paulo State, Brazil (23°02'S, 48°38'W, 850 m a.s.l.). During the last 12 years, the mean annual rainfall and temperature have been 1700 mm and 19.9 °C, respectively. Two distinctive seasons can be observed along the year: a rainy season (October to March) with a cumulative rainfall of about 1146 mm and mean temperature of 21.6 °C, and a dry season (April to September) with lower rainfall and temperature about 544 mm and 18 °C, respectively (Chambi-Legoas et al., 2020). During July and August, monthly rainfall is usually less than 50 mm. The soils are deep ferralsols (>15 m) with 14 to 23% clay content developed on Cretaceous sandstone, Marılia formation, Bauru group (Laclau et al., 2009).

2.2.2. Field experiment description

An experimental plantation in split-plot design was installed on June 20, 2010, with seedlings of a highly productive *E. grandis* clone used in commercial plantations by the Suzano Company (Brazil). Seedlings were spaced at 3 m × 3 m in 12 subplots of 864 m^2 (144 plants per subplot) arranged in three blocks (4 subplots per block). At the time of planting, all plants were fertilized with 75 kg ha^{-1} of P_2O_5, 80 kg ha^{-1} of N ($NH_4(SO_4)_2$), and 20 kg ha^{-1} of FTE BR-12 (micronutrient source) applied in holes next to the plants. Furthermore, 2000 kg ha^{-1} of dolomitic limestone was broadcast on the soil surface.

Three months after planting (September 2010), two levels of water regime (37% throughfall reduction and non-throughfall reduction) as a whole-plot factor and two levels of fertilization (potassium supply and control) as a split-plot factor were applied in subplots. The combination of both factors formed four treatments:

- +K+W: Potassium (K) supply with no throughfall reduction
- −K+W: Non-potassium supply with no throughfall reduction

- +K−W: Potassium supply with 37% throughfall reduction
- −K−W: Non-potassium supply with 37% throughfall reduction

K supply consisted of 335 kg ha^{-1} (or 4.5 kmol ha^{-1}) of KCl broadcast on the soil surface in a single dose 3 months after planting. The 37% throughfall reduction was performed by transparent plastic panels mounted on wooden frames at a height varying between 0.5 m and 1.6 m (Battie-Laclau et al., 2016), covering 37% of the plot area. The experiment was assessed for 6 years. All trees were cut on June 2, 2016.

2.2.3. Fortnightly tree growth monitoring by band dendrometers

Tree growth was monitored through fortnightly increments of the circumference at breast height (CBH) measured by band dendrometers in three trees per subplot (nine trees per treatment). CBH increments were converted to basal area increments to compare the growth between trees of different sizes more appropriately since basal area increment does not depend on the initial CBH of the trees.

Band dendrometers were constructed from steel bands 0.2 mm thickness and 12.5 mm wide, attached to the bole by a spring of 0.8 mm in diameter and 10 mm in length. CBH increments readings at 0.1 mm of precision were made with a vernier measurement scale recorded in the steel bands.

Dendrometers readings were recorded at fortnightly intervals in the early hours of the morning, from October 2011 (16 months after planting) to June 2016 (71 months after planting). The first measurements were recorded one month after band dendrometer installation to avoid underestimating CBH due to initial slack in tree boles (Fuller et al., 1988; Keeland and Sharitz, 1993). In addition, CBH was measured directly with a tape measure at semestral intervals season to verify and correct possible underestimations of band dendrometers.

2.2.4. Xylem traits measurement

The 36 trees, monitored for growth, were cut at 6 years after planting (June 2016) and sampled to measure xylem traits. A cross-sectional disc of 3 cm thick was cut at breast height from each tree. Using dendrometer data, wood density profiles, and wood anatomy images, we delimitated the annual growth rings for each disc to measure xylem traits in each growth ring.

Radial sections (10-15 μm thickness) of the samples were cut on a sliding microtome (Leica SM 2010 R). Histological slides were produced according to standard wood anatomy techniques (Johansen, 1940). Digital images were captured with a microscope (Zeiss Axio Scope A1) at 40x magnification to measure vessel traits (diameter, frequency, and area), and at 100x magnification to measure cell wall fraction (CWF) and cell density (CDen). Measurements were performed using the ImageJ software version 1.52a (Schneider et al., 2012).

Apparent wood density (WD) was measured by microdensitometry method. A thin wood slice of cross-section (1.8 cm thickness, 2 cm wide) was cut from each disc using parallel double circular sawing equipment. The samples were conditioned in a climatic chamber (20°C, 60% HR) for 48 h, with 12-15% wood moisture content. Subsequently, X-ray images of the wood samples were obtained using the Faxitron MX-20 Cabinet X-Ray Imaging System (Faxitron X-Ray Corporation, Lincolnshire, IL, USA). X-ray images were analyzed in R software with the X-ring package (Campelo et al., 2019). A calibration curve was fitted from known values of the density and thicknesses of a step-wedge recorded in each image. Then, the wood density profile was determined based on the grayscale value

of pixels and the thickness of the sample in a region of interest of 2 mm width. The density profile was divided according to growth ring limits, and average ring density was calculated.

Theoretical xylem specific hydraulic conductivity (Kst, kg s^{-1} m^{-1} MPa^{-1}) was calculated according to Fichot et al. (2010), based on the sampled vessels using Hagen–Poiseuille law for ideal capillaries and assuming laminar flow as $Kst = (\pi\varrho/128\eta A_{image}) \times \Sigma d^4$ where ϱ is the density of water at 20 °C (998.2 kg m^{-3}), η is the viscosity of water at 20 °C (1.002×10^{-9} MPa s) and A_{image} is the area of the images analyzed for vessel counts (m^2).

Vulnerability index (VI) was the diameter/density ratio of vessels, indicating the capability of withstanding water stress. The low values of this ratio could be interpreted as a lower risk of the embolism of a given number of vessels under water stress to seriously impair conduction in a plant since vessel density is high (Carlquist, 1977).

2.2.5. Meteorological and soil water measurements

Collection data

Rainfall, mean air temperature (Tmean), minimum air temperature (Tmin), maximum air temperature (Tmax), vapor pressure deficit (VPD), and potential evapotranspiration (PET) data were collected at 30-minute intervals from an automatic weather station installed in a tower at 20 m above ground, located 50 m away from the experiment.

Soil water content (SWC) in m^3 m^{-3}, was measured weekly in the subplots of the first block. In each subplot, three soil moisture sensors (Trase Soilmoisture, Santa Barbara, CA, USA) were installed at 0.15 m, 0.5 m, 1 m, 1.5 m, 3 m, 4.5 m, and 6 m depths, one month before the plantation was established. TDR sensors were calibrated via gravimetry of soil water content and density measurements. During the last year of monitoring, soil water content (SWC) was measured every 30 minutes.

Association with growth measurements

For fortnightly assessment of tree growth, meteorological and soil moisture data were organized into fortnightly periods to match the dendrometers readings. Moreover, daily rainfall data were summarized to obtain cumulative rainfall for six months-interval periods: rainy seasons (October to March) and dry seasons (April to September) for each assessment year.

2.2.6. Data analysis

Mixed-effect models were used to test the effects of water regime, fertilization, age, and the interactions water regime × fertilization, water regime × age, fertilization × age, and interaction water regime × fertilization × age (fixed effects) on fortnightly basal area increment, cumulative basal area increment, and xylem traits by season-year, over 6 years. Blocks and water regime × block were considered as random effects to take account of the split-plot design. A repeated-measures statement was included in the model to take into account the variability within-trees over time.

Pearson correlation was used to assess the individual relationships between meteorological variables, soil water content (SWC), and tree basal area increment in each treatment by season year. Stepwise multiple linear regression analysis for each treatment was used to identify the meteorological variables with the greatest effect on

tree basal area increments and establish models to predict basal area growth rates as a function of meteorological variables and the age of trees. Additional tests were performed, including preceding meteorological data in 1, 2, and 3 days at a given growth interval, to prove the absence of any lag in growth response.

2.3. Results

2.3.1. Meteorological variability and soil water content (SWC) variation

A high inter-annual meteorological variability can be observed over the 6 years. Cumulative rainfall varied from 325 to 589 mm in dry seasons and from 620 to 1763 mm in rainy seasons. Historical data from 2006/2007 to 2018/2019 in Itatinga-SP show an average cumulative rainfall of 1177 mm in rainy and 548 mm in dry seasons.

The driest year occurred in 2014, with 620 mm in the rainy season and 325 mm in dry season, about 47% and 41% lower precipitation than the historical average. By contrast, 2016 was the wettest year, with 1763 mm in the rainy season and 589 mm in the dry season, about 50% and 10% higher precipitation than the historical average (Figure 1).

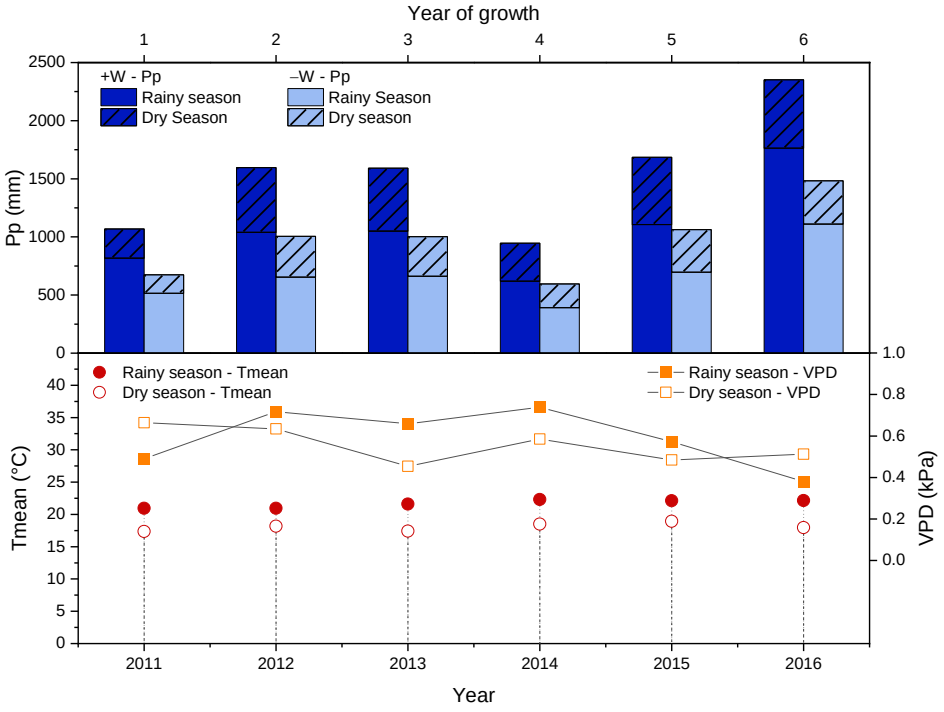

Figure 1. Annual precipitation for +W plots (undisturbed throughfall) and −W plots (37% throughfall reduction) (a), and averages of mean temperature (Tmean) (circle symbol) and vapor pressure deficit (VPD) (square symbol) (b), summarized for rainy season (October to March) and dry season (April to September), at Itatinga Experimental Station, Itatinga, São Paulo, Brazil..

In all plots, soil water content (SWC) in the superficial layers (0.15–1.5 m) was highly responsive to rainfall variability. The recharge of water in the soil superficial layers occurred immediately with the occurrence of rains. In contrast, in the deep layers (3-6m), SWC was less responsive to rainfall events, and groundwater recharge was lag (Figure 3).

The occurrence of extreme drought period from October 2013 to September 2014 affected the groundwater recharge considerably. However, over the 6 years, there was no groundwater recharge in +K−W treatment. On the other hand, high SWC was observed in all treatments during the 6th year of growth due to the abnormally high rainfall in the 2015/2016 rainy season.

In both superficial and deep soil layers, SWC was maximum in the C+W subplots and minimum in the +K−W subplots. +W plots always showed a higher SWC than the −W plots. Throughfall reduction decreased SWC by 12-15% in −K plots and 22–27% in +K plots in the superficial soil layers. In soil deep layers, the reduction of SWC was lower, about 5-9% in −K plots and 15-16% in +K plots. Reductions of SWC were larger in rainy seasons and proportional to high amounts of rainfall over these periods.

The 37% throughfall exclusion affected SWC reduction more strongly than K fertilization in superficial soil layers. In contrast, the effects of K fertilization were stronger in deep soil layers (Figure 2).

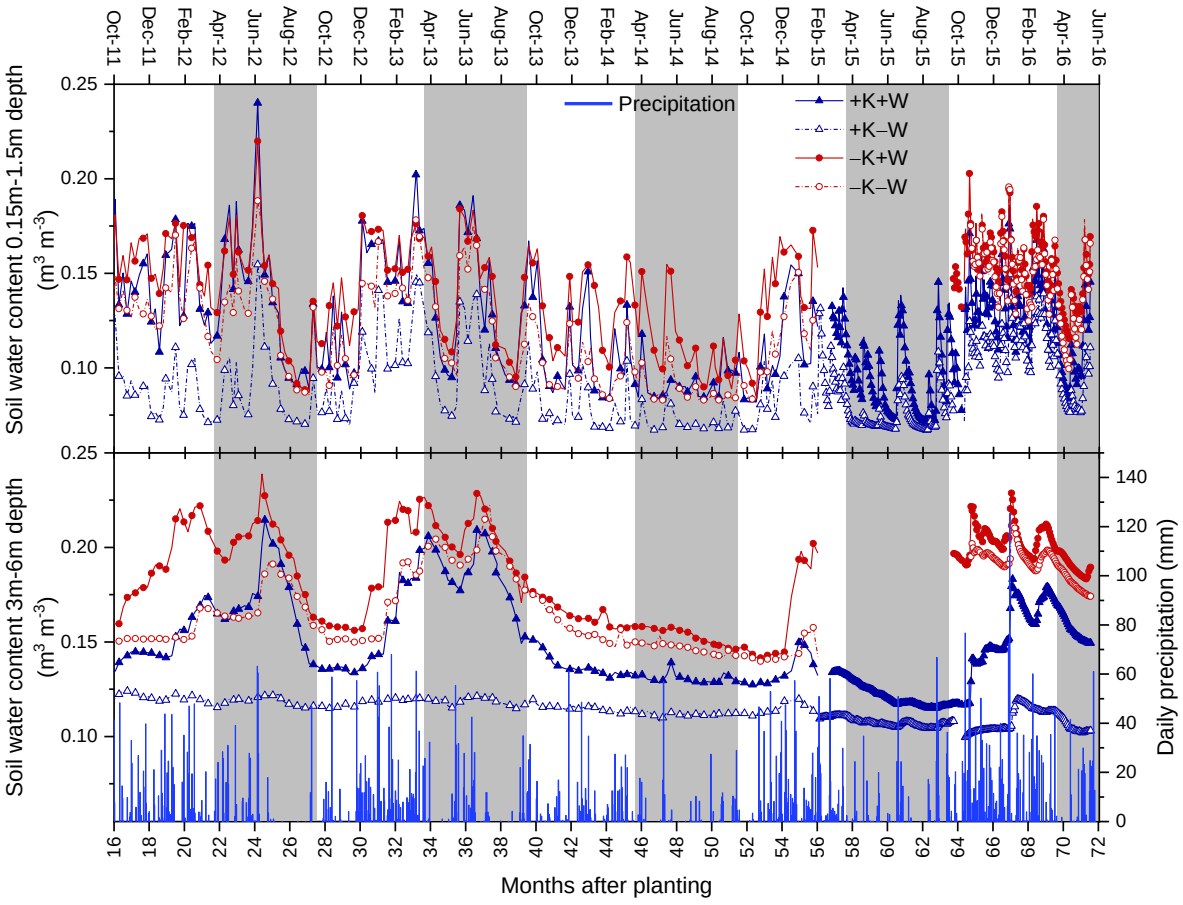

Figure 2. Time series of soil water content (SWC) in 0.15–1.5 m soil layer and in 3–6 m soil layer. Since February 2015, until September 2015 there was no data for −K+W and −K−W treatments, due to TDR sensor malfunction. The blue bars represent the daily rainfall.

2.3.2. Basal area increment (BAI) and climate interactions

Until 16 months after planting K deficient trees already showed significant lower cumulative BAI than K fertilized trees. Cumulative effect of K fertilization was increasing differences between K fertilized and deficient trees

on BAI over time, so much that at 6 years old, K fertilization increased the basal area by 2-fold in +W plots, and by 1.7-fold in −W plots (Figure 3a). In addition, we observed that positive effect of K fertilization was constant across age. K fertilized increased CAI-basal area by 87%, 126%, 40%, 301%, and 100% at 2, 3, 4, 5, and 6 years old, respectively, in +W plots. These positive effects were 35% lower in −W plots.

Effect of K fertilization was highly responsive to precipitation. In non-dry periods K-fertilized trees showed significantly higher fortnightly BAI than K- deficient trees ($p<0.0001$). However, in the driest periods, as from July 2013 to October 2014, K-fertilized trees did not grow, whereas K-deficient trees grew at low rates (approximately 0.3 cm^2 $tree^{-1}$) (Figure 3b). As a result, cumulative BAI during the 2014 dry season was -22% lower in +K+W than −K+W (Figure 4).

Significant interaction fertilization × water regime indicated that 37% throughfall reduction negatively affected BAI only on K-fertilized trees. K-deficient trees were not affected by throughfall reduction over 6 years. In K-fertilized trees, the effects of 37% throughfall reduction decreased across age and were significant only until 30 months after planting ($p=0.03$) (Table 1). Onwards, the effects of 37% throughfall reduction gradually decreased (Figure 3b). For example, the decrease in CAI-basal area in +K−W compared to +K+W trees was 25% at 2 years old but only 14% at 6 years old (Figure 4). Furthermore, +K−W trees grew at the same rate as +K+W during abnormally very wet periods from October 2015 onwards (Figure 3b).

On the other hand, interactions fertilization × season were significant over 6 years. CAI-basal area in rainy seasons was significantly higher than in dry seasons in K fertilized trees, but there were no significant differences between seasons in K-deficient trees. As expected, the BAI decreased progressively across age in all treatments.

Table 1. P-values of the effects of fertilization regime (K addition, non-K addition), water regime (undisturbed rainfall versus 37% of throughfall exclusion), stand age, season (rainy season vs. dry season), and interactions on the fortnightly basal area increment for *Eucalyptus grandis* trees, for the entire period and by stand age.

Factors	Total	Year of growth				
		2	3	4	5	6
Water	0.229	**0.033**	0.892	0.097	0.847	0.495
Fertilization	**<0.001**	**<0.001**	**<.0001**	**<.0001**	**<0.001**	**<0.001**
Season	**<0.001**	**<0.001**	0.416	**<0.001**	0.7493	**0.0061**
Stand age	**<0.001**					
Water × Fertilization	**<0.001**	**0.000**	**0.043**	0.189	**0.001**	0.323
Water × Season	0.608	0.627	0.417	0.539	0.596	0.747
Water × Stand age	**<0.001**					
Fertilization × Season	**<0.001**	**<0.001**	**<0.001**	**<0.001**	**0.9895**	**<0.001**
Fertilization × Stand age	**<0.001**					
Water × Fertilization × Season	0.374	0.674	0.510	**0.023**	0.057	0.650
Water × Fertilization × Stand age	0.126					
Water × Fertilization × Season × Stand age	**<0.001**					

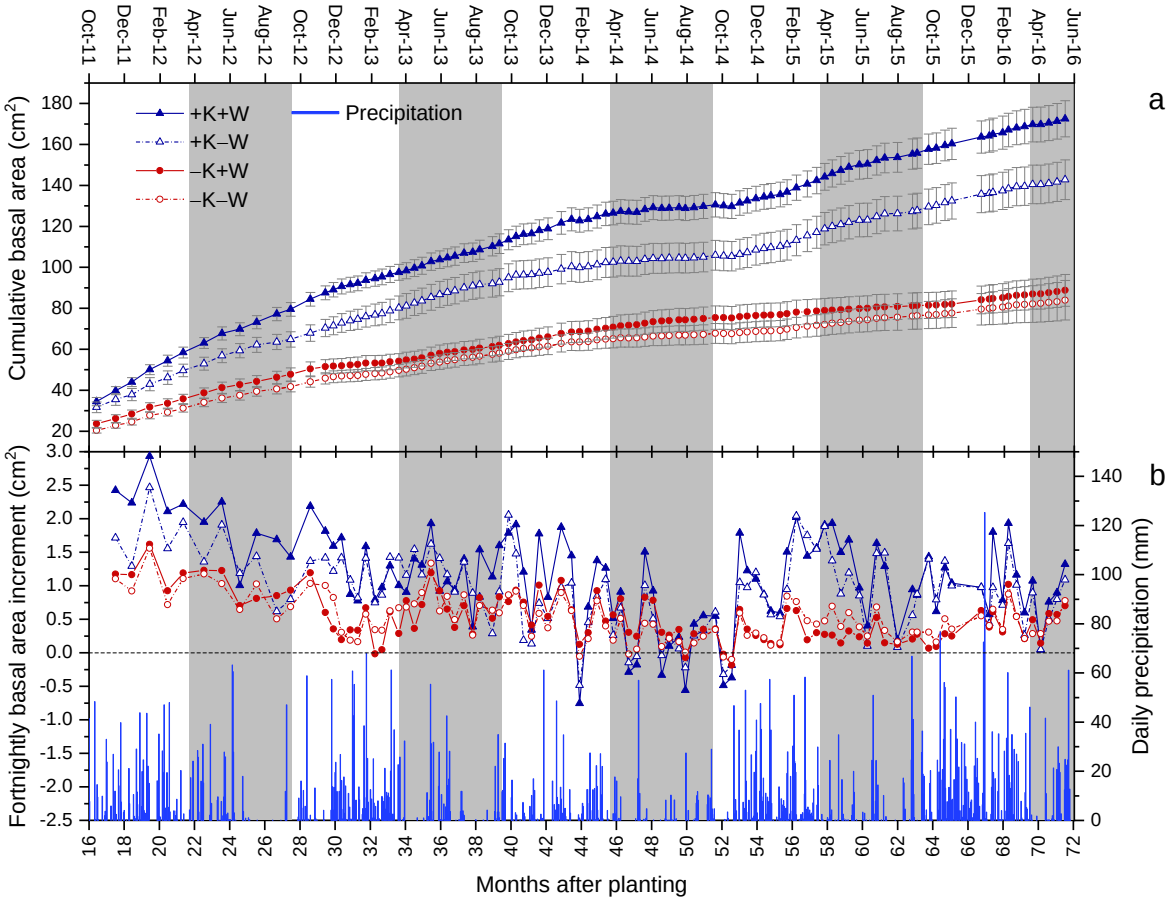

Figure 3. Time series of mean cumulative basal area (a) and mean basal areal fortnightly increment (b) in cm^{-2} $tree^{-1}$. Blue bars indicate daily rainfall (mm). Vertical bars indicate standard errors between trees (n=9).

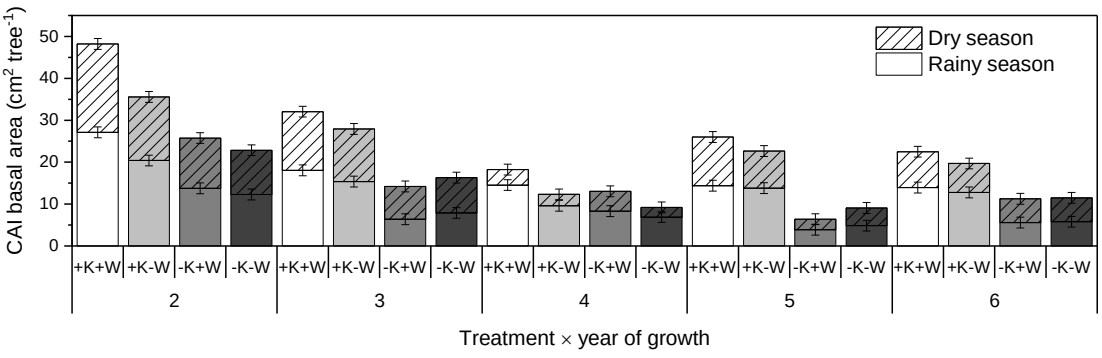

Figure 4. Current annual increment (CAI) basal area during the rainy season and the dry season in bars stacked, by treatment and year of growth. Vertical bars indicate standard errors.

Meteorological variability and age of trees explained about 43% of tree growth. Responsiveness was stronger in +K−W and weaker in −K−W (Table 2). K-fertilized trees were more responsive to precipitation, Tmax, VPD, and ET, while K-deficient trees were more responsive to precipitation, Tmax, and ET (Figure 7).

However, the influence of meteorological variability changes across age. Trees were more responsive to meteorological variability from 4 years old, mainly to precipitation in all treatments. A higher correlation between

precipitation and BAI was observed during the driest year (2014), and a similarly higher correlation between VPD and BAI occurred during 2015 (5 years old).

Table 2. Coefficients of the basal area growth equations and statistical indices by treatment.

Coefficients	Treatments				
	+K+W	+K−W	−K+W	−K−W	Grouped
Intercept	5.22926***	4.35092***	2.73379***	2.81304***	2.76482***
Meteorological variables					
Precipitation	0.00738***	0.00627***	0.00412***	0.00373***	0.0054***
T° mean	0.12054ns	0.2149***		0.13406**	0.13243***
T° min				-0.04204**	-0.02277**
T° max	-0.24547**	-0.28251***	-0.0596**	-0.15001***	-0.18631***
VPD	-0.46839**	-0.49583**			-0.27218**
ET	0.57442**	0.34932***	0.15888**	0.17881**	0.3176***
Time after planting (days)	-0.00157***	-0.00114***	-0.001***	-0.000872***	-0.00115***
R^2_{adj}	0.462	0.489	0.478	0.407	0.432
p-value	<0.0001	<0.0001	<0.0001	<0.0001	<0.0001
RSE	1.042	0.599	0.335	0.374	0.618

Tmean: Mean air temperature; Tmin: Minimum air temperature; Tmax: Maximum air temperature; VPD: Vapor pressure deficit. R^2adj: Adjusted determination coefficient; p-value: significance; RMSE: Root mean square error (cm^2 $tree^{-1}$). n = 387.

2.3.2. BAI and transpiration

Tree transpiration was lower in the dry season than during the rainy season and did not vary significantly across age (Figure 5).

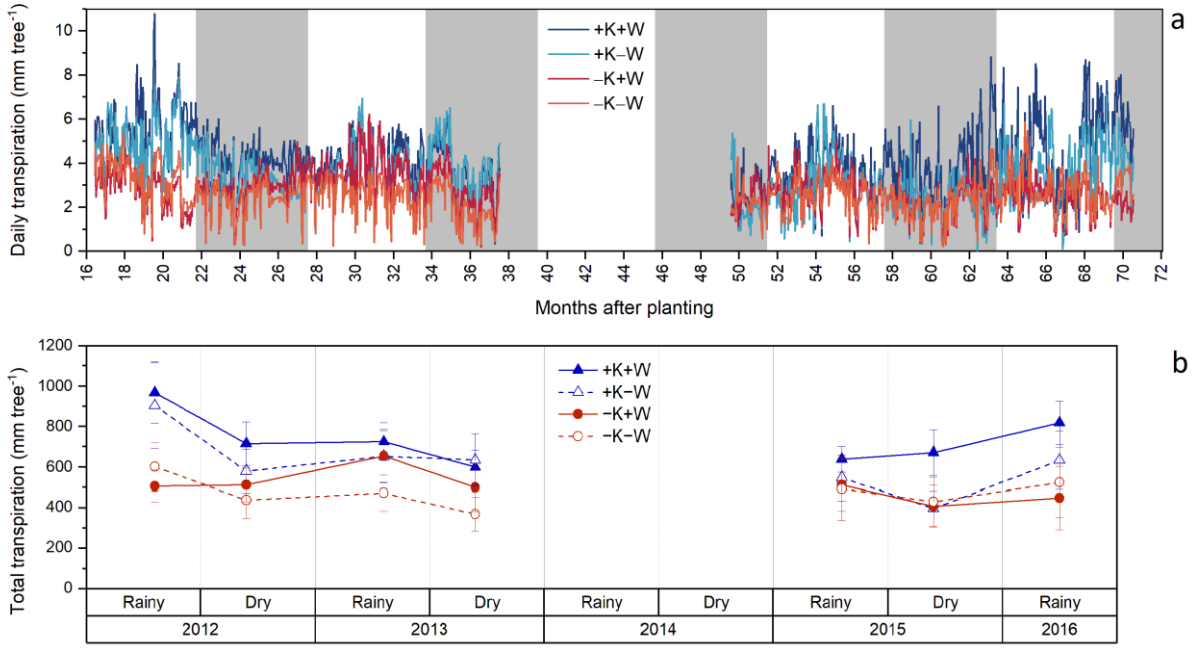

Figure 5. Time series of daily transpiration (a) and total transpiration in rainy and dry season (b) in mm. Vertical bars indicate standard errors between trees (n=9).

Regardless of water availability, the high growth rate observed in K-fertilized trees was strongly related to transpiration rate, while in K-deficient trees, it was moderate (Figure 6).

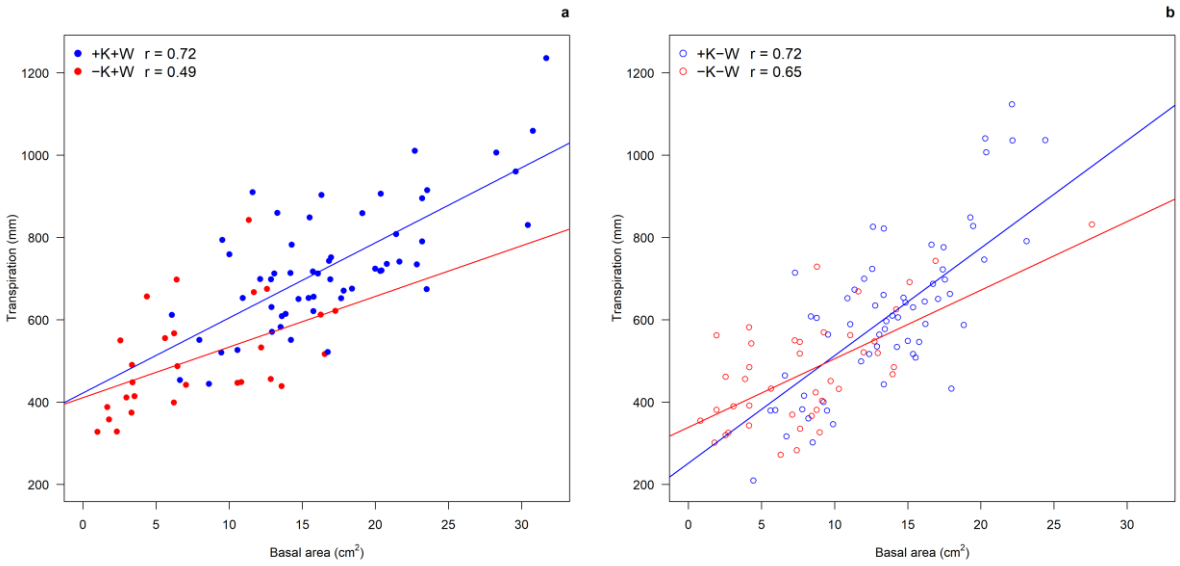

Figure 6. Relationships between basal area and transpiration in undisturbed throughfall plots (+W) (a), and in 37% throughfall reduction plots (−W) (b), by fertilization treatment: K-fertilization (+K) and K-omission (−K). Points are cumulative basal area during rainy or dry seasons by year.

2.3.3. Xylem traits and climate interactions

Fertilization regimes had larger effects on xylem traits than water regimes (Table 3). There was no interaction between fertilization and water regime on vessel traits. K fertilization strongly affected all xylem traits except WD and CWF. In contrast, throughfall reduction affected VD, VI, CWF, and CDen. Significant interactions between fertilization and stand age showed that xylem traits vary across age in K-fertilized trees but not in K-deficient trees. Effects of K-fertilization on most xylem traits remain over 6 years. WD and CWF were lesser affected by treatments. Xylem traits changed significantly between seasons. Transpiration (T) was affected by treatments, season, and age.

Table 3. P-values of the effects of fertilization regime (K addition, non-K addition), water regime (undisturbed rainfall versus 37% of throughfall exclusion), growth year, season (rainy season vs. dry season), and its interactions on tree transpiration (T), apparent wood density (WD), cell wall fraction (CWF), cell density (CDen), theoretical xylem specific hydraulic conductivity (Kst), vessel diameter (VD), vessel density (VDen), vessel area (VA), and vulnerability index (VI). P-value <0.05 in bold indicates significant effect.

Factors	T (mm day^{-1})	WD (g cm^{-3})	CWF (%)	CDen (Cells mm^{-2})	Kst (kg s^{-1} m^{-1} Mpa^{-1})	VD (μm)	VDen (Vessels mm^{-2})	VA (%)	VI
Water	0.520	0.441	**0.022**	**0.012**	0.195	**0.040**	0.051	0.519	**0.041**
Fertilization	**<0.001**	0.730	0.507	**<0.001**	**<0.001**	**<0.001**	**<0.001**	**0.034**	**<0.001**
Season	**<0.001**	**<0.001**	**<0.001**	**<0.001**	0.970	0.145	**<0.001**	**<0.001**	**0.033**
Stand age	**<0.001**	**<0.001**	**<0.001**	**<0.001**	**<0.001**	**<0.001**	**<0.001**	**<0.001**	**<0.001**
Water × Fertilization	**<0.001**	**<0.001**	**0.032**	**<0.001**	**<0.001**	0.230	0.422	0.939	0.060
Water × Season	0.569	0.534	0.582	**<0.001**	0.194	0.085	0.842	0.149	0.488
Water × Stand age	0.672	0.991	0.231	**<0.001**	0.297	0.396	**0.022**	0.388	0.113
Fertilization × Season	0.221	**<0.001**	**0.041**	**<0.001**	0.344	**0.045**	0.561	**0.017**	0.687
Fertilization × Stand age	**<0.001**	**0.016**	**<0.001**	**<0.001**	**<0.001**	**<0.001**	**0.031**	**<0.001**	**<0.001**
Water × Fertilization × Season	0.972	0.275	0.625	**<0.001**	0.754	0.777	0.110	0.720	0.801
Water × Fertilization × Stand age	**<0.001**	0.361	0.334	**<0.001**	0.658	0.928	0.280	0.754	0.707
Water × Fertilization × Season × Stand age	**<0.001**	0.083	0.108	**<0.001**	**<0.001**	**<0.001**	**<0.001**	**<0.001**	**<0.001**

The significant interaction between fertilization and growth year reflected the changes in xylem traits suffered from the extreme drought period of the 2014 dry season. In the 2014 dry season, there was a high increase in WD and CWF and a high decrease in VD, VA, and VI, mainly in K fertilized trees (Figure 7).

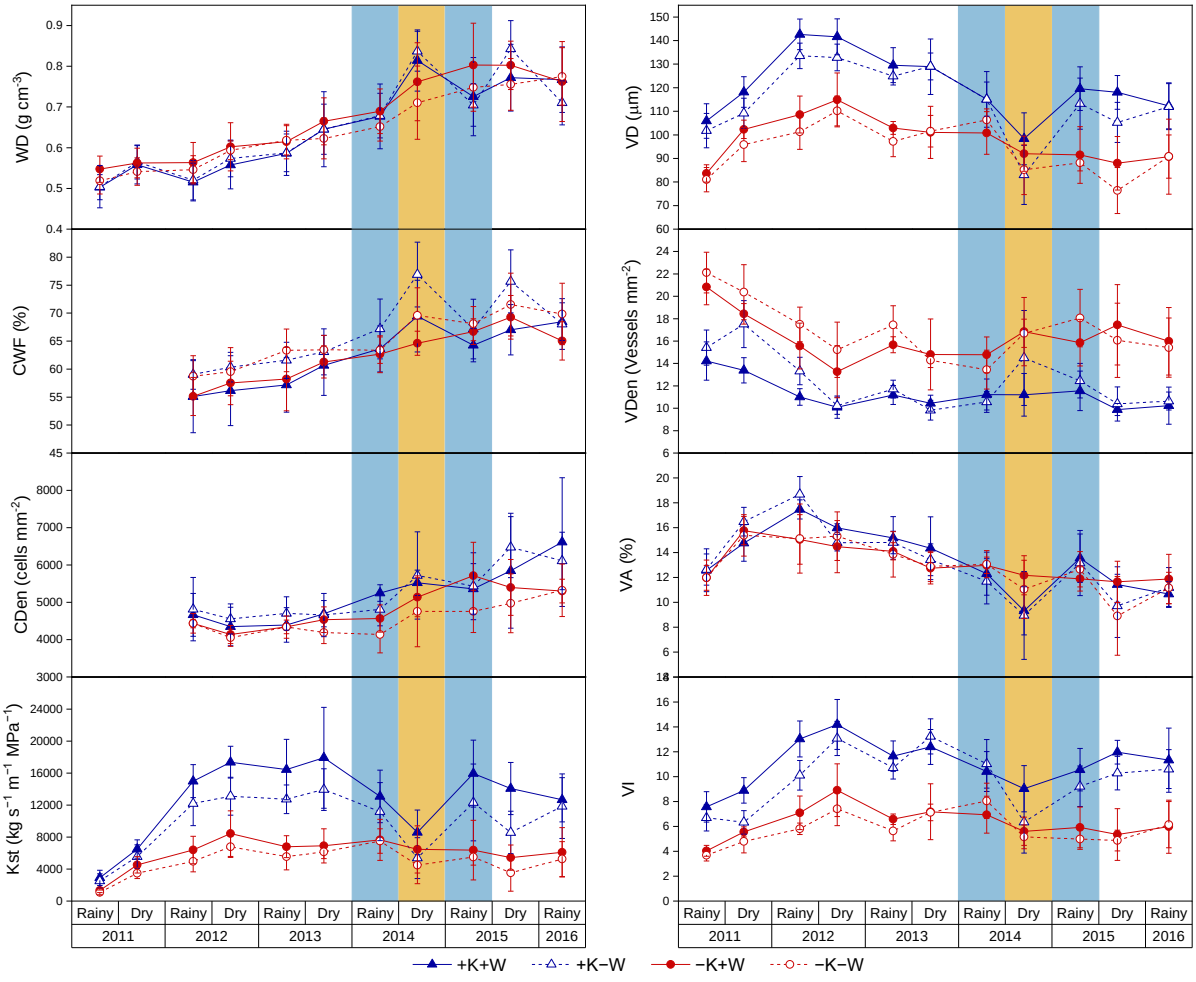

Figure 7. Xylem traits by treatment of fertilization and water regime across years and seasons: Apparent wood density (WD), cell wall fraction (CWF), cell density (CDen), theoretical xylem specific hydraulic conductivity (Kst), vessel diameter (VD), vessel density (VDen), vessel area (VA), and vulnerability index (VI). The yellow region corresponds to the drought period occurring on the 2014 dry season. The blue regions correspond to the periods before and after extreme drought. The vertical bars indicate standard deviation.

The greatest changes in xylem traits were observed in K fertilized trees. In comparison to the values observed of the 2014 rainy season preceding the drought, in +K−W trees, WD, CWF, and VDen increased by around 19%, 15%, and 24%, respectively, whereas xylem traits related to vessels such as Kst, VD, VA, and VI, declined by around 53%, 26%, 33%, and 30%, respectively. In contrast, in K deficient trees on xylem traits, negligible changes were observed, except for Kst and VA, which were lightly reduced in 20% and 12%, respectively (Figure 8a).

Following drought, the % change to the 2015 rainy season was even higher in K fertilized trees. Over this wet period +K−W trees considerably increased Kst, VD, VA, and VI by around 144%, 38%, 76%, and 88%, respectively. WD and CWF dropped moderately. In K deficient trees, the % changes were lower and negligible in most xylem traits (Figure 8b).

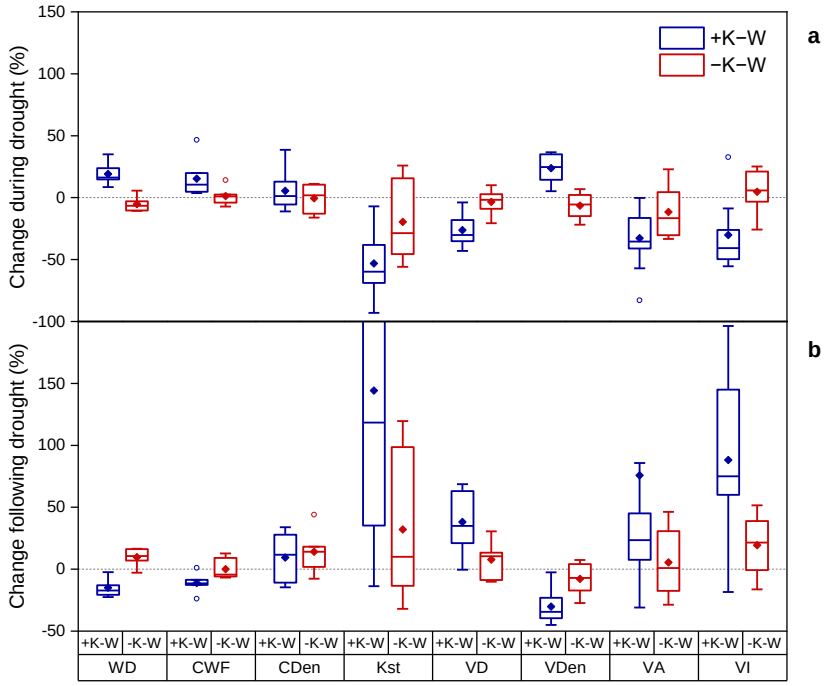

Figure 8. Changes in xylem traits during a drought event of 2014 dry season. Change during drought refers (a) to the percentage increase in the variable's value from rainy season 2014 to drought period (dry season 2014) related to values in rainy season 2014. Change following drought (b) refers to the percentage increase in the variable's value from the drought period to rainy season 2015, related to values in the drought period. Negative values indicate a decrease, while positive values indicate an increase in the value of the respective wood trait variable.

The xylem plasticity in response to severe drought was weakly to moderately correlated to tree basal area. However, the xylem plasticity following drought (in response to rehydration) was not correlated to tree basal area, except for CWF (Table 4).

Table 4. Correlation coefficients between xylem plasticity (percentage of change in xylem trait) and tree basal area, during and following the drought event of 2014 dry season.

Xylem trait	Correlation coefficient	
	During drought	Following drought
WD	0.28	-0.01
CWF	0.64	0.61
CDen	0.46	-0.08
Kst	0.53	0.37
VD	0.63	0.32
VDen	0.10	0.27
VA	0.51	0.04
VI	0.23	0.33

The network correlation showed that relationships between growth rate, xylem traits, and climate were stronger in K-fertilized trees than K-deficient trees. Soil water content was a more critical variable explaining BAI and vessels size changes in K-fertilized trees. Most xylem traits such as CWF, WD, VA, VD, and CDen were highly responsive to the maximum and minimum temperature. In contrast, there was lower responsiveness to temperature

in K-deficient trees. CWF and WD increased with higher temperatures, while VA and VD decreased. Precipitation was more related to BAI, Kst, VD, VA, and VI. Excluding 37% throughfall reduction increased the relationships between growth rate, xylem traits, and climate. VPD and ET were weakly correlated with xylem traits, except in K-deficient trees (Figure 9).

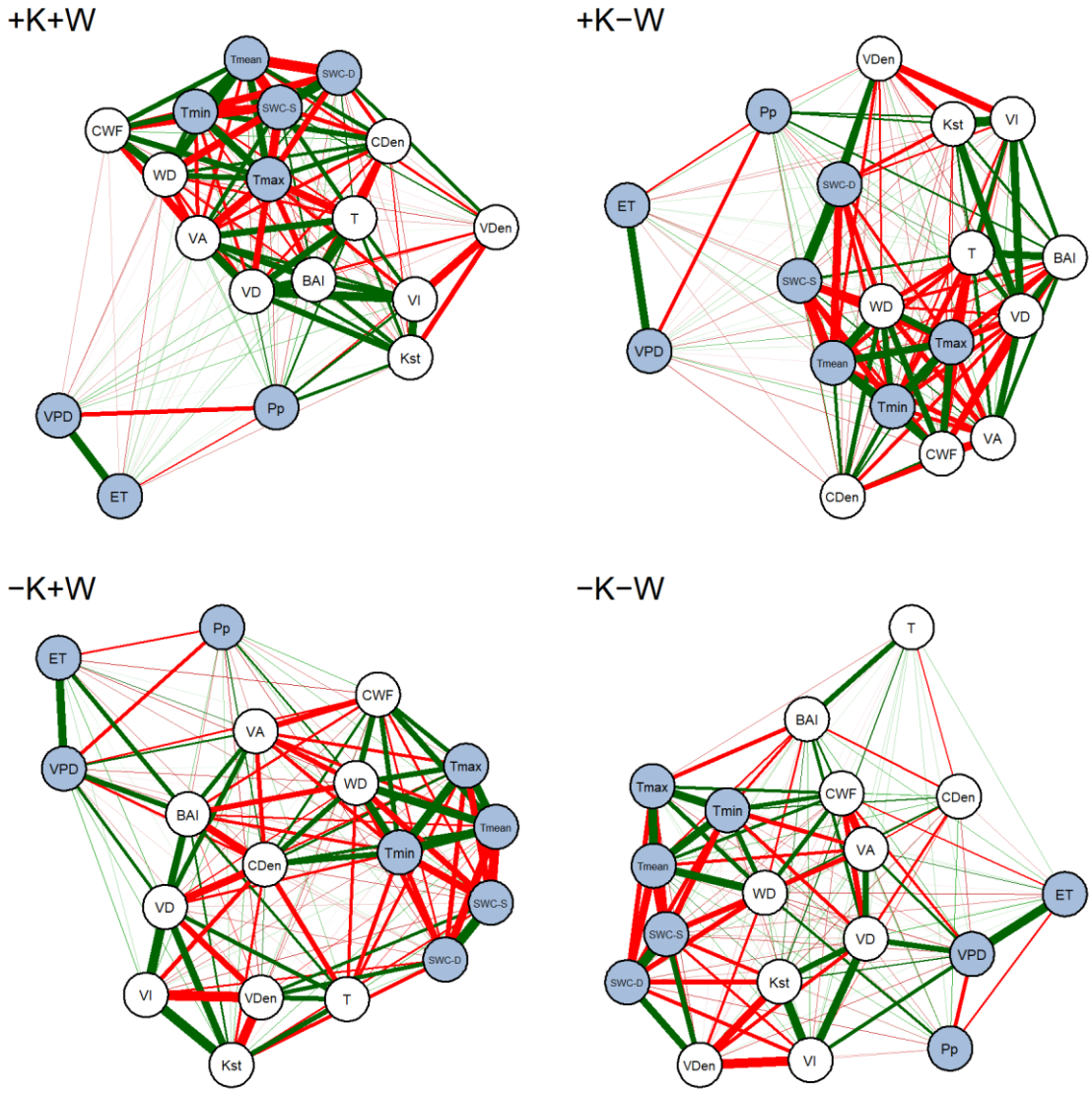

Figure 9. Correlation network between xylem traits of *Eucalyptus grandis* and environmental variables, by treatment, in Itatinga, São Paulo, Brazil. Green edges indicate positive correlation coefficients, and red edges indicate negative correlations coefficients. The color saturation and the width of the edges represent the strength of correlation relative to 1. Correlation from zero to ±0.35 has the smallest edge width. Distance between nodes corresponds very well to the absolute edge weight between those nodes.

2.4. Discussions

Answering the first hypothesis questioned, our results showed that the positive effects of K fertilization on growth rate were constant across age. It highlights the effectiveness of applying a single dose of K in the first year after planting. However, the occurrence of extreme drought during 2014 showed that effects of K are disabled under long-term extreme water deficit. Nevertheless, the sudden BAI in response to any rainfall event (Figure 3) and the highest growth rates following such an extremely dry season in K-fertilized trees demonstrated the high resilience

and recovery ability promoted by K-fertilization (Figure 3b and Figure 4). As a result, during most of the years, K fertilization increased growth until 3-fold.

The Eucalyptus genus is considered among the most resilient trees globally. It is exceptionally well adapted to resist and recover from significant partial tree dieback (Matusick and Fontaine, 2020), to cope with an extreme drought by maintaining high conservation of the integrity of the xylem vascular system, and to have a high ability recovery following drought (Chambi-Legoas et al., 2022). Answering the second hypothesis questioned, the differences in growth patterns between K-fertilized and K-deficient *E. grandis* trees indicated that K fertilization has an additive effect of increasing tree resilience to drought and ability recovery following the drought period.

The significant interaction water regime × fertilization showed 37% throughfall reduction affected tree growth only under K fertilization. However, their negative effects on growth were significant only during the early stage. From 3 years old, K-fertilized trees were not affected by the 37% throughfall reduction. These results can be explained by the high ability of *E. grandis* trees to increase soil exploration and water uptake by enhancing fine root density and distribution in deeper soil profiles. In the same experiment, K-fertilized trees under throughfall reduction reached the water table at a depth of 19 m after 3.5 years, which accounted for a high proportion of the water stock taken up by trees over the dry seasons (Christina et al., 2018, 2017).

The correlations between BAI and transpiration higher in +K than in −K (Figure 6) highlighted the high water consumption of the K-fertilized trees relative to that of the control trees in the deep soil layers (Figure 2). In agreement with Gonçalves et al. (2017), our results demonstrate that precipitation and soil water availability is the main limitation for higher wood production in Eucalyptus plantations in Brazil.

In line with our third hypothesis, K fertilization increases wood plasticity in response to drought. Our results showed that K fertilization multiplied the xylem plasticity in trees by 400% for most wood traits. Reducing 37% throughfall intensified the effects of K on xylem plasticity; however, throughfall reduction per se did not significantly impact most xylem traits, except CWF and CDen. Significant interaction Fertilization × Stand age showed that variation in xylem traits across age was higher in K-fertilized than in K-deficient trees, suggesting that K-fertilization promotes higher inter-annual wood traits variation. It also showed that impacts of K-fertilization on xylem traits are is maintained throughout the full rotation (6 years).

The high xylem plasticity in K fertilized trees was more notorious when extreme drought occurred in the 2014 dry season. In response to these extremely dry conditions, K-fertilized trees suffered greater changes in wood density, fibers, and vessels traits than K-deficient trees. The great changes in vessels, such as the 26% decrease in vessel diameter (VD) and 24% increase in vessel density (VDen), leaded to a high declination in hydraulic conductivity (about 53% of Kst). However, the positive impact was the decrease in vulnerability index (VI) by 30%, indicating a higher capability of withstanding water stress (Carlquist, 1977). In agreement with our results, other anatomical studies also showed high plasticity of the hydraulic architecture in fertilized Eucalyptus trees to water availability in Brazil, which could reduce the risk of embolism (Câmara et al., 2020).

Once such extreme drought ended and a wet period of tree rehydration occurred (2014/2015 rainy season), the high growth recovery was accompanied by a high increase in hydraulic conductivity and vessel area, about 144%, and 76%, respectively recovering or slightly exceeding pre-drought values. This reveals the remarkable capacity of K-fertilized trees for reassembling of xylem vascular system to increase water flow, supporting the high growth recovery following drought (Chambi-Legoas et al., 2022).

The weak or moderate relationships between xylem plasticity and tree basal area (Table 4) showed that xylem plasticity does not depend strongly on tree size in most xylem traits, which suggests that the high xylem

plasticity in K-fertilized trees is not largely due to the high growth rates, but rather to a direct effect of K fertilization. K plays an important osmotic role during cambial cell expansion (Wind et al., 2004), and it has been associated with a significant increase in periclinal cell divisions in the cambium in *Picea abies* (Dünisch and Bauch, 1994) and with an increase in vessels size in poplar (Langer et al., 2002). These previous findings and our results suggest that K is an important nutrient involved in xylogenesis and xylem plasticity.

The effects of high growth rates seem to be more determinant for plasticity of cell wall fraction and vessel diameter. Vessel diameter is considered the most critical anatomical variable related to water transport because hydraulic conductivity is proportional to the radius raised to the fourth power. Therefore, even a small increase or decrease in vessel radius should result in a large change in water conductivity (February et al., 1995). Moreover, their frequency is usually reduced to make more efficient use of resources because of increasing vessels diameter. The high plasticity in vessel diameter and vessel area observed were the main adaptation of K fertilized trees severe water deficit and was controlled by high growth rates promoted by K.

Time-series patterns of SWC reflected that the effective reduction in soil water availability in +K plots was a maximum of 27% and 16% in superficial and deep soil layers, respectively. Although this is a significant reduction in soil water availability, this could not be enough to produce strong water stress on trees, which could explain the negligible or small effects on most xylem traits. Further experiments with greater throughfall reduction are interesting to elucidate the magnitude of long-term severe water deficit impacts on *E. grandis* trees.

Another important finding was the impact of K on wood structure. Our results showed that K fertilization promoted a wood with a higher density of cells per mm^2 (CDen) (meanly fibers, since vessels density were lower in +K) without alteration in cell wall fraction (CWF), i.e., the volume occupied by cell walls or the void volume (porosity) is not affected by K fertilization regardless higher cells density. This structure explains the non-significant effects of K fertilization on wood density over 6 years.

The network correlation allowed to identify the linking between growth rate, xylem traits, and climate. The highest relationships in K-fertilized trees indicated that K fertilization increase responsiveness to climatic variation in *E. grandis* trees. BAI and xylem traits changes were more correlated to soil water content (SWC) than to precipitation. Also, SWC was not highly correlated with precipitation. These results indicate that precipitation does not recharge soil water effectively and simultaneously or that other factors such as root system increased water uptake for trees even under lack of precipitation. Low correlation between SWC and precipitation has been related to both the precipitation spectrum and the time scale of soil moisture retention, suggesting the existence of lagged correlations of precipitation with soil moisture or hydraulic redistribution by trees on soil layers (Sehler et al., 2019; Wei et al., 2008). Thus, measuring SWC rather than precipitation could be a more effective method to evaluate tree responsiveness to water availability.

Minimum and maximum temperature were also important variables affecting xylem traits and growth rate in K-fertilized trees. Mainly, CWF and WD increased with higher temperatures, which could be related to the negative influence of temperature on growth rates. Precipitation and temperature have been reported to strongly affect tree growth in adjacent experiments near our study area (Campoe et al., 2016; Sette Jr et al., 2010). It has been observed in *E. globulus* on a daily time scale (Downes et al., 1999). Temperature is an important meteorological variable involved in biochemical processes, respiration, and stomatal conductance (Lin 2012). In addition, maximum temperature negatively influences stem growth by increasing respiration, reducing stomatal conductance to mitigate a higher transpiration demand, and reducing photosynthesis (Schippers et al., 2015). CWF and WD decrease with

SWC, which was related to the impacts on growth rate. The 37% throughfall reduction intensified the relationships between xylem traits and climate.

2.5. Conclusions

The effects of K fertilization increasing growth rate were maintained over the full rotation, highlighting the effectiveness of applying a single dose of K in the first year after planting. However, these effects depended on water availability, increasing BAI by 3-fold in well-watered seasons but stopping growth in severe seasonal drought periods. Reducing 37% throughfall in plots affected growth only in K-fertilized trees. However, their negative effects on growth only lasted until 2.5 years after planting.

K fertilization increased xylem traits plasticity to precipitation variation. Large trees were not necessarily more plastic, indicating that the effects of K, increasing xylem plasticity, were not due to the high growth rate. Main changes occurred in vessel traits, declining hydraulic conductivity by 53% in severe drought but recovering after drought. High plasticity also was observed for WD, CWF, CDen, and VI. The growth patterns and high xylem plasticity in response to drought of K- fertilized trees suggest an additive effect of K to increase resilience and recovery ability for growth following drought.

Soil water availability and minimum and maximum temperature were the most important environmental variables affecting the xylem traits and growth rate of *E. grandis* trees. K fertilization increased responsiveness to climatic variation.

References

Asensio, V., Domec, J.C., Nouvellon, Y., Laclau, J.P., Bouillet, J.P., Jordan-Meille, L., Lavres, J., Rojas, J.D., Guillemot, J., Abreu-Junior, C.H., 2020. Potassium fertilization increases hydraulic redistribution and water use efficiency for stemwood production in Eucalyptus grandis plantations. Environ. Exp. Bot. 176, 104085. https://doi.org/10.1016/j.envexpbot.2020.104085

Battie-Laclau, P., Delgado-Rojas, J.S., Christina, M., Nouvellon, Y., Bouillet, J.-P., Piccolo, M. de C., Moreira, M.Z., Gonçalves, J.L. de M., Roupsard, O., Laclau, J.-P., 2016. Potassium fertilization increases water-use efficiency for stem biomass production without affecting intrinsic water-use efficiency in Eucalyptus grandis plantations. For. Ecol. Manage. 364, 77–89. https://doi.org/10.1016/j.foreco.2016.01.004

Battie-Laclau, P., Laclau, J.P., Domec, J.C., Christina, M., Bouillet, J.P., de Cassia Piccolo, M., de Moraes Gonçalves, J.L., Moreira, R.M., Krusche, A.V., Bouvet, J.M., Nouvellon, Y., 2014. Effects of potassium and sodium supply on drought-adaptive mechanisms in Eucalyptus grandis plantations. New Phytol. 203, 401–413. https://doi.org/10.1111/nph.12810

Battie-Laclau, P., Laclau, J.P., Piccolo, M. de C., Arenque, B.C., Beri, C., Mietton, L., Muniz, M.R.A., Jordan-Meille, L., Buckeridge, M.S., Nouvellon, Y., Ranger, J., Bouillet, J.P., 2013. Influence of potassium and sodium nutrition on leaf area components in Eucalyptus grandis trees. Plant Soil 371, 19–35. https://doi.org/10.1007/s11104-013-1663-7

Câmara, A.P., Vidaurre, G.B., Oliveira, J.C.L., de Toledo Picoli, E.A., Almeida, M.N.F., Roque, R.M., Tomazello Filho, M., Souza, H.J.P., Oliveira, T.R., Campoe, O.C., 2020. Changes in hydraulic architecture across a water availability gradient for two contrasting commercial Eucalyptus clones. For. Ecol. Manage. 474, 118380. https://doi.org/10.1016/j.foreco.2020.118380

Campelo, F., Mayer, K., Grabner, M., 2019. xRing—An R package to identify and measure tree-ring features using X-ray microdensity profiles. Dendrochronologia 53, 17–21. https://doi.org/10.1016/j.dendro.2018.11.002

Campinhos, Jr., E., 1999. Sustainable plantations of high-yield shape Eucalyptus trees for production of fiber: the Aracruz case. New For. 17, 129–143. https://doi.org/10.1023/A:1006562225915

Campoe, O.C., Munhoz, J.S.B., Alvares, C.A., Carneiro, R.L., de Mattos, E.M., Ferez, A.P.C., Stape, J.L., 2016. Meteorological seasonality affecting individual tree growth in forest plantations in Brazil. For. Ecol. Manage. 380, 149–160. https://doi.org/10.1016/j.foreco.2016.08.048

Carlquist, S., 1977. Ecological Factors in Wood Evolution: A Floristic Approach. Am. J. Bot. 64, 887. https://doi.org/10.2307/2442382

Chambi-Legoas, R., Chaix, G., Tomazello-Filho, M., 2020. Effects of potassium/sodium fertilization and throughfall exclusion on growth patterns of Eucalyptus grandis W. Hill ex Maiden during extreme drought periods. New For. 51, 21–40. https://doi.org/10.1007/s11056-019-09716-x

Chambi-Legoas, R., Tomazello-Filho, M., Guedes, F.T.P., Chaix, G., 2022. High growth recovery ability of Eucalyptus grandis trees following a 3-year period of 80% throughfall reduction. For. Ecol. Manage. 503, 119766. https://doi.org/10.1016/J.FORECO.2021.119766

Christina, M., le Maire, G., Nouvellon, Y., Vezy, R., Bordon, B., Battie-Laclau, P., Gonçalves, J.L.M., Delgado-Rojas, J.S., Bouillet, J.P., Laclau, J.P., 2018. Simulating the effects of different potassium and water supply regimes on soil water content and water table depth over a rotation of a tropical Eucalyptus grandis plantation. For. Ecol. Manage. 418, 4–14. https://doi.org/10.1016/j.foreco.2017.12.048

Christina, M., Nouvellon, Y., Laclau, J.P., Stape, J.L., Bouillet, J.P., Lambais, G.R., le Maire, G., 2017. Importance of deep water uptake in tropical eucalypt forest. Funct. Ecol. 31, 509–519. https://doi.org/10.1111/1365-2435.12727

Coelho, C.A.S., de Oliveira, C.P., Ambrizzi, T., Reboita, M.S., Carpenedo, C.B., Campos, J.L.P.S., Tomaziello, A.C.N., Pampuch, L.A., Custódio, M. de S., Dutra, L.M.M., Da Rocha, R.P., Rehbein, A., 2016. The 2014 southeast Brazil austral summer drought: regional scale mechanisms and teleconnections. Clim. Dyn. 46, 3737–3752. https://doi.org/10.1007/s00382-015-2800-1

Deslauriers, A., Fonti, P., Rossi, S., Rathgeber, C.B.K., Gričar, J., 2017. Ecophysiology and Plasticity of Wood and Phloem Formation, in: Amoroso, M., Daniels, L., Baker, P., Camarero, J. (Eds.), Dendroecology. Ecological Studies (Analysis and Synthesis). Springer, pp. 13–33. https://doi.org/10.1007/978-3-319-61669-8_2

Downes, G., Beadle, C., Worledge, D., 1999. Daily stem growth patterns in irrigated Eucalyptus globulus and E. nitens in relation to climate. Trees - Struct. Funct. 14, 102–111. https://doi.org/10.1007/s004680050214

Dünisch, O., Bauch, J., 1994. Influence of mineral elements on wood formation of old growth spruce (picea abies [L.] karst.). Holzforschung 48, 5–14. https://doi.org/10.1515/hfsg.1994.48.s1.5

February, E.C., Stock, W.D., Bond, W.J., Le Roux, D.J., 1995. Relationships between water availability and selected vessel characteristics in Eucalyptus grandis and two hybrids. IAWA J. 16, 269–276. https://doi.org/10.1163/22941932-90001410

Fichot, R., Barigah, T.S., Chamaillard, S., Le Thiec, D., Laurans, F., Cochard, H., Brignolas, F., 2010. Common trade-offs between xylem resistance to cavitation and other physiological traits do not hold among unrelated Populus deltoides × Populus nigra hybrids. Plant, Cell Environ. 33, 1553–1568. https://doi.org/10.1111/j.1365-3040.2010.02164.x

Freitas, P.D.C. e, Sette Jr, C.R., Castro, V.R. De, Chaix, G., Laclau, J.P., Tomazello Filho, M., 2015. Efeito da disponibilidade hídrica e da aplicação de potássio e sodio nas característica anatômicas do lenho juvenil de Eucalyptus grandis. Árvore 39, 405–416. https://doi.org/10.1590/0100-67622015000200020

Fuller, L.G. (School of F. and W.R.B.V., Cattelino, P.J., Reed, D.D., 1988. Correction equations for dendrometer band measurements of five hardwood species. North. J. Appl. For.

Gonçalves, J.L. de M., Alvares, C.A., Higa, A.R., Silva, L.D., Alfenas, A.C., Stahl, J., Ferraz, S.F. de B., Lima, W. de P., Brancalion, P.H.S., Hubner, A., Bouillet, J.-P.D., Nouvellon, Y., Epron, D., 2013. Integrating genetic and silvicultural strategies to minimize abiotic and biotic constraints in Brazilian eucalypt plantations. For. Ecol. Manage. 301, 6–27. https://doi.org/10.1016/j.foreco.2012.12.030

Gonçalves, J.L.M., Alvares, C.A., Rocha, J.H.T., Brandani, C.B., Hakamada, R., 2017. Eucalypt plantation management in regions with water stress. South. For. 79, 169–183. https://doi.org/10.2989/20702620.2016.1255415

IBÁ, 2020. Annual Report 2020. São Paulo.

Johansen, D.A., 1940. Plant microtechnique. McGraw-Hill Publishing Company, Ltd., London.

Keeland, B.D., Sharitz, R.R., 1993. Accuracy of tree growth measurements using dendrometer bands. Can. J. For. Res. 23, 2454–2457. https://doi.org/10.1139/x93-304

Laclau, J.P., Almeida, J.C.R., Gonalves, J.L.M., Saint-Andr, L., Ventura, M., Ranger, J., Moreira, R.M., Nouvellon, Y., 2009. Influence of nitrogen and potassium fertilization on leaf lifespan and allocation of above-ground growth in Eucalyptus plantations. Tree Physiol. 29, 111–124. https://doi.org/10.1093/treephys/tpn010

Langer, K., Ache, P., Geiger, D., Stinzing, A., Arend, M., Wind, C., Regan, S., Fromm, J., Hedrich, R., 2002. Poplar potassium transporters capable of controlling K+ homeostasis and K+-dependent xylogenesis. Plant J. 32, 997–1009. https://doi.org/10.1046/J.1365-313X.2002.01487.X

Matusick, G., Fontaine, J., 2020. Causes of large-scale eucalyptus tree dieback and mortality : research priorities. A report for the NSW Natural Resources Commission. WA.

Nobre, C.A., Marengo, J.A., Seluchi, M.E., Cuartas, A., Alves, L.M., 2016. Some Characteristics and Impacts of the Drought and Water Crisis in Southeastern Brazil during 2014 and 2015 Some Characteristics and Impacts of the Drought and Water Crisis in Southeastern Brazil during 2014 and 2015. J. od Water Resour. Prot. 8, 252–262. https://doi.org/10.4236/jwarp.2016.82022

Schippers, P., Sterck, F., Vlam, M., Zuidema, P.A., 2015. Tree growth variation in the tropical forest: understanding effects of temperature, rainfall and CO 2. Glob. Chang. Biol. 21, 2749–2761. https://doi.org/10.1111/gcb.12877

Schneider, C.A., Rasband, W.S., Eliceiri, K.W., 2012. NIH Image to ImageJ: 25 years of image analysis. Nat. Methods 9, 671–675. https://doi.org/10.1038/nmeth.2089

Sehler, R., Li, J., Reager, J., Ye, H., 2019. Investigating Relationship Between Soil Moisture and Precipitation Globally Using Remote Sensing Observations. J. Contemp. Water Res. Educ. 168, 106–118. https://doi.org/10.1111/J.1936-704X.2019.03324.X

Sette Jr, C.R., Tomazello Filho, M., Dias, C.T. dos S., Laclau, J.P., 2010. Crescimento em diâmetro do tronco das árvores de Eucalyptus grandis W. Hill. ex. Maiden e relação com as variáveis climáticas e fertilização mineral. Rev. Árvore 34, 979–990. https://doi.org/10.1590/S0100-67622010000600003

Stape, J.L., Binkley, D., Ryan, M.G., Fonseca, S., Loos, R.A., Takahashi, E.N., Silva, C.R., Silva, S.R., Hakamada, R.E., Ferreira, J.M. de A., Lima, A.M.N., Gava, J.L., Leite, F.P., Andrade, H.B., Alves, J.M., Silva, G.G.C., Azevedo, M.R., 2010. The Brazil Eucalyptus Potential Productivity Project: Influence of water, nutrients and stand uniformity on wood production. For. Ecol. Manage. 259, 1684–1694. https://doi.org/10.1016/j.foreco.2010.01.012

Wei, J., Dickinson, R.E., Chen, H., 2008. A Negative Soil Moisture–Precipitation Relationship and Its Causes. J. Hydrometeorol. 9, 1364–1376. https://doi.org/10.1175/2008JHM955.1

Wind, C., Arend, M., Fromm, J., 2004. Potassium-Dependent Cambial Growth in Poplar. Plant Biol. 6, 30–37. https://doi.org/10.1055/s-2004-815738

Wu, Z., Dijkstra, P., Koch, G.W., Peñuelas, J., Hungate, B.A., 2011. Responses of terrestrial ecosystems to temperature and precipitation change: A meta-analysis of experimental manipulation. Glob. Chang. Biol. 17, 927–942. https://doi.org/10.1111/j.1365-2486.2010.02302.x

3. HIGH GROWTH RECOVERY ABILITY OF *Eucalyptus grandis* TREES FOLLOWING A 3-YEAR PERIOD OF 80% THROUGHFALL REDUCTION

Published in the journal: Forest Ecology and Management, v. 503, p. 119766, 2022

Roger Chambi-Legoas [1, 4]*, Mario Tomazello-Filho [1], Fernanda Trisltz Perassolo Guedes [1], Gilles Chaix [1, 2, 3]

[1] Universidade de São Paulo, ESALQ, Departamento de Ciências Florestais, 13418-900, Piracicaba, SP, Brazil

[2] CIRAD, UMR AGAP Institut, F-34398 Montpellier, France

[3] UMR AGAP Institut, Univ Montpellier, CIRAD, INRAE, Institut Agro, F-34398 Montpellier, France

[4] Universidad Nacional Autónoma de Chota, Escuela Profesional de Ingeniería Forestal y Ambiental, Chota, Perú

*Corresponding author: rchambilegoas@gmail.com

Abstract

Eucalyptus plantations are already planted in - or expanding to - water-limited regions with a high risk of severe drought. In future drier and more variable climate including extreme events, the ability of trees to recover after severe droughts emerges as a crucial for the sustainability of forest plantations.An original experiment involving 80% reduction in throughfall was set up in Brazil to gain insight into the responses of *Eucalyptus grandis* trees to prolonged (3-year) extreme water deficit and the ability of this species to recover following water stress. Our study focused on the changes in basal area, stem radius, and total height measured by high-temporal resolution dendrometers and periodical surveys of trees affected by 80% throughfall reduction (treatment group) and in a control group. The differences in basal area, stem radius, and total height growth rate were compared between groups over (i) 37 months of 80% throughfall reduction and (ii) 31 months following the end of 80% throughfall reduction. The correlations among growth rates, stem radius fluctuations, and meteorological variables in each group were determined to gain insights into the trees' responses to environmental conditions and stem water status.The 80% reduction in throughfall over 3 years significantly reduced tree growth rates by 73% in basal area and 95% in total height. However, under normal water availability following throughfall reduction, the basal area growth rate of water-stressed trees was 97% higher than that of the control trees while total height growth rate was only 8% higher. Despite the severe water stress, no tree mortality was observed. Trees recovered 51% of their basal area over the 31-month recovery period. In contrast, only 5% of total height was recovered.In the treatment group, rapid responses to variation in rainfall events were observed during the 80% throughfall reduction period. Also, correlations between stem radius fluctuations and vapor pressure deficit indicate increased transpiration following the end of throughfall reduction. These relationships indicate high conservation of the integrity of the xylem vascular system over the 3 years of 80% throughfall reduction, a key factor in the increased resilience of the trees. In the absence of tree mortality, our results suggest the 80% throughfall reduction had a severe impact on tree growth but demonstrate great recovery ability of *E. grandis* trees in basal area growth following such a severe water deficit.

Keywords: Drought; Climate change; Dendrometer; Forest management; Tree resilience; Xylem vascular system.

3.1. Introduction

Climate change scenarios predict a rise in global temperature and changes in precipitation amounts and patterns worldwide (IPCC, 2021). A decrease in precipitation and aggravation of the intensity and frequency of seasonal dry periods are expected in most subtropical regions (Lee et al., 2021). Forest plantation for wood production occupied 131.1 million hectares in 2020 (FAO, 2020), of which about 20 million hectares (15%) were *Eucalyptus* species (Carle and Holmgren, 2009). Due to their rapid growth, high wood yield, easy propagation, and

wide genetic variation, *Eucalyptus* plantations are rapidly expanding worldwide for wood supply in different zones (FAO, 2020), many of which are water-limited areas under the risk of severe drought (Gonçalves et al., 2017). Episodes of drought-induced tree mortality have been reported for *Eucalyptus* in some areas (Allen et al., 2010; Gonçalves et al., 2017).

In regions where the productivity of *Eucalyptus* plantation is strongly limited by rainfall amount, including Brazil, the effects of water deficit on tree growth and mortality are one of the main concerns (Binkley et al., 2010; Stape et al., 2010). *Eucalyptus* responses to water stress have been addressed in some studies. Diverse changes: reduced stomatal conductance and inhibition of cell expansion resulting in reduced carbon assimilation leading to slower growth rates have been reported depending on the duration and intensity of the water deficit (Correia et al., 2014; Costa E Silva et al., 2004). If water stress persists, plants can modify carbon partitioning in favor of root system development (Costa E Silva et al., 2004; Li et al., 2000) or even enable access to water in deeper soil layers (Battie-Laclau et al., 2014; Christina et al., 2018). Nevertheless, trees conserve high water use efficiency (Li et al., 2000). As water stress becomes more persistent and increases in severity, the risk of death caused by hydraulic failure or combined with carbon starvation is high, and maintaining the integrity of the xylem vascular system and a positive carbon balance is critical to avoid death (McDowell et al., 2008; Sevanto et al., 2014).

Although the growth response to water deficit has been well characterized for *Eucalyptus* species, studies of the growth recovery ability following water stress are rare. In contexts where drought is inevitable, tree resilience to severe water stress is crucial for the sustainability of forest plantations. Drought recovery capacity has been described in other species, including Scots pine and black pine, both of which showed limited resiliency capacity to drought, were unable to recover their previous growth rates, and susceptible to death (Guada et al., 2016). The limitation of growth recovery of Scots pine was related to the number of green leaves and the levels of carbon reserves after drought. The depletion in carbon reserves resulting from reduced photosynthetic tissue led to tree mortality. In surviving trees, severe drought leads to delayed recovery (Galiano et al., 2011). A decline in natural forests after severe drought has been observed in Borneo, Indonesia (Nishimua et al., 2007). In contrast, *Eucalyptus globulus* clone seedlings growing in plastic containers subjected to water limitation revealed high recovery ability when water again became available, overcompensation of CO2, and greater growth (Correia et al., 2014). However to date, no studies have measured the resilience of *Eucalyptus* trees in field conditions, and responses may differ considerably due to increased physiological activity or to the exposure of the xylem hydraulic system to cavitation.

Prolonged water deficit conditions have been duplicated in throughfall exclusion experiments to better understand the potential impacts of severe droughts on trees (Wu et al., 2011). In planted *Eucalyptus* forests, two experiments excluding 37% and 33% throughfall were conducted that had little effect on the tree growth rate (Battie-Laclau et al., 2016; Binkley et al., 2017). Trees were shown to be able to reduce their basal area growth by 17% without mortality over a 6-year period of 37% throughfall reduction (Chambi-Legoas et al., 2020), while another study showed that stem volume decreased by around 16% under 30% throughfall reduction (Binkley et al., 2020). In contrast, *Eucalyptus* growth recovery capacity after water deficit relief has not been assessed. In a context of variability and unpredictability of precipitation scenarios, more water availability experiments are needed at different levels of rainfall reduction to elucidate the impacts of a wide range of possible scenarios (Wu et al., 2011).

In forest research, dendrometers have been widely used to monitor changes in stem size (Drew and Downes, 2009) to identify long-term growth patterns as a function of short-term environmental variability. Temporally high-resolution automatic dendrometers provide the daily patterns of stem variation needed to study cambial activity and tree water status and help identify periods of cell division and plant response to water deficit.

The fluctuations in stem radius measured by automatic dendrometers are known to be due to elastic movements caused by reversible changes in bark water use controlled by xylem water potential and by fluctuations related to growth, which incorporates both irreversible growth and elastic changes in bark osmotic content (Chan et al., 2016; Mencuccini et al., 2017). Moreover, reversible fluctuations in stem radius are mainly determined by the course of transpiration (Zweifel et al., 2001). Since environmental variables such as vapor pressure deficit and temperature drive tree transpiration, linking fluctuations in stem radius and environmental variables can provide insights into tree water use.

In this framework, we ask if *E. grandis* trees will cope with a long-term 80% water deficit and, if so, to what extent they can recover over time following such a severe water deficit. Proportionally to the previous results with lower water deficits in *Eucalyptus* described above, we hypothesize that *E. grandis* trees should stop growing under 80% throughfall reduction. Furthermore, the high growth recovery after rehydration showed by *Eucalyptus* seedlings and the high water use efficiency of *E. grandis* trees could suggest a remarkable resilience following the end of throughfall reduction, capable of rapidly regaining growth.

To address these issues, an original experiment was conducted to reproduce severe drought conditions in *E. grandis* plantation by 80% throughfall reduction in plots located in Itatinga, São Paulo, Brazil. The aim was to evaluate growth responses to three years of 80% throughfall reduction and tree recovery ability for 2.6 years following the end of the throughfall reduction by measuring stem girth using temporally high-resolution dendrometers and by monitoring tree height. We also aimed to identify correlations among growth rates, stem radius fluctuations, and meteorological variables to gain insights into the responsiveness to environmental conditions and the stem water status of trees during and after a severe water deficit.

3.2. Material and Methods

3.2.1. Study area

The study was conducted at the Itatinga Experimental Station of the University of São Paulo, São Paulo State, Brazil (23°02'S, 48°38'W, 850 m a.s.l.). Mean annual rainfall over the last 14 years was 1 730 mm, and the mean annual temperature was 20 °C. The soils are deep ferralsols (>15 m) with 14-23% clay content developed on Cretaceous sandstone, Marılia formation, Bauru group (Laclau et al., 2009).

3.2.2. Field experiment

The study was carried out in an existing plantation of *E. grandis* half-sib progeny, planted in July 2012, under 3m x 2m spacing and with standard fertilization consisting of 335 kg ha^{-1} of KCl, 75 kg ha^{-1} of P_2O_5, 80 kg ha^{-1} of N ($NH_4(SO_4)_2$), 20 kg ha^{-1} of FTE BR-12 (micronutrient source), and 2 000 kg ha^{-1} of dolomitic limestone. At the beginning of our study, the plants were 2.4 years old.

The experimental design included two groups: control (C) and treatment (T), assessed in three *steps* .

- **The control group (C)** comprised trees growing under hydric conditions that remained normal over time (Figure 1b).

– **The treatment group (T)** comprised trees subjected to 80% throughfall reduction for 37 months; throughfall reduction was then stopped, and their recovery ability was monitored for the following 31 months. The growth of the trees in the T group was monitored in three *Step*s:

- ***Step 0:*** November 2014 to August 2015. Period of normal water conditions before the beginning of the 80% throughfall reduction.
- ***Step* 1:** September 2015 to October 2018 (37 months). Period of 80% throughfall reduction in T trees. The 80% throughfall reduction was achieved by mounting transparent plastic sheets on wooden frames that covered 80% of the plot area. The highest point was 1.6 m decreasing to 0.5 m (Figure 1a). Water flowed by gravity from the plastic sheets into a collection channel that carried it away from the experiment. The throughfall reduction device was removed in October 2018.
- ***Step* 2:** November 2018 to May 2021 (31 months). Period of normal water conditions following removal of the throughfall reduction device. The growth recovery of the trees was monitored following the severe water stress.

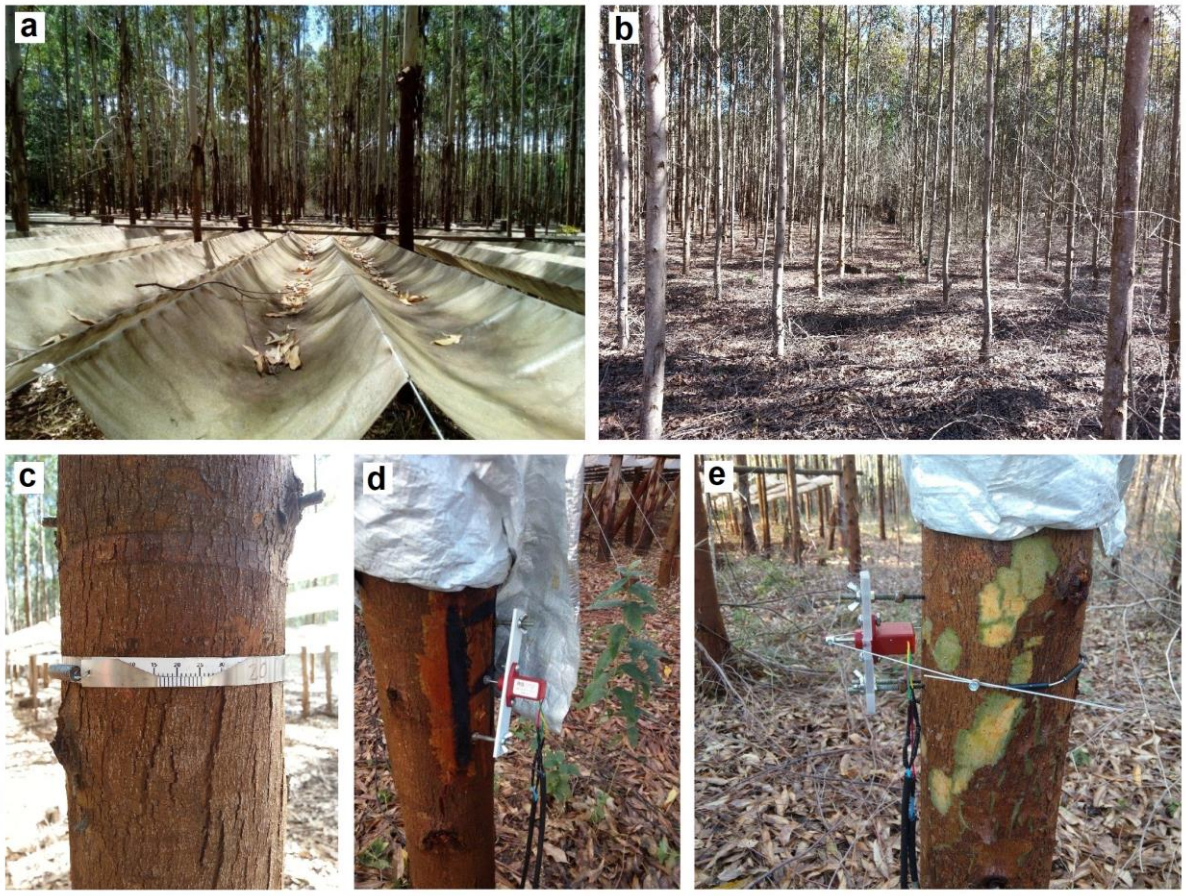

Figure 1. 80% throughfall reduction experiment conducted at the Itatinga Experimental Station of the University of São Paulo in Brazil 4 years after *Eucalyptus grandis* trees were planted. Throughfall reduction was achieved by covering 80% of the plot with plastic sheets (a). Control plot with no throughfall reduction (b). Band dendrometer (c). Automatic dendrometers of point (d) and girth (e).

3.3.3. Growth monitoring in basal area and total height

Basal area growth was monitored at fortnightly intervals (14-day) from November 2014 to May 2021 using band dendrometers installed on 10 trees by group (Figure 1c). Band dendrometers readings provided circumference increments at breast height (CBH) that were converted into basal area increments (BAI). The first measurements were recorded one month after the band dendrometers were installed to avoid underestimation of CBH owing to initial slack in tree boles (Fuller et al., 1988; Keeland and Sharitz, 1993). In addition, CBH was measured directly with a tape measure at 6-month intervals to check and correct possible underestimations by the band dendrometers. The total height of the trees was measured in four surveys of all the trees in the plots covered by *Step 1* and *Step 2* from May 2016 to January 2021.

3.3.4. Stem radius variation monitoring

Variations in stem radius were measured at 30-minute intervals from November 2016 to October 2020 using automatic point and girth dendrometers installed at breast height in 10 trees per group (Figure 1d and Figure 1e). The automatic dendrometers consisted of a linear potentiometer (RS Components SAS, LM10 Series, Beauvais, France) mounted in a carbon fiber frame fixed to the stem by three stainless steel thread rods inserted into the inactive heartwood and shielded from direct sunlight and potential damage by weather by aluminum foil. In the point dendrometer, a weight supported on the sensing rod of the potentiometer presses lightly against the tree stem. As the stem expands and contracts, the sensing rod transmits the movements to the potentiometer. Similarly, in the girth dendrometer, a stainless-steel cable is attached to half of the stem circumference and passed into a metal cylindrical piece supported on the shaft of the sensing rod of the potentiometer. The cable is joined at its ends and fitted to the stem with a grub screw nipple. The cable is wrapped in strips of Teflon to reduce friction with the bark. As the stem expands and contracts, the stainless-steel cable transmits the movements to the potentiometer. Changes in resistance of the potentiometer are linearly related to the changes in the displacement of the body. The typical output coefficient of the potentiometer was about 523 mV mm^{-1}. Potentiometer measurements were automatically recorded with a data logger (Model CR1000, Campbell Scientific, Logan, UT).

The variations in stem radius recorded at 30-minute intervals revealed cyclic patterns of shrinking and swelling of the stem (*stem cycle*) covering approximately 24 h. We used the *stem cycle* approach (Deslauriers et al., 2007; Downes et al., 1999; Drew and Downes, 2009) to extract the variations in stem radius recorded by the dendrometers by dividing the cycle into two phases (Figure 2):

- Contraction phase, the period between the morning maximum and afternoon minimum
- Expansion phase, the total period from the minimum to the following maximum

The maximum daily shrinkage (MDS) and the stem radius increment (ΔR) were calculated for each cycle. The MDS is the amplitude of the contraction phase that accounts for most of the reversible change in the stem radius driven by tree water status. ΔR was calculated as the difference between the maximum expansion of the current radius and the maximum expansion of the previous radius. ΔR accounted for most of the irreversible change in stem radius (radial growth). When the maximum value of the previous cycle was reached, a +ΔR was calculated, otherwise a –ΔR. MDS and ΔR were extracted using a SAS routine adapted from Deslauriers et al. (2011).

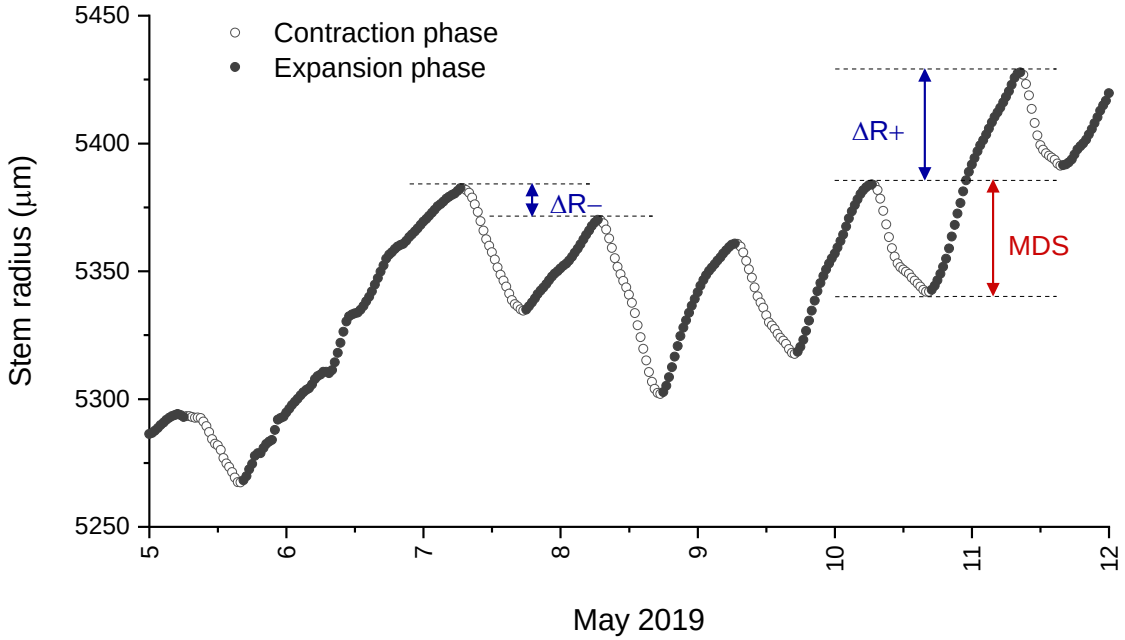

Figure 2. The stem cycle is divided into two distinct phases: a contraction phase and an expansion phase. The contraction phase is the period between the morning maximum and afternoon minimum, and the expansion phase is the total period from the current minimum to the following maximum. +ΔR: Positive stem radius increment. –ΔR: Negative stem radius increment. MDS: Maximum daily shrinkage.

3.3.5. Meteorological data

Rainfall, mean air temperature (Tmean), minimum air temperature (Tmin), maximum air temperature (Tmax), vapor pressure deficit (VPD), and potential evapotranspiration (ET) data were collected at 30-minute intervals from an automatic weather station installed in a tower 20 m above ground level, located at a distance of 50 m from the experiment. The rainfall in T plots during *Step 1* was equivalent to 20% of the total rainfall recorded since throughfall reduction device covered 80% of the area of the plots.

Two distinct seasons can be observed (Obregón et al., 2014): a rainy season (October to March) with mean total rainfall of about 1 170 mm and mean temperature of 21.7 °C, and a dry season (April to September) with less rainfall (531 mm) and lower temperatures (about 18 °C) (Figure 3 and Table 1). In July and August, monthly rainfall is usually less than 50 mm. Severe drought conditions occurred during the first four months of 2018 dry season, with monthly rainfall < 35 mm. During application of 80% throughfall reduction in the T plots, monthly rainfall ranged from 15.5 mm in the driest seasons to 59 mm in the wettest seasons (Table 1).

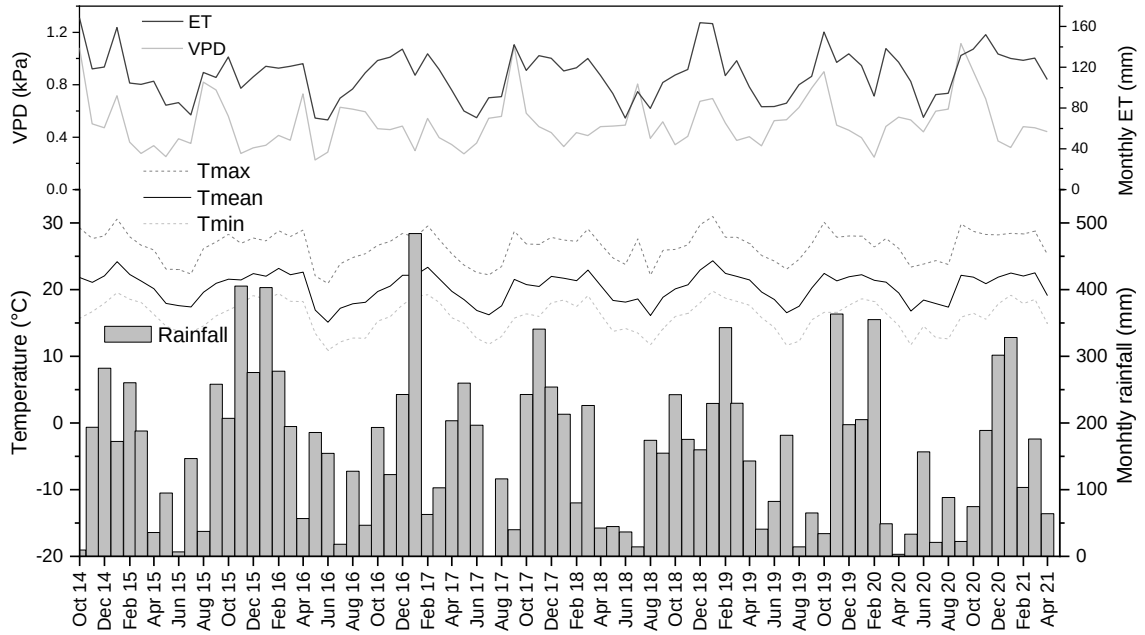

Figure 3. Monthly variations in vapor pressure deficit (VPD), evapotranspiration (ET), monthly rainfall, mean air temperature (Tmean), minimum air temperature (Tmin), and maximum air temperature (Tmax) (b) from October 2014 to July 2019, at Itatinga Experimental Station, Itatinga, São Paulo, Brazil.

Table 1. The three *Steps* of growth monitoring showing the duration, stand age, and rainfall in control (C) and treatment (T) plots in the rainy and "dry" seasons. Numbers in bold show the low rainfall values in the treatment (T) plots resulting from the 80% throughfall reduction applied in *Step* 1.

Step	Season	Date	Stand age (years)	Total rainfall (mm)	
				C plots	T plots
0	Rainy 2014/2015	Oct 2014 - Mar 2015	2	1106	1106
	"Dry" 2015	Apr 2015 - Sep 2015	2	580	580
1	Rainy 2015/2016	Oct 2015 - Mar 2016	3	1763	**353**
	"Dry" 2016	Apr 2016 - Sep 2016	3	589	**118**
	Rainy 2016/2017	Oct 2016 - Mar 2017	4	1209	**242**
	"Dry" 2017	Apr 2017 - Sep 2017	4	816	**163**
	Rainy 2017/2018	Oct 2017 - Mar 2018	5	1357	**271**
	"Dry" 2018	Apr 2018 - Sep 2018	5	467	**93**
2	Rainy 2018/2019	Oct 2018 - Mar 2019	6	1380	1380
	"Dry" 2019	Apr 2019 - Sep 2019	6	527	527
	Rainy 2019/2020	Oct 2019 - Mar 2020	7	1204	1204
	"Dry" 2020	Apr 2020 - Sep 2020	7	325	325
	Rainy 2020/2021	Oct 2020 - Mar 2021	8	1058	1058

Meteorological data were organized in 14-day periods to match band dendrometer data. Daily rainfall data were summed to obtain cumulative rainfall for 6-month periods, the rainy season (October to March) and the dry season (April to September) for each assessment year. To assess daily radial growth, meteorological data were coupled with the respective phases of the stem cycle based on the beginning, end, and duration of each phase, using a SAS protocol adapted from Deslauriers et al. (2011).

3.3.6. Data analysis

The mixed model for repeated measures was used to assess the effects of *Group, Stand age, season* and their interactions on cumulative BAI in each *Step*. *Season* × *Stand age* was considered as a repeated-measures factor. Pearson correlation analysis was used to assess the individual relationships between meteorological variables and fortnightly BAI by *Group*, S*eason,* and *Step*.

Multiple regressions per *Group* for each *Step* were used to estimate BAI growth rate as a function of the meteorological variables and to investigate whether the influence of meteorological variability on tree growth differed between *Groups* and *Steps*. Regressions were performed using the MIXED procedure (linear mixed model) with a repeated-measure factor (*date*) and random factor (*tree*). We used the autocorrelation function (ACF) test to determine how many lag periods affect the measured BAI based on the ACF-lag plot. We found a clear time auto-correlation at lag 1, and incorporated it in the regression model. Finally, among all possible candidate linear regression models, the best one was chosen based on the AIC value.

ΔR values were grouped in monthly periods to eliminate the high oscillation of stem radius in daily series (Deslauriers et al., 2007; Giovannelli et al., 2007). A boxplot with ΔR grouped at monthly intervals was drawn separately for each *Step* and *Group*. A Student's T-test was used to assess whether the ΔR in a specific monthly period differed from zero ($\mu=0$). The relationships between meteorological variables, ΔR, and MDS were examined using Pearson correlation analysis. Statistical analyses were performed using SAS Enterprise Guide 7.1 (SAS Institute Inc., Cary, NC, USA).

3.3. Results

3.3.1. Basal area growth

Before installing the throughfall exclusion device, a similar BAI was observed in the two groups of trees. However, during the three years of 80% throughfall exclusion in the treatment (T) group, trees experienced severe growth reduction from the second month on, with almost no BAI most of the time (Figure 4b), leading to a total reduction of 38 cm^2 of cumulative BAI compared to control trees (Figure 4a). Then, following throughfall exclusion, T trees grew at a similar rate to C trees during the first four months, but subsequent growth recovery by T trees was fast, with higher BAI than in C trees (range 0.5 to 1.5 cm^2) for 20 months. T trees grew at the same growth rates as C trees in the last nine months (Figure 4b). After almost three years of recovery, the difference in cumulative BAI between T and C trees was 18 cm^2, representing 51% growth compensation. An upward trend of cumulative BAI was observed in T trees (Figure 4a).

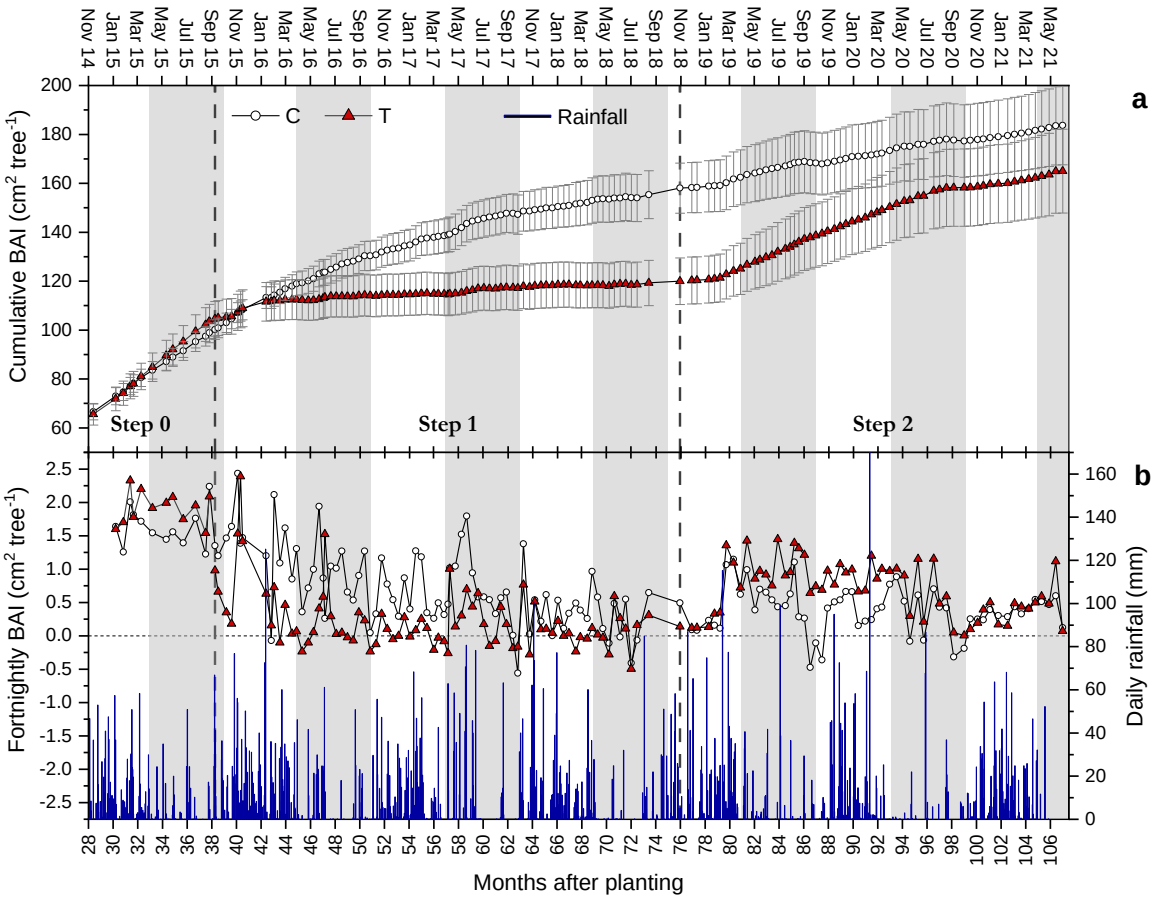

Figure 4. Time series of cumulative (a) and fortnightly (b) basal area increment (BAI). Blue bars indicate daily rainfall (mm). Vertical bars indicate standard errors between trees (n=10). C and T refer to group of the control and treatment trees, respectively. In C group trees, hydric conditions remained normal over time. In T group trees, hydric conditions changed over time (Step 0, 1, and 2): Step 0: Period of normal water conditions before the beginning of the 80% throughfall reduction; Step 1: Period of 80% throughfall reduction; and Step 2: Period of normal water conditions following removal of the throughfall reduction device. The vertical dashed lines indicate the dates of installation and removal of throughfall reduction device in T group.

Analysis of variance showed significant differences in current annual increment of basal area (CAI-basal area) between T and C groups during and after throughfall exclusion (Table 2). Before throughfall exclusion was applied to T trees, their CAI-basal area did not differ significantly from the C group, indicating similar initial growth conditions between groups. Then, during the 80% throughfall reduction in T plots, tree CAI-basal area decreased significantly by 66%, 82%, and 72% at three, four, and five years of age, respectively. However, after throughfall exclusion ended, T trees recovered quickly, with a CAI-basal area of about 76% and 117% greater than control trees, at respectively, six and seven years old. Unexpectedly, 8-year-old T trees did not grow at high growth rates (Figure 5).

CAI-basal area was significantly higher in rainy seasons than in dry seasons, with no significant interaction with groups over the three *Steps* (Table 2). However, significant interactions between season and stand age indicated that exceptionally, the growth rate in the 2017 and 2019 dry season (4 and 6 yr old) was equal to or higher than in the rainy season. On the other hand, as expected, the growth rate of C trees decreased continuously over time (Figure 5). A low CAI-basal area was observed in 5-year-old trees due to severe drought conditions during the 2018 dry season (Table 1).

Table 2. P-values of the effects of two groups (C: Control; T: Treatment), season (rainy season and dry season), stand age, and their interactions on the current annual increment basal area (CAI-basal area) of *E. grandis* trees, by Steps. Step 0, Step 1, and Step 2, refer to the period of before, during, and after throughfall reduction, respectively, applied in T group trees. P-values < 0.05, bold indicates a significant effect.

Factors	Step 0	Step 1	Step 2
Group	0.117	**<0.001**	**0.046**
Season	0.301	**0.019**	0.616
Stand age	-	**<0.001**	**0.046**
Group × Season	0.081	0.265	0.411
Group × Stand age	-	**<0.001**	0.134
Season × Stand age	-	**<0.001**	**0.001**
Group × Season × Stand age	-	0.667	**0.007**

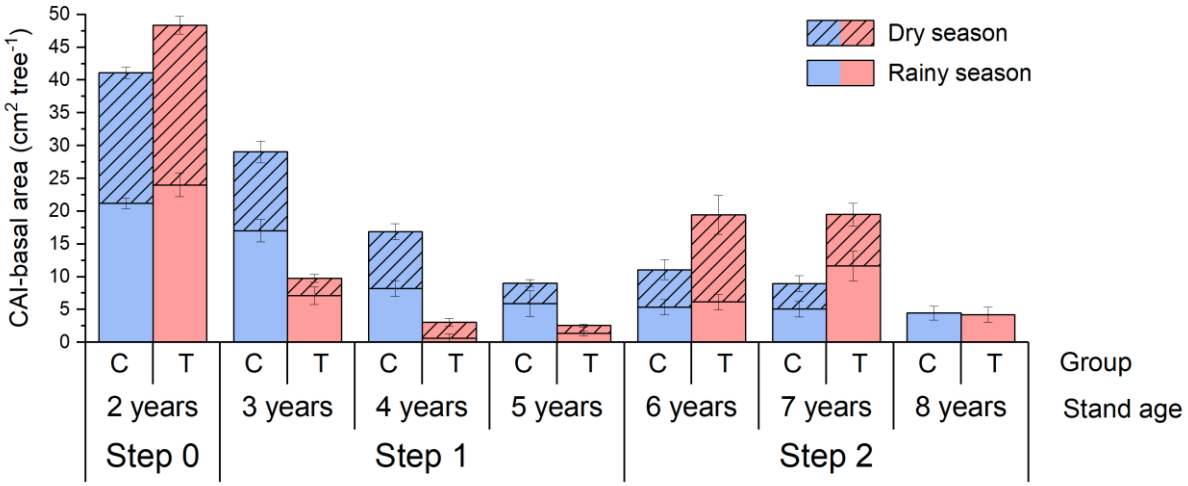

Figure 5. Current annual increment basal area (CAI-basal area) in the rainy season and the dry season in stacked bars, per *Group*, *Stand age*, and *Step*. Vertical bars indicate standard errors between trees (n=10). C and T refer to the group of the control and treatment trees, respectively. In C group trees, hydric conditions remained normal over time. In T group trees, hydric conditions changed over time (Step 0, 1, and 2): Step 0: Period of normal water conditions before the beginning of the 80% throughfall reduction; Step 1: Period of 80% throughfall reduction; and Step 2: Period of normal water conditions following removal of the throughfall reduction device.

3.3.2. Total height growth

There was no growth in total height during the three years of 80% throughfall exclusion in T trees. Then, when throughfall exclusion ended, T trees experienced sudden notable total height growth, higher than or equal to that in C trees, over two years (Figure 6).

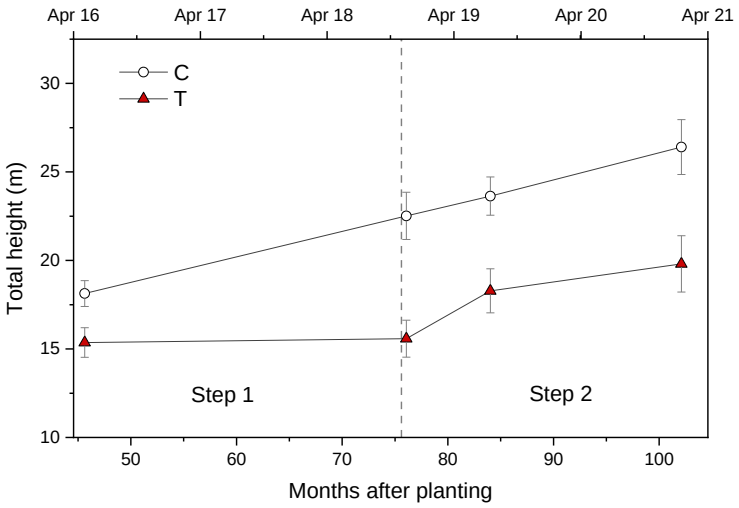

Figure 6. Total height growth over time in the control group (C) and treatment group (T). The vertical bars indicate standard error between trees (n=10). C and T refer to group of the control and treatment trees, respectively. In C group trees, hydric conditions remained normal over time. In T group trees, hydric conditions changed over time (Step 1 and 2): Step 1: Period of 80% throughfall reduction; and Step 2: Period of normal water conditions following removal of the throughfall reduction device. The vertical dashed line indicates the date of removal of throughfall reduction device in T group.

3.3.3. Daily radial growth

Information extracted from the automatic dendrometers also showed the difference in growth between C and T over time. During the two years of 80% throughfall reduction in T trees, radial growth was 0.55 mm, 8 times lower than C trees, which reached 4.72 mm of radial growth. However, at *Step 2*, following throughfall reduction, T trees showed great growth recovery ability, growing 5.6 mm in radius, almost 2 times that in C trees (Figure 7a).

The daily mean ΔR value was 0.007 mm for C and 0.001 mm for T during *Step* 1, and 0.006 mm for C, and 0.009 mm for T during *Step* 2. These average values showed marked variability over time with a higher amplitude of ΔR calculated for T than for C over four years (Figure 7b). Standard deviations ranged from 0.047 mm to 0.067 mm, revealing marked interindividual variability in each group.

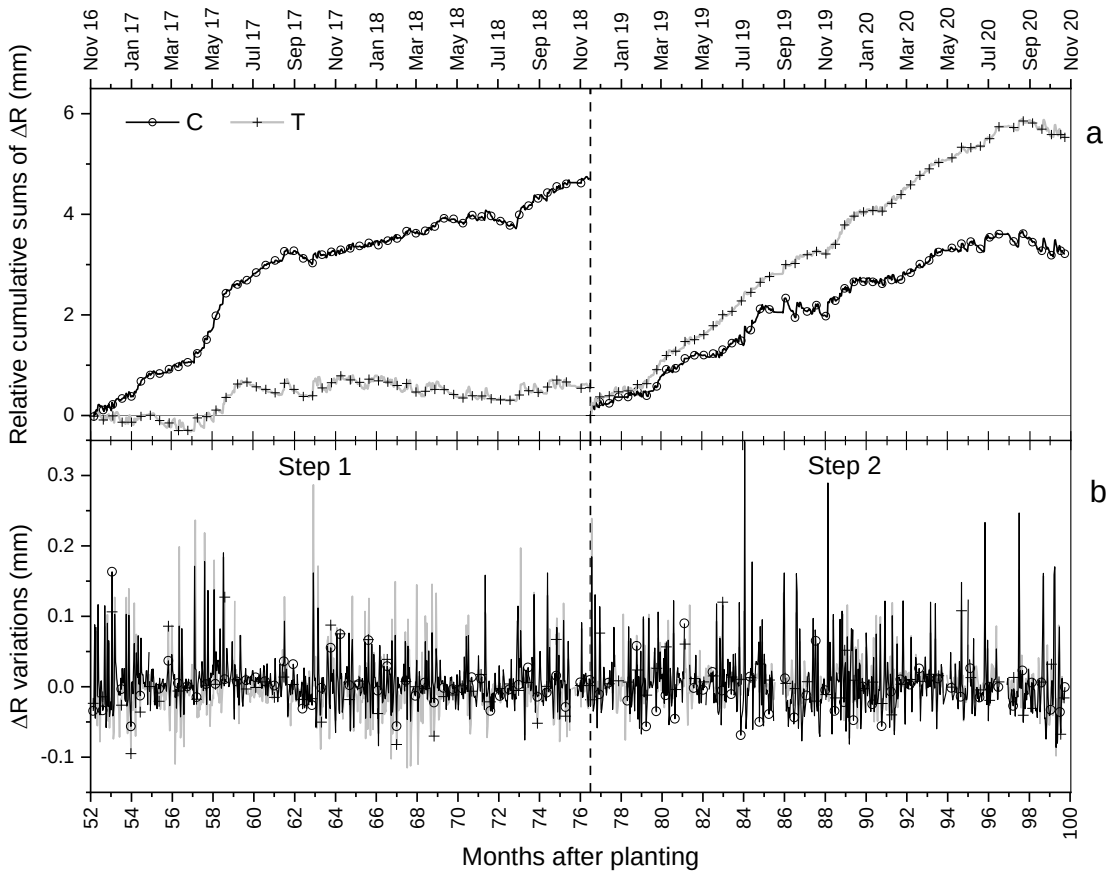

Figure 7. Cumulative ΔR relative to zero (a) and daily variation in ΔR (b) in *Eucalyptus grandis* trees in the control group (C) and in the treatment group (T) during *Step* 1 (during 80% throughfall reduction in T) and *Step* 2 (rehydration period in T following removal of 80% throughfall reduction). The vertical dashed line indicates the date of removal of the throughfall reduction device.

Stem growth was considered to occur when the value distributions of ΔR were positive and significantly different from zero. On a monthly scale, we identified periods of radial growth in C trees that occurred in a temporal pattern that was not clearly defined but lasted mainly from February to June (end of the rainy season and beginning of the dry season) with higher ΔR values (Figure 8). From July to October (end of the dry season), ΔR differed non-significantly from zero or was even negative. In contrast, from November to January (beginning of the rainy season), ΔR was moderate. Nevertheless, high ΔR occurred mainly in months with a moderate rainfall volume. In contrast, in very dry or excessively wet months, no radial growth occurred. In exceptional cases, the driest periods, like that at the beginning of the 2018 dry season and at the end of the 2020 dry season, led to the lowest ΔR.

In T trees in *Step 1*, radial growth was zero or even negative, except in January, May, and June 2017, when rainfall volume was high. However, following water stress, intensive periods of radial growth were identified over more than two years, with the same temporal patterns observed in C trees.

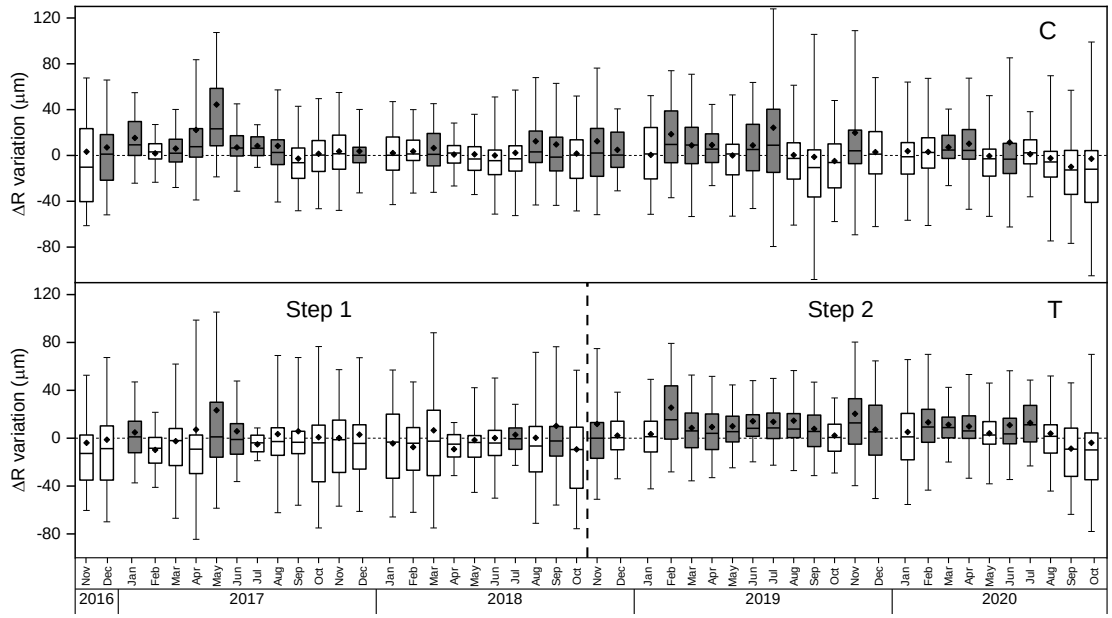

Figure 8. Boxplots of daily variation in ΔR (µm) in *Eucalyptus grandis* trees in the control group (C) and in the treatment group (T), during *Step* 1 (during 80% throughfall reduction in T) and *Step* 2 (rehydration period in T following removal of 80% throughfall reduction). Distribution highlighted in grey differed significantly from zero (one-sample t-test $p<0.05$). The diamonds represent the mean, and the horizontal lines the medians.

3.3.4. Relationships with meteorological variability

During *Step 1*, despite the throughfall reduction, the BAI of T trees was sensitive to meteorological variability, which explained about 38% of the variation in BAI, similar to the responsiveness of C trees. In *Step 2*, following throughfall reduction, responsiveness to meteorological variability increased slightly, explaining about 45% of BAI variability, similar to the responsiveness of C trees. As observed in C trees in *Step 1* and *Step 2*, responsiveness to meteorological variables did not decrease with time.

ACF plots and regression models showed that BAI depended significantly on its previous value (Lag1) (see supplementary material, Figure S1). Rainfall was the only variable present in all models. Temperature and ET were also important variables predictors of BAI over time (Table 3). Predicted vs. observed plots showed that prediction models from meteorological variables slightly underestimate BAI (see supplementary material, Figure S2).

Table 3. Coefficients of multivariate equations of fortnightly basal area increment (BAI) by group of trees (C: Control group; T: Treatment group) and Step (Step 1: period of 80% throughfall reduction in T group; Step 2: period following removal of 80% throughfall reduction in T group). P-values < 0.05, bold indicates a significant effect.

Variables		*Step 1*		*Step 2*	
		C	T	C	T
Intercept		-7.7487	-4.6544	-1.8975	1.6111
Lag1(BAI)		0.1172	0.1778	0.2718	0.4011
Meteorological variables	Rainfall	0.0024	0.0027	0.0006	0.0010
	Tmean	0.4707	0.6922	0.5265	
	Tmin	-0.4169	-0.5460	-0.4404	
	Tmax		-0.0771		-0.0458
	VPD	1.2999		-1.6813	
	ET	-0.0284	-0.0246	-0.0129	
	RH	0.0738	0.0313		

Tmean=Mean temperature; Tmin=Minimum temperature; Tmax= Maximum temperature; VPD=Vapor pressure deficit; ET=Evapotranspiration; RH=Relative humidity. Lag1(BAI) means that the current fortnightly BAI depends on the BAI of the previous period.

During *Step 1*, responsiveness to meteorological variables was similar in C and T trees. BAI growth was moderately correlated with rainfall (r = 0.4 to 0.5) and RH (r = 0.2 to 0.5) in both C and T trees. However, in *Step 2*, these relationships were less robust in both C and T trees. Correlation analysis per season showed that during *Step 1,* BAI growth was more sensitive to temperature (i.e., affected tree growth negatively) in the dry season than in the rainy season in both C and T trees. In *Step 2*, the relationships with the meteorological variables did not vary with the season (Figure 9).

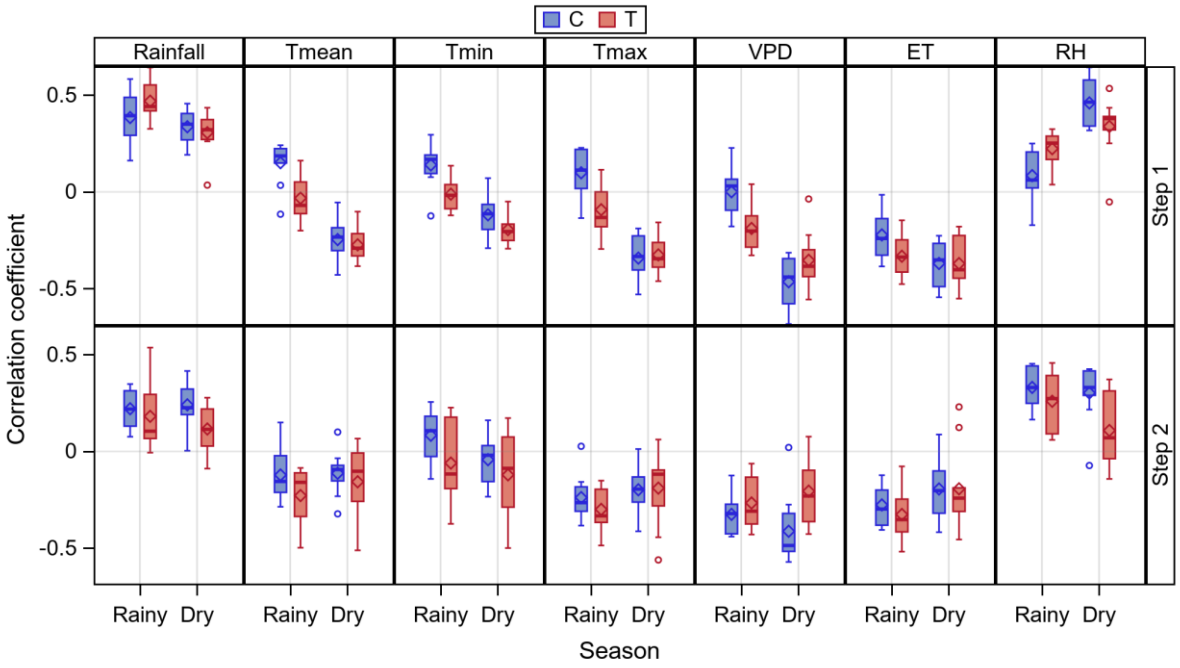

Figure 9. Boxplot of correlation coefficients between the fortnightly BAI and meteorological variables for trees of control group (C) and treatment group (T), in *Step 1* (upper panel) and *Step 2* (lower panel), per season. Step 1 refers to the period of 80% throughfall reduction in T group, and Step 2 refers to the period of normal water conditions following removal of the throughfall reduction device in T group. Hydric conditions remained normal over time in C group.

The Pearson correlation coefficients for the relationships between MDS (maximum daily shrinkage) and the meteorological variables highlighted the greater sensitivity of MDS to environmental variables. MDS was positively correlated with temperature, VPD, ET, and negatively correlated with RH (Figure 10). The MDS of T trees subjected to throughfall reduction was less sensitive to meteorological variables than the MDS of C trees. However, following throughfall reduction, the MDS of T trees was more sensitive to meteorological variables than the MDS of C trees.

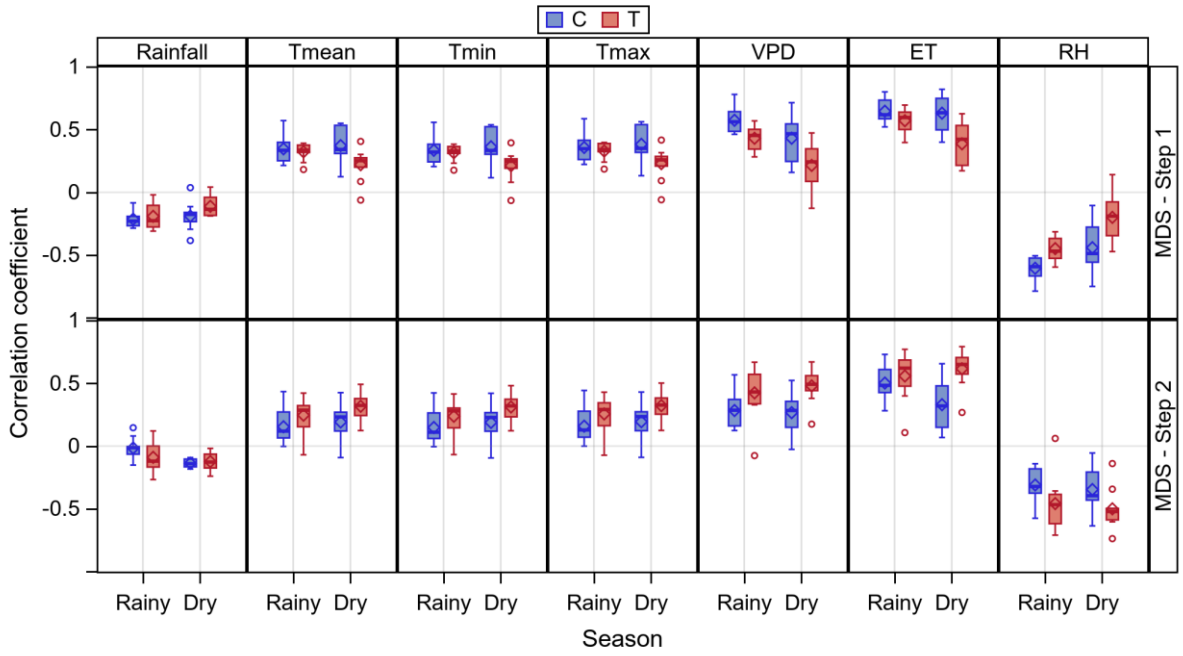

Figure 10. Boxplot of correlation coefficients between MDS and meteorological variables for trees of control group (C) and treatment group (T), in *Step* 1 (upper panel), and *Step* 2 (lower panel), per season. Step 1 refers to the period of 80% throughfall reduction in T group, and Step 2 refers to the period of normal water conditions following removal of the throughfall reduction device in T group. Hydric conditions remained normal over time in C group.

3.4. Discussion

As we hypothesized, 80% throughfall reduction severely reduced tree growth, which can be attributed to the reduction in photosynthetic uptake caused by the stomatal closure to prevent hydraulic failure (McDowell et al., 2008). Hydraulic failure alone or combined with carbon starvation is the main mechanism behind plant mortality during extreme water limitation (McDowell et al., 2008; Sevanto et al., 2014). Particularly in *Eucalyptus* species, hydraulic failure could be a major threat to survival under drought stress due to a high xylem embolism vulnerability (Chen et al., 2020). However, in our study, despite the 80% throughfall reduction, there was no tree mortality. We suspect that, in our study, *E. grandis* trees protected the integrity of their hydraulic system and maintained sufficient carbon balance to avoid death. We base this hypothesis on the sudden major increase in BAI in T trees during 80% throughfall reduction in response to high rainfall volume events, evidence for the great water use efficiency of stressed trees and the integrity of the xylem vascular system. Anatomical studies also showed high plasticity of the hydraulic architecture of *Eucalyptus* species to water availability in Brazil, which could reduce the risk of embolism (Câmara et al., 2020). It is also possible that trees could have enhanced access to water stored in the deepest soil layers by modifying their root system, thus allowing some water uptake to maintain vital physiological processes (McDowell et al., 2008). In fact, in a neighboring experiment with 37% throughfall reduction, the roots of *E. grandis* trees reached the water table at a depth of 19 m (Asensio et al., 2020; Christina et al., 2018).

Nevertheless, *E. grandis* and other *Eucalyptus* species could be well-adapted genotypes with enhanced ability to use water when available, thereby maximizing short-term carbon gain (Pita et al., 2005). In addition, *E. grandis* trees have been reported to cope with water restriction through efficient stomatal regulation, leading to a more gradual use of soil water (Battie-Laclau et al., 2014; Pita et al., 2005; Sperry, 2000). For these reasons, large-scale

mortality events in *Eucalyptus* short-cycle plantations caused by drought are rarely reported, like the mortality of clonal stands of 4-year-old *Eucalyptus urophylla* trees, little tolerant to drought, occurred after an atypically long severe drought in Brazil (Gonçalves et al., 2017). Even mature *Eucalyptus* have historically low tree mortality rates due to drought in natural forests (Matusick and Fontaine, 2020).

Under 80% throughfall reduction, tree basal area growth was 5.12 cm^2 $year^{-1}$ in basal area, and total height was 0.08 m $year^{-1}$, 73%, and 95% lower than control trees, respectively (Figure 5 and Figure 6). These effects show the effectiveness of 80% throughfall reduction in creating severe drought conditions in T trees, with monthly rainfall ranging from around 16 mm in the driest period to 59 mm in the wettest periods (Table 1). Other 6-year experiments with less water limitation showed a much lower response of *Eucalyptus* trees, decreasing basal area and total height by 17% and 7%, respectively, at 37% throughfall reduction (Chambi-Legoas, 2016; Chambi-Legoas et al., 2020) and decreasing stem volume by 16% at 30% throughfall reduction (Binkley et al., 2020). Our results show the high dependence of *Eucalyptus* trees on rainfall and the severe impacts of extreme drought on wood production. Even in control trees, dry periods of less than 40 mm monthly rainfall severely impacted tree growth, as observed at the beginning of the 2018 dry season and the end of the 2020 dry season. It thus appears that most drought tolerance mechanisms tend to enhance survival rather than growth (Pereira and Pallardy, 1989).

During the first four months after the end of water stress, the basal area growth rates of T trees were about 51% higher than those of control trees. This supports the hypothesis that trees maintained the integrity of the xylem vascular system to reinitialize high water uptake. As time passed, T trees grew increasingly faster, mostly 100% to 400% higher than C trees, suggesting that the xylem vascular system reassembled to increase water flow. However, during the last nine months, 8-year-old T trees grew at low rates due to the lowest total rainfall observed in 2020 dry season (325 mm) and 2020/2021 rainy season (1058 mm) (Table 1). Nevertheless, over a 2.6-year recovery period, trees recovered 51% of the basal area growth previously lost during the period of severe water deficit (Figure 4a), whereas total height recovery was 5% (Figure 6). Similarly, water-limited seedlings have been shown to have a higher biomass and height growth rate than well-watered seedlings when water becomes available, increasing stomatal conductance and transpiration rate (Correia et al., 2014). Moreover, drought hardening treatments of *Eucalyptus* seedlings enhanced survival after transplantation (Thomas, 2009).

In contrast, other species such as Scots pine and black pine showed very limited resilience to drought. The delay in - and shortening of - the onset and duration of xylem formation caused by drought disable the recovery of previous growth rates and becoming more prone to die (Guada et al., 2016). The number of green leaves and the levels of carbon reserves after drought determine tree survival. However, even if pine trees survive, severe drought delays recovery and leads to low recovery rates (Galiano et al., 2011).

Our results support our hypothesis that *E. grandis* trees have a great ability to recover basal area growth following drought, and to a lesser extent, total height growth. This is the first study to assess tree growth in field trials after prolonged and extreme water deficit. Consistent with our findings, Matusick and Fontaine (2020) state that *Eucalyptus* genus is among the most resilient trees globally and are exceptionally well adapted to resist and recover from significant partial tree dieback. In addition, our results showed that after severe water stress, trees allocate resources to grow preferentially in diameter rather than in height, which favors the increase and repair of hydraulic conductivity to sustain rapid tree recovery.

Field observations worldwide have shown that tree height is the strongest predictor of tree mortality during intense drought, with large trees becoming twice more vulnerable to die than small trees (Bennett et al., 2015; McIntyre et al., 2015; Stovall et al., 2019). This is consistent with Darcy's law because tree height constrains leaf-

specific hydraulic conductance and evapotranspiration such that the margin of safety is reduced (McDowell et al., 2008). Under this framework, effects of severe drought on long-cycle *Eucalyptus* plantations with large trees (more mature trees) may differ greatly from what was found in our study with short-cycle plantations. Further studies should address older trees and test these hypotheses.

High-resolution measurement of stem radius using automatic dendrometers enabled extraction of reversible fluctuations in stem radius caused by the stem water status, represented by the MDS variable. We found that correlations between MDS and VPD were lower in T trees than in C trees during the 80% throughfall reduction period, but higher in T trees than in C trees following the end of water stress (Figure 10). Reversible fluctuations in stem radius, measured by MDS, are mainly determined by the course of transpiration (Zweifel et al., 2001). Since VPD drives tree transpiration, the relationships between MDS and VPD showed a weak impact of VPD on transpiration in T trees during 80% throughfall reduction, suggesting reduced transpiration. In the same way, it indicated high transpiration rates in T trees after the end of water stress, i.e., increased water use, supporting the high growth recovery observed.

Linear regression models and relationships between meteorological variables and BAI showed that trees were equally responsive to rainfall despite the 80% throughfall reduction (Table 3, Figure 9). Any rainfall event, even limited, contributed to tree growth. Major rainfall events, mainly at the end of the rainy season and onset of the dry season, led to significant increases in basal area or in radial growth. In the dry season, temperatures and VPD were important variables that negatively affected tree growth, mainly in T trees, due to the reduction of stomatal conductance in response to low water availability. However, during dry seasons with high rainfall such as in 2017 and 2019 (Table 1), trees experienced equal or higher growth rates than those during rainy seasons. It seems that moderate rainfall accompanied by lower temperatures and VPD, as observed in 2017 and 2019 dry seasons, promoted high growth rates.

We expected the growth rates to be highest in the wettest months and lowest in the driest months. However, the ΔR results showed a different growth pattern over the years (Figure 8). The lowest daily growth occurred as the dry season was ending, low to moderate daily growth at the beginning of the rainy season with the wettest months, and the highest daily growth at the end of the rainy season and the beginning of the dry season when both rainfall and temperature are moderate. This pattern suggests that during the wettest months, at the onset of the rainy season, trees allocate resources preferentially to increasing foliar area and to the formation of fine roots to the detriment of cambial meristems (Laclau et al., 2005). Then, in the following months when rainfall is moderate, trees can dedicate resources to higher cambial activity, thereby increasing growth rates.

3.5. Conclusions

The extreme drought conditions created by 80% throughfall reduction throughout three years severely impacted tree growth, decreasing basal area and total height growth rates by 73% and 95%, respectively. However, trees responded immediately to rehydration when water stress ended, with higher growth rates than control trees, about 97% and 9% for basal area and total height, respectively. Furthermore, 51% of tree basal area was recovered over the 2.6-year recovery period, whereas only 5% of tree total height was recovered. No mortality events occurred despite the severe water stress. Our findings suggest 6-y-old *E. grandis* trees have a great capacity for recovery after drought, but for growth in diameter rather than in height.

Even with 80% throughfall reduction, tree growth response to rainfall events was rapid. Relationships between MDS and VPD suggest an increase in the transpiration rate upon the end of water stress. These findings indicate high conservation of the integrity of the xylem vascular system during prolonged extreme drought, a key factor in the high resilience of *E. grandis* trees.

Future studies should address vessel anatomy and hydraulic conductance of the trees to understand the adjustment of the xylem vascular system to this severe water deficit and rehydration. Also, wood properties under these conditions need to be studied to know if *E. grandis* trees maintain good wood quality during the recovery period.

CRediT authorship contribution statement

Roger Chambi-Legoas: Conceptualization, Methodology, Formal analysis, Investigation, Data curation, Writing - original draft, Visualization. **Mario Tomazello-Filho:** Conceptualization, Methodology, Investigation, Data curation, Writing - review & editing, Supervision, Project administration, Funding acquisition. **Fernanda Trisltz Perassolo Guedes:** Investigation, Data curation, Writing - review & editing. **Gilles Chaix:** Conceptualization, Methodology, Investigation, Data curation, Writing - review & editing, Supervision, Project administration, Funding acquisition.

Declaration of Competing Interest

The authors declare that they have no known competing financial interests or personal relationships that could have appeared to influence the work reported in this paper.

Acknowledgments

We gratefully acknowledge Rildo M. Moreira and staff of the Itatinga Research Station (ESALQ/USP) for authorization to conduct the experiment and Eder Araujo da Silva (http://www.floragroapoio.com.br) for technical support in the installation of the throughfall exclusion device and growth monitoring. We also thank Dr. Juan Sinforiano Delgado Rojas for support in installing, maintaining, and reading the automatic dendrometers.

Funding Sources

This research was funded by the Agropolis Foundation under reference ID1203-003 through the «*Investissements d'avenir*» program (LabexAgro/ANR-10-LABX-0001-01), *Conselho Nacional de Desenvolvimento Científico e Tecnológico* (CNPq) (444793/2014-3), and *Fondo Nacional de Desarrollo Científico, Tecnológico y de Innovación Tecnologica* (FONDECYT-CONCYTEC, Perú) (Award Number 239-2018).

Roger Chambi- Legoas was supported by a scholarship from FONDECYT-CONCYTEC (Award Number 239-2018), and by a grant for yearly stays in Montpellier from the *Centre de coopération internationale en recherche agronomique pour le développement* (CIRAD) "*Action incitative-Soutien aux doctorants*".

References

Allen, C.D., Macalady, A.K., Chenchouni, H., Bachelet, D., McDowell, N., Vennetier, M., Kitzberger, T., Rigling, A., Breshears, D.D., Hogg, E.H. (Ted), Gonzalez, P., Fensham, R., Zhang, Z., Castro, J., Demidova, N., Lim, J.-H., Allard, G., Running, S.W., Semerci, A., Cobb, N., 2010. A global overview of drought and heat-induced tree mortality reveals emerging climate change risks for forests. For. Ecol. Manage. 259, 660–684. https://doi.org/10.1016/j.foreco.2009.09.001

Asensio, V., Domec, J.C., Nouvellon, Y., Laclau, J.P., Bouillet, J.P., Jordan-Meille, L., Lavres, J., Rojas, J.D., Guillemot, J., Abreu-Junior, C.H., 2020. Potassium fertilization increases hydraulic redistribution and water use efficiency for stemwood production in Eucalyptus grandis plantations. Environ. Exp. Bot. 176, 104085. https://doi.org/10.1016/j.envexpbot.2020.104085

Battie-Laclau, P., Delgado-Rojas, J.S., Christina, M., Nouvellon, Y., Bouillet, J.-P., Piccolo, M. de C., Moreira, M.Z., Gonçalves, J.L. de M., Roupsard, O., Laclau, J.-P., 2016. Potassium fertilization increases water-use efficiency for stem biomass production without affecting intrinsic water-use efficiency in Eucalyptus grandis plantations. For. Ecol. Manage. 364, 77–89. https://doi.org/10.1016/j.foreco.2016.01.004

Battie-Laclau, P., Laclau, J.P., Domec, J.C., Christina, M., Bouillet, J.P., de Cassia Piccolo, M., de Moraes Gonçalves, J.L., Moreira, R.M., Krusche, A.V., Bouvet, J.M., Nouvellon, Y., 2014. Effects of potassium and sodium supply on drought-adaptive mechanisms in Eucalyptus grandis plantations. New Phytol. 203, 401–413. https://doi.org/10.1111/nph.12810

Bennett, A.C., Mcdowell, N.G., Allen, C.D., Anderson-Teixeira, K.J., 2015. Larger trees suffer most during drought in forests worldwide. Nat. Plants 1. https://doi.org/10.1038/nplants.2015.139

Binkley, D., Campoe, O.C., Alvares, C., Carneiro, R.L., Cegatta, Í., Stape, J.L., 2017. The interactions of climate, spacing and genetics on clonal Eucalyptus plantations across Brazil and Uruguay. For. Ecol. Manage. 405, 271–283. https://doi.org/10.1016/j.foreco.2017.09.050

Binkley, D., Campoe, O.C., Alvares, C.A., Carneiro, R.L., Stape, J.L., 2020. Variation in whole-rotation yield among Eucalyptus genotypes in response to water and heat stresses: The TECHS project. For. Ecol. Manage. 462, 117953. https://doi.org/10.1016/j.foreco.2020.117953

Binkley, D., Stape, J.L., Bauerle, W.L., Ryan, M.G., 2010. Explaining growth of individual trees: Light interception and efficiency of light use by Eucalyptus at four sites in Brazil. For. Ecol. Manage. 259, 1704–1713. https://doi.org/10.1016/j.foreco.2009.05.037

Câmara, A.P., Vidaurre, G.B., Oliveira, J.C.L., de Toledo Picoli, E.A., Almeida, M.N.F., Roque, R.M., Tomazello Filho, M., Souza, H.J.P., Oliveira, T.R., Campoe, O.C., 2020. Changes in hydraulic architecture across a water availability gradient for two contrasting commercial Eucalyptus clones. For. Ecol. Manage. 474, 118380. https://doi.org/10.1016/j.foreco.2020.118380

Carle, J.B., Holmgren, L.P.B., 2009. Wood from planted forests: Global outlook to 2030, in: Evans, J. (Ed.), Planted Forests: Uses, Impacts and Sustainability. CABI, pp. 47–59. https://doi.org/10.1079/9781845935641.0047

Chambi-Legoas, R., 2016. Efeito do potássio e do sódio no crescimento e nas propriedades do lenho de árvores de Eucalyptus grandis sob duas condições de regime hídrico. Universidade de São Paulo, Escola Superior de Agricultura Luiz de Queiroz.

Chambi-Legoas, R., Chaix, G., Tomazello-Filho, M., 2020. Effects of potassium/sodium fertilization and throughfall exclusion on growth patterns of Eucalyptus grandis W. Hill ex Maiden during extreme drought periods. New For. 51, 21–40. https://doi.org/10.1007/s11056-019-09716-x

Chan, T., Hölttä, T., Berninger, F., Mäkinen, H., Nöjd, P., Mencuccini, M., Nikinmaa, E., 2016. Separating water-potential induced swelling and shrinking from measured radial stem variations reveals a cambial growth and osmotic concentration signal. Plant Cell Environ. 39, 233–244. https://doi.org/10.1111/pce.12541

Chen, X., Zhao, P., Ouyang, L., Zhu, L., Ni, G., Schäfer, K.V.R., 2020. Whole-plant water hydraulic integrity to predict drought-induced Eucalyptus urophylla mortality under drought stress. For. Ecol. Manage. 468, 118179. https://doi.org/10.1016/j.foreco.2020.118179

Christina, M., le Maire, G., Nouvellon, Y., Vezy, R., Bordon, B., Battie-Laclau, P., Gonçalves, J.L.M., Delgado-Rojas, J.S., Bouillet, J.P., Laclau, J.P., 2018. Simulating the effects of different potassium and water supply regimes on soil water content and water table depth over a rotation of a tropical Eucalyptus grandis plantation. For. Ecol. Manage. 418, 4–14. https://doi.org/10.1016/j.foreco.2017.12.048

Correia, B., Pintó-Marijuan, M., Neves, L., Brossa, R., Dias, M.C., Costa, A., Castro, B.B., Araújo, C., Santos, C., Chaves, M.M., Pinto, G., 2014. Water stress and recovery in the performance of two Eucalyptus globulus clones: Physiological and biochemical profiles. Physiol. Plant. 150, 580–592. https://doi.org/10.1111/ppl.12110

Costa E Silva, F., Shvaleva, A., Maroco, J.P., Almeida, M.H., Chaves, M.M., Pereira, J.S., 2004. Responses to water stress in two Eucalyptus globulus clones differing in drought tolerance. Tree Physiol. 24, 1165–1172. https://doi.org/10.1093/treephys/24.10.1165

Deslauriers, A., Rossi, S., Anfodillo, T., 2007. Dendrometer and intra-annual tree growth: What kind of information can be inferred? Dendrochronologia 25, 113–124. https://doi.org/10.1016/j.dendro.2007.05.003

Deslauriers, A., Rossi, S., Turcotte, A., Morin, H., Krause, C., 2011. A three-step procedure in SAS to analyze the time series from automatic dendrometers. Dendrochronologia 29, 151–161. https://doi.org/10.1016/j.dendro.2011.01.008

Downes, G., Beadle, C., Worledge, D., 1999. Daily stem growth patterns in irrigated Eucalyptus globulus and E. nitens in relation to climate. Trees - Struct. Funct. 14, 102–111. https://doi.org/10.1007/s004680050214

Drew, D.M., Downes, G.M., 2009. The use of precision dendrometers in research on daily stem size and wood property variation: A review. Dendrochronologia 27, 159–172. https://doi.org/10.1016/j.dendro.2009.06.008

FAO, 2020. Global Forest Resources Assessment 2020 Main report. Rome. https://doi.org/10.4060/ca9825en

Fuller, L.G. (School of F. and W.R.B.V., Cattelino, P.J., Reed, D.D., 1988. Correction equations for dendrometer band measurements of five hardwood species. North. J. Appl. For.

Galiano, L., Martínez-Vilalta, J., Lloret, F., 2011. Carbon reserves and canopy defoliation determine the recovery of Scots pine 4 yr after a drought episode. New Phytol. 190, 750–759. https://doi.org/10.1111/J.1469-8137.2010.03628.X

Giovannelli, A., Deslauriers, A., Fragnelli, G., Scaletti, L., Castro, G., Rossi, S., Crivellaro, A., 2007. Evaluation of drought response of two poplar clones (Populus×canadensis Mönch 'I-214' and P. deltoides Marsh. 'Dvina') through high resolution analysis of stem growth. J. Exp. Bot. 58, 2673–2683. https://doi.org/10.1093/jxb/erm117

Gonçalves, J.L.M., Alvares, C.A., Rocha, J.H.T., Brandani, C.B., Hakamada, R., 2017. Eucalypt plantation management in regions with water stress. South. For. 79, 169–183. https://doi.org/10.2989/20702620.2016.1255415

Guada, G., Camarero, J.J., Sánchez-Salguero, R., Cerrillo, R.M.N., 2016. Limited Growth Recovery after Drought-Induced Forest Dieback in Very Defoliated Trees of Two Pine Species. Front. Plant Sci. 7, 418. https://doi.org/10.3389/fpls.2016.00418

IPCC, 2021. Climate Change 2021: The Physical Science Basis. Contribution of Working Group I to the Sixth Assessment Report of the Intergovernmental Panel on Climate Change, In Press. ed. Cambridge University Press.

Keeland, B.D., Sharitz, R.R., 1993. Accuracy of tree growth measurements using dendrometer bands. Can. J. For. Res. 23, 2454–2457. https://doi.org/10.1139/x93-304

Laclau, J.P., Almeida, J.C.R., Gonalves, J.L.M., Saint-Andr, L., Ventura, M., Ranger, J., Moreira, R.M., Nouvellon, Y., 2009. Influence of nitrogen and potassium fertilization on leaf lifespan and allocation of above-ground growth in Eucalyptus plantations. Tree Physiol. 29, 111–124. https://doi.org/10.1093/treephys/tpn010

Laclau, J.P., Ranger, J., Deleporte, P., Nouvellon, Y., Saint-André, L., Marlet, S., Bouillet, J.P., 2005. Nutrient cycling in a clonal stand of Eucalyptus and an adjacent savanna ecosystem in Congo: 3. Input-output budgets and consequences for the sustainability of the plantations. For. Ecol. Manage. 210, 375–391. https://doi.org/10.1016/j.foreco.2005.02.028

Lee, J.Y., Marotzke, J., Bala, G., Cao, L., Corti, S., Dunne, J.P., Engelbrecht, F., Fischer, E., Fyfe, J.C., Jones, C., Maycock, A., Mutemi, J., Ndiaye, O., Panickal, S., Zhou, T., 2021. Future Global Climate: Scenario-Based Projections and Near-Term Information, in: Masson-Delmotte, V., Zhai, P., Pirani, A., Connors, S.L., Péan, C., Berger, S., Caud, N., Chen, Y., Goldfarb, L., Gomis, M.I., Huang, M., Leitzell, K., Lonnoy, E., Matthews, J.B.R., Maycock, T.K., Waterfield, T., Yelekçi, O., Yu, R., Zhou, B. (Eds.), Climate Change 2021: The Physical Science Basis. Contribution of Working Group I to the Sixth Assessment Report of the Intergovernmental Panel on Climate Change. Cambridge University Press, p. 195.

Li, C., Berninger, F., Koskela, J., Sonninen, E., 2000. Drought responses of Eucalyptus microtheca provenances depend on seasonality of rainfall in their place of origin Chunyang. Aust. J. Plant Physiol. 27, 231–238. https://doi.org/10.1071/PP99056

Matusick, G., Fontaine, J., 2020. Causes of large-scale eucalyptus tree dieback and mortality : research priorities. A report for the NSW Natural Resources Commission. WA.

McDowell, N., Pockman, W.T., Allen, C.D., Breshears, D.D., Cobb, N., Kolb, T., Plaut, J., Sperry, J., West, A., Williams, D.G., Yepez, E.A., 2008. Mechanisms of plant survival and mortality during drought: Why do some plants survive while others succumb to drought? New Phytol. 178, 719–739. https://doi.org/10.1111/j.1469-8137.2008.02436.x

McIntyre, P.J., Thorne, J.H., Dolanc, C.R., Flint, A.L., Flint, L.E., Kelly, M., Ackerly, D.D., 2015. Twentieth-century shifts in forest structure in California: Denser forests, smaller trees, and increased dominance of oaks. Proc. Natl. Acad. Sci. U. S. A. 112, 1458–1463. https://doi.org/10.1073/pnas.1410186112

Mencuccini, M., Salmon, Y., Mitchell, P., Hölttä, T., Choat, B., Meir, P., O'Grady, A., Tissue, D., Zweifel, R., Sevanto, S., Pfautsch, S., 2017. An empirical method that separates irreversible stem radial growth from bark water content changes in trees: theory and case studies. Plant Cell Environ. 40, 290–303. https://doi.org/10.1111/pce.12863

Nishimua, T.B., Suzuki, E., Kohyama, T., Tsuyuzaki, S., 2007. Mortality and Growth of Trees in Peat-swamp and Heath Forests in Central Kalimantan After Severe Drought. Plant Ecol. 188, 165–177. https://doi.org/10.1007/s11258-006-9154-z

Obregón, G.O., Marengo, J.A., Nobre, C.A., 2014. Rainfall and climate variability: Long-term trends in the Metropolitan Area of São Paulo in the 20th century. Clim. Res. 61, 93–107. https://doi.org/10.3354/cr01241

Pereira, J.S., Pallardy, S., 1989. Water Stress Limitations to Tree Productivity, in: Biomass Production by Fast-Growing Trees. Springer Netherlands, pp. 37–56. https://doi.org/10.1007/978-94-009-2348-5_3

Pita, P., Cañas, I., Soria, F., Ruiz, F., Toval, G., 2005. Use of physiological traits in tree breeding for improved yield in drought-prone environments. The case of Eucalyptus globulus. Investig. Agrar. Sist. y Recur. For. 14, 383. https://doi.org/10.5424/srf/2005143-00931

Sevanto, S., Mcdowell, N.G., Dickman, L.T., Pangle, R., Pockman, W.T., 2014. How do trees die? A test of the hydraulic failure and carbon starvation hypotheses. Plant, Cell Environ. 37, 153–161. https://doi.org/10.1111/pce.12141

Sperry, J.S., 2000. Hydraulic constraints on plant gas exchange. Agric. For. Meteorol. 104, 13–23. https://doi.org/10.1016/S0168-1923(00)00144-1

Stape, J.L., Binkley, D., Ryan, M.G., Fonseca, S., Loos, R.A., Takahashi, E.N., Silva, C.R., Silva, S.R., Hakamada, R.E., Ferreira, J.M. de A., Lima, A.M.N., Gava, J.L., Leite, F.P., Andrade, H.B., Alves, J.M., Silva, G.G.C., Azevedo, M.R., 2010. The Brazil Eucalyptus Potential Productivity Project: Influence of water, nutrients and stand uniformity on wood production. For. Ecol. Manage. 259, 1684–1694. https://doi.org/10.1016/j.foreco.2010.01.012

Stovall, A.E.L., Shugart, H., Yang, X., 2019. Tree height explains mortality risk during an intense drought. Nat. Commun. 10, 1–6. https://doi.org/10.1038/s41467-019-12380-6

Thomas, D.S., 2009. Survival and growth of drought hardened Eucalyptus pilularis Sm. seedlings and vegetative cuttings. New For. 38, 245–259. https://doi.org/10.1007/s11056-009-9144-9

Wu, Z., Dijkstra, P., Koch, G.W., Peñuelas, J., Hungate, B.A., 2011. Responses of terrestrial ecosystems to temperature and precipitation change: A meta-analysis of experimental manipulation. Glob. Chang. Biol. 17, 927–942. https://doi.org/10.1111/j.1365-2486.2010.02302.x

Zweifel, R., Item, H., Häsler, R., 2001. Link between diurnal stem radius changes and tree water relations. Tree Physiol. 21, 869–877. https://doi.org/10.1093/treephys/21.12-13.869

Appendix. Supplementary material

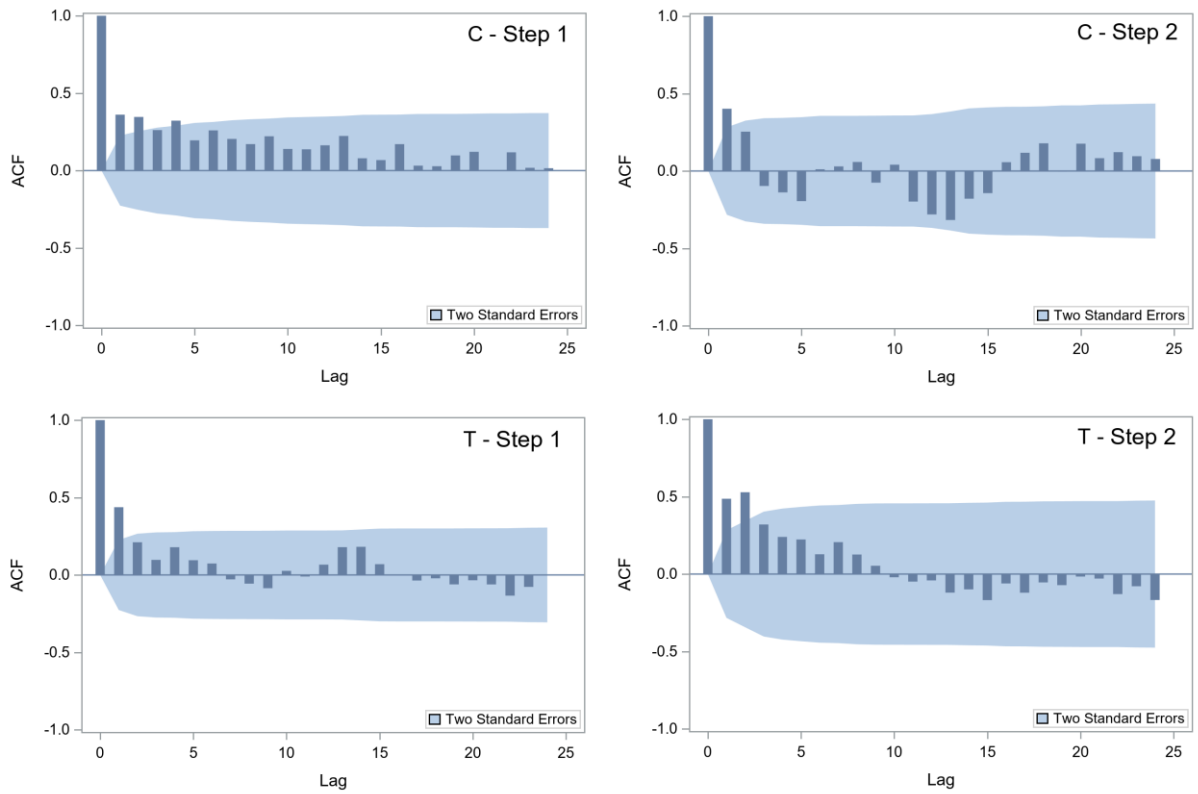

Figure S1: Autocorrelation function plots (ACF) between 2-weekly BAI and meteorological variables, per groups and step.

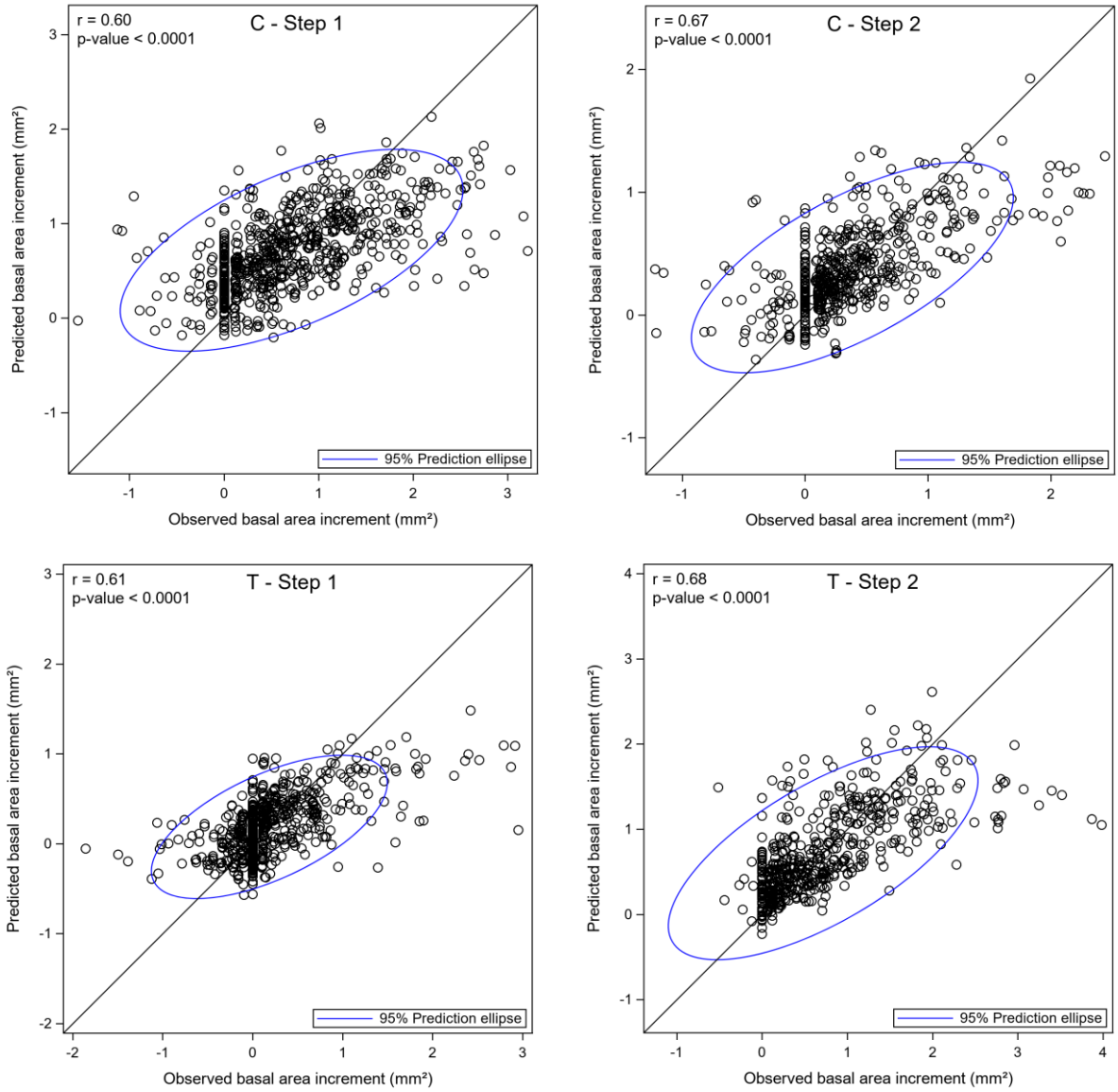

Figure S2: Relationship between predicted and observed 2-weekly BAI per group and step. Predicted 2-weekly BAI is the result of regression from meteorological variables. Regressions were performed using a linear mixed model with a repeated-measure factor (date) and random factor (tree). The comparison was tested using the Akaike information criterion (AIC).

4. INTER-ANNUAL EFFECTS OF POTASSIUM/SODIUM FERTILIZATION AND WATER DEFICIT ON WOOD QUALITY OF *Eucalyptus grandis* TREES OVER A FULL ROTATION

Published in the journal: Forest Ecology and Management, v. 496, p. 119415, 2021

Roger Chambi-Legoas [1]*, Gilles Chaix [1,2,3], Vinicius Resende Castro [4], Mariana Pires Franco [5], Mario Tomazello-Filho [1],

[1] Universidade de São Paulo, ESALQ, Departamento de Ciências Florestais, 13418-900, Piracicaba, SP, Brazil

[2] CIRAD, UMR AGAP Institut, F-34398 Montpellier, France

[3] UMR AGAP Institut, Univ Montpellier, CIRAD, INRAE, Institut Agro, F-34398 Montpellier, France

[4] Universidade Federal de Viçosa, Departamento de Engenharia Florestal, 36570-900, Viçosa, MG, Brazil

[5] Universidade Federal de Goiás, Escola de Agronomia, 74690900, Goiânia, GO, Brazil

*Corresponding author: rchambilegoas@gmail.com

Abstract

In Brazil, most *Eucalyptus* plantations are located in regions experiencing periods of water shortage, where fertilizers such as potassium (K) are intensively used to achieve high productivity. Recently, sodium (Na) has also been considered a potential nutrient in K-deficient soils. K and Na supply can increase water stress in *Eucalyptus grandis* trees, which could negatively impact forest productivity over prolonged droughts. Wood properties are determinants of the quality and yield of products. They are important factors to consider when measuring the impacts of silvicultural practices and water deficit on forest productivity. However, alterations in wood properties due to interactions between K/Na fertilization, water availability, and stand age are not well documented. Through annual sampling of *E. grandis* trees throughout a complete rotation (6 years) in Brazil, we evaluated the interactive effects of K/Na fertilization, water availability, and stand age on stem volume, sapwood/heartwood ratio, wood density, fiber, and vessel features. We also evaluated the relationships between growth rate, wood density, and fiber and vessel features. The split-plot experimental design consisted of two water supply regimes (37% throughfall reduction versus undisturbed throughfall) and three fertilization regimes (K, Na, and control). Until six years of age, K and Na fertilization increased stem volume by three and 2-fold, respectively, and only K-fertilized trees affected stem volume by 37% throughfall reduction. Both K and Na detrimentally affected wood density and beneficially affected fiber length. The sapwood/heartwood ratio was highly and negatively related to the growth rate of trees. Wall thickness was not affected by either K or Na. As expected, K and Na affected vessel size due to an increase in basal area growth. However, the effects of Na were more pronounced than those of K. Significant interactions between fertilization and water availability suggest that, under water deficit, wood density will not be affected by K fertilization. In contrast, the effect of Na and control treatments were invariable regardless of water availability. The effects of fertilization on wood properties changed over time, with non-significant effects in the first year and stronger effects from two years of age of trees. The variations in wood density were strongly related to variations in the fiber wall thickness. High increases in basal area growth promoted by K and Na were not related to significant decreases in wood density, but they were related to increases in fiber length. These findings highlight the significant effects of K addition on stem volume without significant losses in wood quality, even under water stress over a complete rotation. The negative impacts observed on wood density and lower productivity in commercial *E. grandis* plantations with the use of Na as a substitute for K should be considered.

Keywords: Throughfall reduction; Fertilization; Fiber size; Vessels size; Heartwood content; Forest productivity

4.1. Introduction

Fertilization is widely used in Brazil to increase wood productivity in *Eucalyptus* plantations. In regions where potassium (K) is a limiting factor, K fertilization is a widespread practice because K is the main driver for an increase in aboveground biomass and growth rates of Eucalyptus trees (Laclau et al., 2009). On the other hand, sodium (Na) has been considered a potential fertilizer because *Eucalyptus grandis* growth showed a positive response to NaCl application in a partial replacement of KCl (Almeida et al., 2010).

Fertilization increases water use efficiency and resistance to drought, which is a key advantage in water-limited conditions (Asensio et al., 2020; Tariq et al., 2019; Wang et al., 2019). However, fertilization also increases tree water demand and reduces water reserves in soils, increasing the risk of death by embolism during severe drought (Battie-Laclau et al., 2014). Because of this, the study of the interaction of fertilizers with water deficit on tree development is considered of great importance for the revision of management practices in regions at risk of prolonged drought (Battie-Laclau et al., 2014; Christina et al., 2018; Gonçalves et al., 2013). The great positive effects of K and Na nutrients in interaction with water availability on tree growth and have been reported (Battie-Laclau et al., 2014; Chambi-Legoas et al., 2020); however, there is scarce information about their effects on wood anatomy and basic density.

Wood quality is also an important factor in forest management because it influences the transformation process and quality of end-use wood products. Higher wood density, larger fiber size, and higher sapwood/heartwood ratio are desirable attributes for higher yield and quality of pulp and paper products (Gonçalves et al., 2004). The greater the fiber length, the higher the tearing resistance of paper, while the lesser the fiber wall thickness, the higher the burst and tensile strengths but lower the tear resistance (Rana et al., 2011; Shmulsky and Jones, 2011). Heartwood has a higher content of extractives than sapwood, increasing chemical consumption and decreasing pulp yield and pulp brightness (Lourenço et al., 2011; Morais and Pereira, 2007). Environmental conditions, including silvicultural practices, can affect wood formation in trees (Gonçalves et al., 2004; Pillai et al., 2013; Thomas et al., 2007), and, consequently, the wood anatomy and density, and other physical properties (Zobel and van Buijtenen, 1989). Thus, applying silvicultural techniques to changing environmental conditions must consider the potential impacts on wood quality.

The effects of fertilization under different rainfall regimes on wood properties are confusing. The addition of fertilizer (nitrogen and phosphorus) may be detrimental to some wood properties at drier sites but has no major effects on wetter sites (Raymond and Muneri, 2000). In particular, for K and Na, a previous study using juvenile stages of Eucalyptus trees (1-3 years old) showed that the effects of K and Na fertilization on fiber and vessel properties are not significant, regardless of water availability (Freitas et al., 2015). Juvenile wood formed in the first years could influence the absence of effects of K and Na on wood density, fibers, and vessel features (Freitas et al., 2015; Júnior et al., 2009; Sette Jr et al., 2012). However, in 6-year-old *E. grandis* trees, Na fertilization was shown to modify fiber features, but both K and Na did not affect wood density (Sette Jr et al., 2014). In addition, wood density is not significantly affected by throughfall reduction conditions (Câmara et al., 2020; Castro et al., 2020; Searson et al., 2004), but trees growing in drier sites were shown to be able to produce wood with a higher density (Naidoo et al., 2007; Pfautsch et al., 2016). Nevertheless, as seen, published results cannot unequivocally establish that water limitation increases wood density in *Eucalyptus* species under water stress. On the other hand, fiber features can be affected mainly by a water surplus (Drew et al., 2011, 2009), but the effects under water stress conditions are unknown.

On the other hand, the decrease in vessel diameter and increase in vessel density in *Eucalyptus* trees (Arend and Fromm, 2007; Câmara et al., 2020; February et al., 1995; Searson et al., 2004) have been reported as a key measure of the "fitness" of trees to ensure sufficient water transport to maintain physiological functioning of leaves while minimizing risks of loss of conductivity due to embolism (February et al., 1995; Pfautsch et al., 2016). Changes in diameter and density of vessels are an important variable to measure in silvicultural trials and changing environmental conditions because it reflects the adaptation of hydraulic architecture to water availability.

Studies in phloem and leaf cells in water-deficient *Eucalyptus* trees showed that both K and Na increase the sieve tube cross-sectional area, resulting in a higher velocity of phloem transport (Epron et al., 2015). Likewise, K and Na increase the cell size of the leaves and cell turgor from a higher concentration of osmotica (Battie-Laclau et al., 2013). From these studies, we can suppose that K and Na could affect the cambial cells, which could lead to changes in the anatomy of adult xylem cells and therefore affect wood properties.

In this context, assessment of wood property changes under different water deficit conditions, throughout a complete rotation, from one to six years of age, is crucial for more accurate conclusions about the impacts of K and Na, to define more appropriate management practices in regions with risk of prolonged drought. New wood tissues are formed during each growing period; however, unlike coniferous species and some other broad-leaved species, *Eucalyptus* trees do not form distinguishable annual rings, making reliable assessments of inter-annual variability in wood properties difficult. Therefore, yearly systematic tree sampling can overcome these constraints. Knowing the inter-annual variability of wood properties allows for weighing the effects of treatments on the whole stem of trees.

The goal of our study was to evaluate the interactive effects of K/Na fertilization, water availability, and stand age on stem volume and wood properties. Here, we evaluated the effects of K and Na fertilization under water reduction and non-water reduction conditions on stem volume, sapwood/heartwood ratio, basic and apparent density, and fiber and vessel attributes, from one to six years of age. In addition, we evaluated whether variabilities in wood properties are induced by changes in the growth rate promoted by K and Na fertilization.

We intend, therefore, to answer the following questions: (i) How do additions of K and Na affect tree wood properties? (ii) do wood properties change under 37% throughfall reduction? (iii) do the effects of fertilization and water regimes change according to tree age? and (iv) are the changes in wood properties related to the basal area growth rate promoted by the K and Na supply?

We hypothesized that, under normal water availability, K and Na decrease wood density and increase fiber size, mainly at the final years of the rotation. Under 37% throughfall reduction, which reduces tree growth rate, the effects of fertilization would be weak or insignificant. Vessel diameter and vessel density would be highly responsive to the reduction of water availability and fertilization with K and Na. We also hypothesized the interaction of these effects with stand age.

4.2. Material and Methods

4.2.1. Study area

The experiment was conducted at the Itatinga Experimental Station of the University of São Paulo, São Paulo, Brazil (23°02 S, 48°38 W). The mean annual rainfall and temperature were 1360 mm and 19.9°C, respectively. The experiment was set up on an elevated terrain with a 3% slope at an altitude of 850 m. The soils are deep

Ferralsols with 14 to 23% clay content (for more details about the soil characteristics, see Battie-Laclau et al. 2014 and Laclau et al. 2010).

4.2.2 Experimental plantation description

The experiment is described in detail in Battie-Laclau et al. (2014). Seedlings of a highly productive clone of *E. grandis* were planted in June 2010 in an area of 10370 m^2, spaced 2 m × 3 m. At the time of planting, standard fertilization used in the region was applied except K. Plants were fertilized with 75 kg ha^{-1} of P_2O_5, 80 kg ha^{-1} of N ($NH_4(SO_4)_2$), and 20 kg ha^{-1} of FTE BR-12 (micronutrient source) applied close to the plants. Furthermore, 2000 kg ha^{-1} of dolomitic limestone was broadcast on the soil surface. Three months after planting, two levels of water regime, 37% throughfall reduction (−W) and no throughfall reduction (+W), and three levels of fertilization: potassium addition (+K), sodium addition (+Na), and control (C), were applied to the plantation in a split-plot design.

The water regime was applied as the whole-plot factor, whereas fertilization was considered as the split-plot factor (nested within each plot) in three blocks (repetitions), producing six treatments:

- C+W: control, without K and Na fertilization, and no throughfall reduction,
- +Na+W: 0.45 mol Na m^{-2} applied as NaCl and no throughfall reduction,
- +K+W: 0.45 mol K m^{-2} applied as KCl and no throughfall reduction,
- C−W: control, without K and Na fertilization, and 37% throughfall reduction,
- +Na−W: 0.45 mol Na m^{-2} applied as NaCl, and 37% throughfall reduction,
- +K−W: 0.45 mol K m^{-2} applied as KCl, and 37% throughfall reduction.

K and Na supply were broadcast on the soil surface in a single dose 3 months after planting. The 37% throughfall reduction was performed using transparent plastic panels mounted on wooden frames at a height varying between 0.5 m and 1.6 m (Battie-Laclau et al., 2016) and covering 37% of the plot area (Figure 1) and installed in September 2010. The experiments were assessed for 6 years, and trees were cut on 02 May 2016.

Figure 1. Throughfall reduction experiment conducted at the Itatinga Experimental Station of the University of São Paulo in Brazil, at 5 years after planting *Eucalyptus grandis* trees.

4.2.3 Wood sampling

Sampling was carried out annually in May, from one to six years of age. According to the annual inventory of trees, the sampled trees were distributed in four to nine diametric classes (one tree per diametric class). Extreme classes were not sampled. We sampled 24 trees at 1 and 2 years of age (4 trees per treatment), 48 trees at 3 and 4 years of age (8 trees per treatment), 54 trees at 5 years old (9 trees per treatment), and 36 trees at 6 years old (6 trees per treatment). In total, 234 trees were sampled over the six-year experiment.

A log of 50 cm length was cut at breast height from each tree and then divided into several cross-sectional discs. To assess inter-annual variability of wood quality, we analyzed the outer region of the discs, which corresponds to the wood formed in the last year. The basic density and sapwood/heartwood ratio was calculated based on the whole disc.

4.2.4 Estimation of trunk volume and basal area growth of trees

The trunk volume under the bark was calculated by the Smalian method annually from 1 to 6 years of age, from the trees cut to obtain the wood samples. Each trunk was divided into logs of 2 m in length. The bottom diameter, upper diameter, and bark thickness of each log were measured. Log volume was calculated from the diameters inside the bark, which were obtained by discounting the bark thickness. Trunk volume was calculated as the sum of the volume of each log.

The basal area growth (at breast height) was calculated each year from sampled trees, expressed as the mean annual increment of basal area (basal area MAI) and current annual increment of basal area (basal area CAI). The basal area MAI was calculated by dividing the basal area by sample age. While the basal area CAI was calculated

as the difference between the current basal area and the basal area at the previous year (obtained from yearly measurements of trunk circumference at breast height).

4.2.5 Sapwood/Heartwood ratio

Thin cross-sectional discs (5 mm) were taken from each sample log at 4 and 6 years of age only. Each disc was polished to obtain a good contrast between the macroscopic characteristics of the transverse surface. Subsequently, the polished discs were scanned at 1200 dpi resolution to use the color difference for the visual delimitation of heartwood. When heartwood borders were not distinguishable, discs were stained with dimethyl yellow solution (1%) and scanned to support heartwood delimitation. This chemical solution reacts to the difference in pH between heartwood and sapwood (lower pH in heartwood) with a characteristic orange-red color in heartwood and yellow color in sapwood. From both images, the sapwood and heartwood areas were measured for the calculation of sapwood/heartwood ratio using the open-source image processing software ImageJ version 1.52a (Schneider et al., 2012).

4.2.6 Wood basic density

The wood basic density was calculated for each tree disc sampled annually from 1 to 6 years of age. The discs without bark were divided into four segments, and two opposite segments free of defects (knots, rot, etc.) were sampled and placed in water until completely saturated. The wood volume of each saturated segment was measured using the water displacement method. The dry mass was determined after drying at 105°C ± 2°C. The basic density of each segment was calculated by dividing the dry mass by the volume. The average basic density of the two segments represents the total basic density of the disc sample.

4.2.7 Wood apparent density by X-ray microdensitometer

Wood density profiles were obtained at 4, 5, and 6 years of age. Rectangular sections, bark-to-bark (2 cm width, pith-centered), were cut from the discs at breast height and glued to wooden supports. Then, a thin wood slice (1.8 cm thickness) was transversally cut from each section using a parallel double circular sawing equipment. The samples were conditioned in a climatic chamber (20°C, 60% HR) for 48 h, with 12-15% wood moisture content. Subsequently, X-ray images of the wood samples were obtained using the Faxitron MX-20 Cabinet X-Ray Imaging System equipment (Faxitron X-Ray Corporation, Lincolnshire, IL, USA). X-ray images were analyzed in R software with the X-ring package (Campelo et al., 2019), where a calibration curve was fitted from known values of the density and thicknesses of a step-wedge recorded in each image. Then, using the calibration curve, the wood density profile was determined based on the grayscale value of pixels and the thickness of the sample in a region of interest of 2 mm width. From the density profile, we identified and selected the region of the last annual growth ring and averaged its density.

4.2.8 Fibers and vessels features

Fiber and vessel features were measured in the outer region of each disc (corresponding to the wood formed in the previous year) sampled at 1, 2, 3, 4, and 6 years old. We did not measure fiber and vessels at 5 years of age because of technical problems. The outer radial represents the wood formed in the last year (last annual growth ring). Fibers were dissected by maceration using Franklin's method (Franklin, 1945). To measure vessels, sections (10-15 μm thickness) from the transverse surface of the samples were cut on a sliding microtome (Leica SM 2010 R). Histological slides were produced according to standard wood anatomy techniques (Johansen, 1940), then digital images were captured with a digital camera (Axio Cam MRC-Zeiss) integrated into a microscope (Zeiss Axio Scope A1). Images for fiber length, vessel density, and vessel area were captured at 25x magnification. Images for vessel diameter were captured at 40x magnification, and images for thickness, diameter, and lumen diameter of fibers were captured at 100x magnification. Fiber features were measured for at least 35 fibers for each sample. The fiber thickness was calculated as half of the difference between the fiber diameter and fiber lumen diameter. Vessels, diameter (μm), and density (vessels mm^{-2}), and occupied areas (%) were measured over the entire area of the histological section. Measurements were performed using the ImageJ software version 1.52a (Schneider et al., 2012).

In addition, we measured the total vessel area of sapwood each year. As indicated in section 2.5, sapwood area and width were measured directly only at 4 and 6 years old. We fit a linear regression (sapwood area ~ diameter, and sapwood width ~ diameter) at 4 and 6 years to be used to estimate sapwood area and width at 1, 2, and 3 years. Then vessel area was measured over the histological section comprising the sapwood width and projected to the sapwood area of trees.

4.2.9 Data analysis

Mixed-effect models were used to test, by variance analysis, the effects of water regime, fertilization regime, stand age, and interaction water regime × fertilization, water regime × stand age, fertilization × stand age, water regime × fertilization × stand age (as fixed effects) on trunk volume, sapwood/heartwood ratio, wood basic density, and fiber and vessel properties. Blocks and water regime × blocks were considered as random effects to take account of the split-plot design. Pearson's correlation was used to assess the relationship between wood properties and basal area growth. Statistical analysis was performed using SAS Enterprise Guide 7.1 (SAS Institute Inc., Cary, NC, USA).

4.3. Results

Wood density increased as the stand age increased, from 0.35-0.38 g cm^{-3} in the first year to 0.51-0.55 g cm^{-3} in the sixth year, whereas the sapwood/heartwood ratio decreased from 1.32-2.36 in the fourth year to 1.04-2.05 in the sixth year. There were significant interactions between fertilization and stand age on trunk volume and wood density. Significant effects of fertilization regimes took place only from 2 years of age. Likewise, there was a significant effect of fertilization regime on trunk volume and the sapwood/heartwood ratio, without significant interaction between water supply and fertilization regime (Table 1). In contrast, the significant interaction between water supply and fertilization regime showed that K did not reduce the wood basic density under lower water availability, but it did under normal water availability.

Table 1. Effects of water regime, fertilization regime, stand age, and its interactions on trunk volume, wood basic density, and the sapwood/heartwood ratio. p-value<0.05, bold indicates significant effect.

Factors	Trunk volume	Basic density	Sapwood/Heartwood ratio
Water	**0.040**	**<0.001**	0.086
Fertilization	**<0.001**	**<0.001**	**<0.001**
Stand age	**<0.001**	**<0.001**	**0.001**
Water × Fertilization	0.301	**0.014**	0.699
Water × Stand age	0.630	**0.000**	0.368
Fertilization × Stand age	**<0.001**	**0.001**	0.190
Water × Fertilization × Stand age	0.997	0.679	0.377

From the second year, significant effects of K and Na fertilization on trunk volume, wood basic density, and the sapwood/heartwood ratio were observed. K and Na increased trunk volume by three and two-fold, respectively; however, it generally decreased the wood basic density and sapwood/heartwood ratio. The effects of fertilizers on trunk volume were stronger in older age groups (Figure 2). The 37% throughfall reduction significantly affected trunk volume, mainly under K fertilization, decreasing the trunk volume of trees by 15% at 6 years of age. Wood density decreased significantly with fertilization, and the decrease was higher under Na fertilization than under K fertilization, mainly under normal water availability. Under 37% throughfall reduction, the effects of K fertilization on wood density were not significant. The effect of throughfall reduction was significant mainly at 4 years of age for Na fertilization.

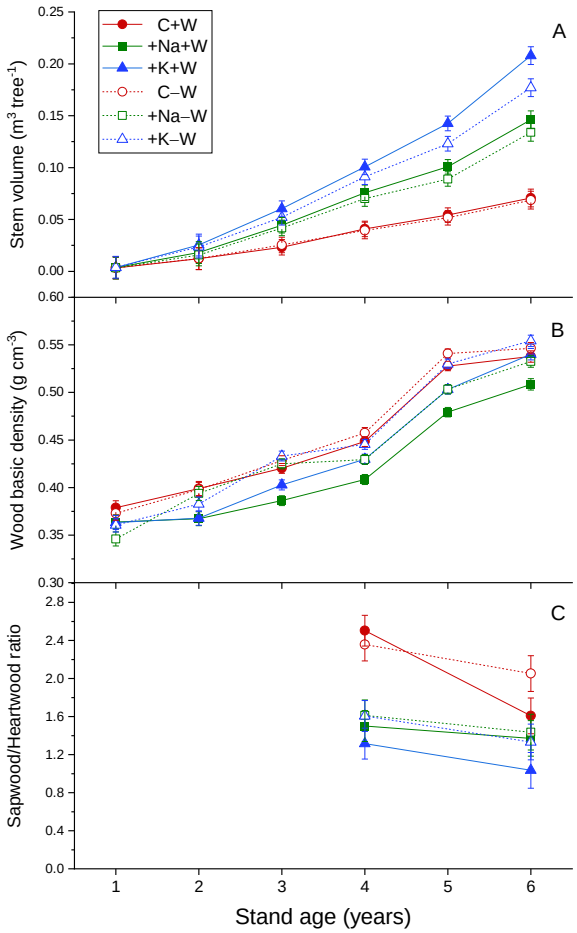

Figure 2. Trunk volume (A), wood basic density (B), and the sapwood/heartwood ratio (C) by treatment of fertilization and water regime over the stand age of *Eucalyptus grandis* trees. The vertical bars indicate standard error.

Fertilization regimes significantly affected fiber and vessel features, except fiber wall thickness. Throughfall reduction did not significantly affect the fiber and vessel features. Non-significant interactions between water supply and fertilization regime on fiber and vessel features (except for fiber diameter) showed that effects of K and Na did not change with the different water availability conditions (Table 2). In addition, there were significant interactions between fertilization regime and stand age in many fiber and vessel features. In these, effects of K and Na were significant only from 2 years of age. In contrast, fiber diameter was significantly affected by K and Na were only at 1 and 2 years of age.

Table 2. Effects of water regime, fertilization regime, stand age, and its interactions with fiber and vessel features. p-value<0.05, bold indicates significant effect.

Factors	Fiber length	Fiber diameter	Wall thickness	Vessel diameter	Vessel density	Vessel area	Sapwood total vessel area
Water	0.155	0.113	0.609	0.281	0.386	0.422	0.317
Fertilization	**<0.001**	**0.002**	0.902	**<0.001**	**<0.001**	**<0.001**	**<0.001**
Stand age	**<0.001**	**<0.001**	**<0.001**	**<0.001**	**<0.001**	**<0.001**	**<0.001**
Water × Fertilization	0.508	**0.025**	0.079	0.303	0.451	0.780	0.637
Water × Stand age	0.721	**0.009**	0.085	0.560	0.437	0.571	0.918
Fertilization × Stand age	**0.013**	**0.028**	0.157	0.093	**0.033**	**0.033**	**0.004**
Water × Fertilization × Stand age	0.084	0.323	0.928	0.641	0.928	0.951	0.980

Fiber length increased significantly under K and Na fertilization from 2 years of age, regardless of water availability. The effects of fertilization on fiber diameter were not consistent over time. Fiber wall thickness was not affected by fertilization or water availability over time (Figure 3). In all treatments, the length and diameter of fibers increased from the first to the fourth year and decreased slightly in the sixth year of growth. In contrast, an increase in wall thickness over 6 years was observed (Figure 3).

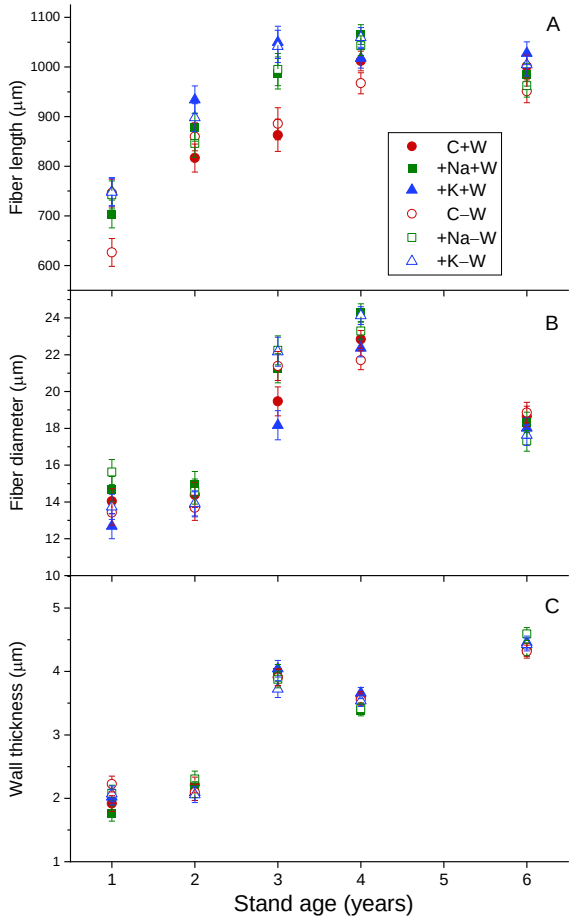

Figure 3. Variations of fiber length (A), fiber diameter (B), and wall thickness (C), throughout the stand age (wood formed in the last year) by treatment of fertilization and water regime on *Eucalyptus grandis* trees. The vertical bars indicate standard error.

Unlike what was observed in the fibers, vessel features were more responsive to K and Na supply. The effects of K and Na on the diameter and density of vessels were significant and consistent from 2 to 6 years of age (Figure 4). K fertilization considerably increased vessel diameter and decreased vessel density, and Na fertilization had an intermediate effect. On the other hand, K and Na fertilization significantly increased the sapwood total vessel area; however, these had a contrary effect on the percentage vessel area. The diameter and percentage area of vessels increased until the third year and then decreased. Vessel density decreased over time, and the sapwood total vessel area increased consistently over time in all treatments (Figure 4).

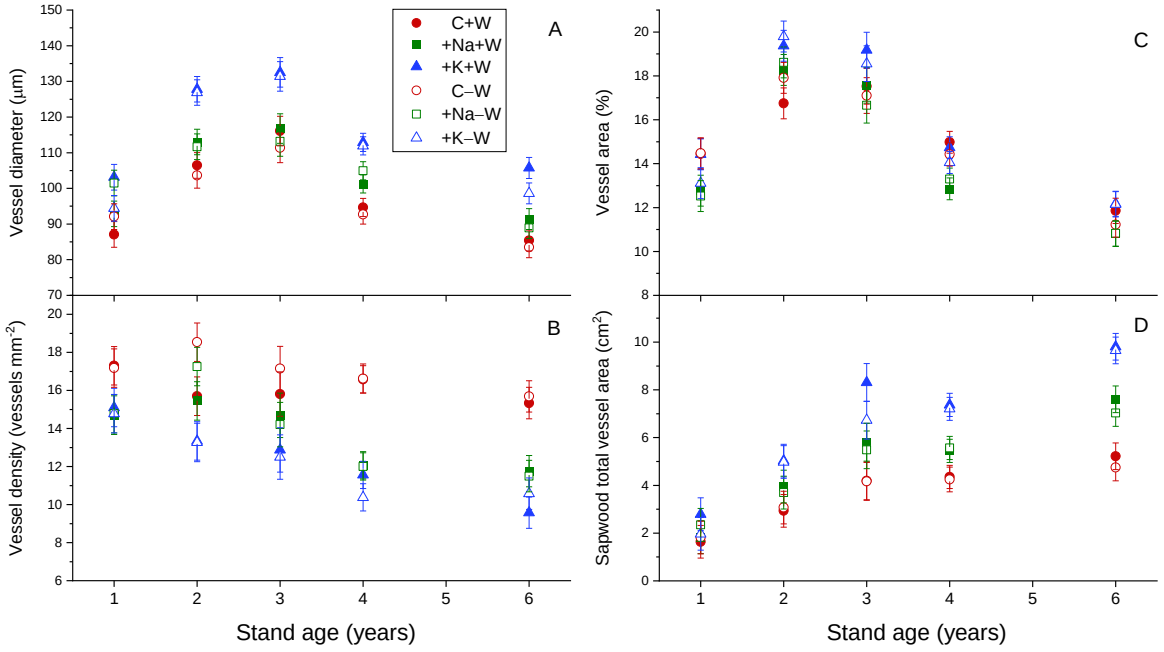

Figure 4. Variations of vessel diameter (A), vessel density (B), vessel area (as a percentage of sapwood area) (C), and sapwood total vessel area (D), throughout the stand age (wood formed in the last year) by treatment of fertilization and water regime, on *Eucalyptus grandis* trees. The vertical bars indicate standard error.

The trees showed a strong negative correlation between basal area MAI and the sapwood/heartwood ratio, and a weak negative correlation between basal area MAI and basic wood density (Figure 5). Removing the variability due to tree size by analysis of covariance (basal area as covariate) showed non-significant effects of fertilization on sapwood/heartwood ratio ($p = 0.09$). In contrast, the significant decrease in basic density in fertilized trees was not strongly induced by the increase in tree growth rate promoted by K and Na.

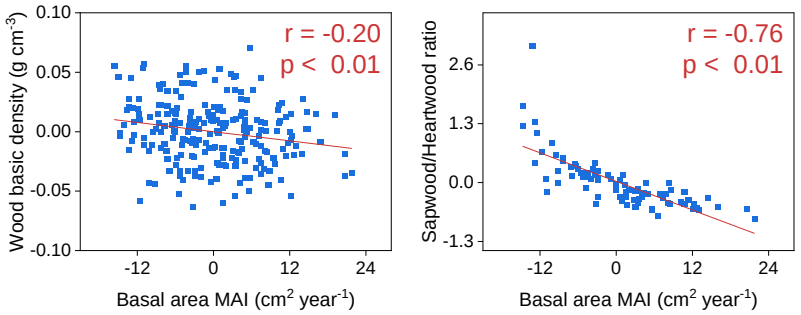

Figure 5. Partial correlation matrix plot between basal area MAI, sapwood/heartwood ratio, and wood basic density, controlling the variable "Stand age." Partial correlations were obtained by the correlations between the residuals of variables after regression on the controlling variable "Stand age". Diagonal cells show histograms of the variables.

As shown for wood basic density and basal area MAI, there was a weak negative correlation between wood apparent density and basal area CAI ($r = -0.22$, $p<0.04$). In addition, as expected, basal area CAI was strongly correlated with vessel diameter ($r = 0.73$, $p<0.001$), vessel density ($r = -0.71$, $p<0.001$), and fiber length ($r = 0.40$, $p<0.001$) (Figure 6A). On the other hand, strong relationships between wood apparent density and wood anatomical features among treatments were observed. Wood apparent density was strongly correlated with fiber diameter ($r = -$

0.74, p<0.001), wall thickness (r = 0.77, p<0.001), vessel diameter (r = -0.48, p<0.001), and vessel area percentage (r = -0.64, p<0.001). A weak correlation was observed with fiber length (-0.35, p<0.05) and a non-significant correlation with vessel density (Figure 6A).

Weaker relationships within each treatment were found between basal area CAI, apparent density, and wood anatomical features (Figure 6B), indicating that the strong relationships observed were caused mainly by inter-treatment variability.

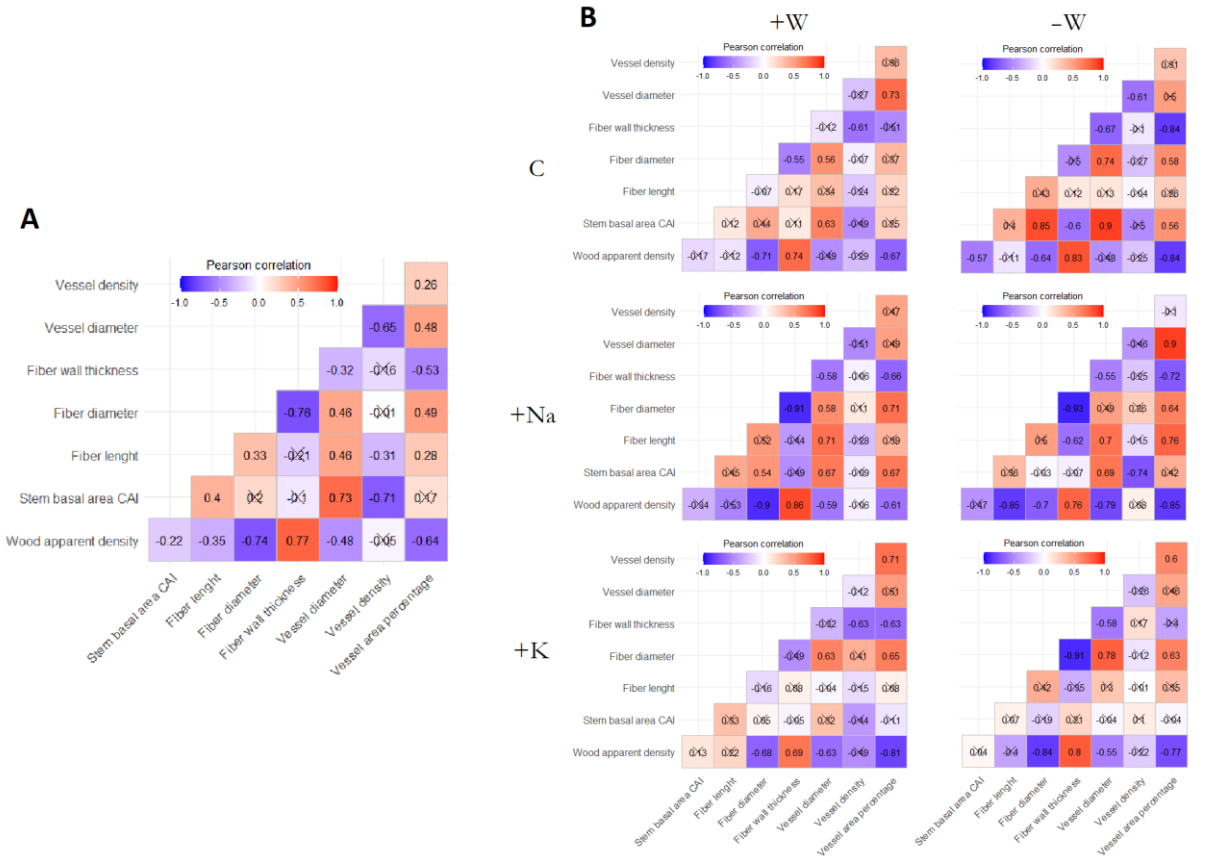

Figure 6. Heatmap plot correlation matrix, between wood apparent density, basal area CAI, and fiber and vessel features, among treatments (A) and within each treatment (B) from four to six years of age. Cross indicates a non-significant correlation coefficient (p>0.05).

4.4. Discussion

4.4.1 Effects on volume and sapwood/heartwood ratio

The positive effects of K and, to a lesser extent, Na on trunk volume, demonstrate the importance of basic fertilization to increase wood production in *E. grandis* plantations in the Itatinga region of Brazil. Similarly, our results confirmed the beneficial effect of these nutrients on tree growth observed during the previous years, where K and Na significantly increased diameter and total height (Castro et al., 2017; Chambi-Legoas et al., 2020), as well as stemwood biomass accumulation, aboveground net primary production, and gross primary production (Battie-Laclau et al., 2016, 2014; Christina et al., 2015).

During the first and second years, trunk volume of trees was not affected by the 37% throughfall reduction; however, from 3 years of age, the throughfall reduction affected the trunk volume only in K-fertilized trees (Figure 2A). Similar effects were reported for trunk biomass accumulation at 2 years of age and basal area at 4 years of age (Battie-Laclau et al., 2014; Chambi-Legoas et al., 2020). In the first year, even a 37% throughfall reduction is not enough to produce a significant decrease in tree growth. However, in the following years, as trees grow, the effects of throughfall reduction were stronger, mainly in K-fertilized trees. This is because of the low water demand of trees and the large amounts of water stored in soils after clear-cutting, which supported fast growth rates at 1 year of age, and to the increase of water consumption of the older trees to maintain high growth rates promoted by the K supply. In contrast, control trees were not affected at all, owing to their low demand for water and higher water reserves in the plot soil (Battie-Laclau et al., 2016; Christina et al., 2018).

Heartwood proportion varied from 33% in C–W and up to 49% in +K+W at 6-year-old K-fertilized *E. grandis* trees. In similar conditions to +K+W, it has been reported 51% of heartwood proportion in *E. grandis* × *E. urophylla* at 6 years old (Gominho et al., 2001) or 56% at 7 years old (Tomazello Filho, 2006). On the other hand, our yearly sampling showed that heartwood formation in *E. grandis* starts between 3 and 4 years of age, regardless of the treatments. The beginning of heartwood formation has only been reported for *E. globulus* between 3 and 5 years of age (Gominho and Pereira, 2005, 2000). Knowing the proportion of heartwood and sapwood at the end of the rotation and understanding its variability due to fertilizers and water availability is important for estimation of pulp yield expected since a lower proportion of heartwood is desired because of the negative impact of heartwood extractives on pulp yield and process efficiency (Lourenço et al., 2011; Morais and Pereira, 2007).

4.4.2 Interactive effects of fertilization × water deficit on wood properties

As we hypothesized, K and Na decreased wood density, the effect of K fertilization being less detrimental than that of Na, from 2 to 6 years of age. However, the effects of K fertilization on wood density were non-significant under 37% throughfall reduction, which could be related to its strong decrease in trunk volume, which alternatively helped improve wood density. In contrast, the effects of Na fertilization were detrimental, regardless of the water regime (Table 1 and Figure 2B). Similarly, increasing water availability by irrigation treatment, a greater decrease in basic wood density by fertilizers is expected (Tomazello et al., 2008).

In contrast, Sette Jr et al. (2014) and Franco (2014) found that the effects of both K and Na fertilization were non-significant on 6-and 8 years old *E. grandis* trees. These differences can be related to the lower Na and K doses applied in these studies: 68 kg ha^{-1} and 116 kg ha^{-1}, respectively (Almeida et al., 2010; Franco, 2014; Sette Jr et al., 2014), approximately 34% lower than the doses applied in our study. There is a tendency for a higher fertilization dose to have a greater effect on the decrease in wood density (Barbosa et al., 2014). The impacts of other nutrients on the wood density of eucalypt trees, such as nitrogen (N) and phosphorus (P) are inconsistent (Assis, 2013; Debell et al., 2001; Wilkins, 1990).

Regarding the fibers, the results partially verified our hypothesis. It showed that from 2 to 6 years of age, K and Na supply affected the fiber length beneficially, regardless of water availability, but did not affect fiber diameter and wall thickness. In another study, no effects of K supply on fiber size were observed (Sette Jr et al., 2014). Other nutrients (or combinations) such as P, N, and NP in older *E. grandis*, *E. grandis* × *E. urophylla,* and *E. globulus* trees also had no effects on fiber properties (Assis, 2013; Pillai et al., 2013; Raymond and Muneri, 2000).

The decrease in vessel diameter and an increase in vessel density reflect adaptation of hydraulic architecture to lower water availability, to maintain sufficient water transport minimizing risks of embolism (February et al., 1995; Pfautsch et al., 2016). Thus, under a 37% throughfall reduction, we expected significant changes in vessel dimensions; however, this did not occur over the 6 years (Figure 4). In other younger trees, changes were also reported not to be significant (Freitas et al., 2015). These results suggest that a 37% throughfall reduction was not enough to cause strong water stress in trees. High root development and distribution in deep soil layers have been identified as a possible factor for improving water availability in –W plots (Christina et al., 2018). In contrast, K and Na fertilization significantly altered vessel anatomy (Table 2), increasing diameter and decreasing density over time as a response to the high water consumption observed in K-and Na-fertilized trees, which are necessary to maintain high growth rates promoted by these nutrients (Battie-Laclau et al., 2016).

4.4.3 The role of stand age

Many studies have assessed the effect of stand age on wood radial variation from pith to bark. Although this is a practical method, it does not provide information on inter-annual variability of wood properties in *Eucalyptus* trees due to the difficulty of delimiting their growth rings. Our study, with independent samples collected annually over 6 years, allowed us to evaluate the inter-annual variability inferring suitably on the effects of stand age on wood properties.

As we hypothesized, there were significant interactions between fertilization and stand age, indicating that the effects of fertilization changed over time. This revealed no effects of K and Na at 1 year of age on wood density, fiber, and vessel features, which could be due to the high intra-annual variability in fiber and vessel size formed at the early stage of growth (juvenile wood) (Zobel and van Buijtenen, 1989). As the plants grow, less juvenile wood is formed (less variability in cell size); therefore, the effects of fertilization and water regimes on wood density, fibers, and vessel size were stronger at older ages.

For many species, as typical of juvenile wood, wood anatomical radial variation is characterized by a continuous increase in fiber size and vessel diameter and a decrease in vessel density from the pith to the bark (Bowyer et al., 2007; Lachenbruch et al., 2011). However, with independent samples over time, our study shows the particular influence of age on the anatomical characteristics of *E. grandis* trees. Although the wall thickness increased and vessel density decreased over 6 years, the length and diameter of fibers increased until the fourth year and then decreased. The diameter and percentage area of vessels increased until the third year and then decreased (Figure 3 and Figure 4). Similarly, in 6.5 years old and 10-to 25-year-old *E. grandis* trees, a lack of upward tendency of radial variation for length, diameter, and lumen width of fibers has been observed (Pillai et al., 2013; Silva et al., 2007).

4.4.4 Relationships between basal area growth and wood properties

The weak correlation between basic density and basal area MAI (Figure 5) and between apparent density and basal area CAI (Figure 6) indicate that differences in growth rate between treatments per se have negligible influences on wood density over the 6 years. Similar results were found in *E. globulus* and *E. saligna* (Debell et al., 2001; Miranda et al., 2001; Raymond and Muneri, 2000).

The strong correlation between sapwood/heartwood ratio and basal area MAI (Figure 5) and the analysis of covariance indicated that the increase in heartwood proportion in K-and Na-fertilized trees is an effect of the

higher growth rates (promoted by the fertilizers) rather than a direct effect of K and Na. The strong influence of trunk diameter on heartwood proportion has been well documented in *E. globulus* (Gominho and Pereira, 2005; Miranda et al., 2006). Therefore, fertilization practices aiming at increasing individual tree radial growth also increase heartwood.

The large basal area CAI promoted by K and Na is associated with increased fiber length, which is desirable for pulp and paper production (Gonçalves et al., 2004); however, the wall thickness, another critical parameter, was not influenced by the basal area growth. As expected, the diameter and density of vessels were correlated with basal area CAI since they are variables involved in the increase of hydraulic conductivity (February et al., 1995), which are higher in trees growing at a high growth rate (as those fertilized with K and Na) in response to the higher demand for water.

Nevertheless, the stronger relationships found between wood apparent density and wood anatomical characteristics (Figure 6) suggest that changes in fiber size (length, diameter, and wall thickness) and vessel size (diameter and area percentage) were the major drivers influencing changes in wood density.

4.5. Conclusions

K and Na fertilization detrimentally affected wood basic density, with more pronounced effects under Na fertilization. However, both K and Na increased the fiber length. The wood density of trees was not affected by K fertilization when growing under conditions of 37% throughfall reduction. In contrast, the effect of Na fertilization on all wood properties assessed was invariable regardless of the water regime. Sapwood/heartwood ratio was highly and negatively correlated with growth rate, indicating an effect due to growth rate rather than fertilization.

Both the K and Na supply considerably increased the trunk volume by approximately three and two-fold, respectively. A 37% throughfall reduction would negatively affect trunk volume only in K-fertilized trees. Thus, the beneficial effects of K and Na on trunk volume, even under lower water availability, largely compensate for the loss in wood density.

As expected, throughout the complete rotation, the density of the wood and the quality of the fiber increased steadily with stand age across treatments. However, the vessel size increased only until the third year and then decreased. The effects of fertilization and water regimes on trunk volume and wood properties changed over time, with significant effects from 2 years of age and non-significant effects in the first year. Another important finding was the significant correlation between fiber length and basal area growth rate among treatments, which indicates that fiber length enhancement could have been induced by a higher growth rate promoted by K and Na. The weak correlation between the basal area growth rate and wood density indicated that high basal area growth does not worsen wood density. Although K and Na did not significantly affect the wall thickness, large variations in the wood density were strongly related to small variations in the fiber wall thickness.

These findings highlight the significant effects of K addition on trunk volume without significant losses on wood quality, even under water stress, in commercial *E. grandis* plantations. Na as a substitute for K should consider the negative impacts on the wood density of *E. grandis* trees and their lower productivity. Future studies should address the interactive effects of fertilization, water availability, and stand age, on the chemical properties of wood, as it is likely that there is an effect on chemical properties (lignin and cellulose content), and the benefits or detriment of K and Na on wood quality could be enhanced or balanced by chemical effects on wood.

CRediT authorship contribution statement

Roger Chambi-Legoas: Conceptualization, Methodology, Formal analysis, Investigation, Data curation, Writing - original draft, Writing - review & editing, Visualization. **Gilles Chaix:** Conceptualization, Methodology, Investigation, Resources, Writing - review & editing, Supervision, Project administration, Funding acquisition. **Vinicius R. Castro:** Data curation, Investigation, Writing - review & editing. **Mariana P. Franco:** Data curation, Investigation, Writing - review & editing. **Mario Tomazello-Filho:** Methodology, Resources, Writing - review & editing, Supervision, Project administration, Funding acquisition.

Declaration of Competing Interest

The authors declare that they have no known competing financial interests or personal relationships that could have appeared to influence the work reported in this paper.

Acknowledgments

We gratefully acknowledge Rildo M. Moreira and the staff of the Itatinga Research Station (ESALQ/USP) for their technical support in sample collection. We also thank Luiz Santini, Maria Aparecida Bermudez, and Aparecido Candido Siqueira for their excellent support in the preparation of wood samples and histological plates. Roger Chambi-Legoas was supported by a scholarship from Fondo Nacional de Desarrollo Científico, Tecnológico y de Innovación Tecnológica (FONDECYT-CONCYTEC, Perú) (Award Number 239-2018).

Funding Sources

This research was partially funded by the Agropolis Foundation under the reference ID1203-003 through the «Investissements d'avenir» program (LabexAgro/ANR-10-LABX-0001-01), Conselho Nacional de Desenvolvimento Científico e Tecnológico (CNPq) (444793/2014-3 and 014/2012), and Fundação de Amparo à Pesquisa do Estado de São Paulo (Fapesp) (2013/25642-5).

References

Almeida, J.C.R., Laclau, J.P., Gonçalves, J.L. de M., Ranger, J., Saint-André, L., 2010. A positive growth response to NaCl applications in Eucalyptus plantations established on K-deficient soils. For. Ecol. Manage. 259, 1786–1795. https://doi.org/10.1016/j.foreco.2009.08.032

Arend, M., Fromm, J., 2007. Seasonal change in the drought response of wood cell development in poplar. Tree Physiol. 27, 985–992. https://doi.org/10.1093/treephys/27.7.985

Asensio, V., Domec, J.C., Nouvellon, Y., Laclau, J.P., Bouillet, J.P., Jordan-Meille, L., Lavres, J., Rojas, J.D., Guillemot, J., Abreu-Junior, C.H., 2020. Potassium fertilization increases hydraulic redistribution and water use efficiency for stemwood production in Eucalyptus grandis plantations. Environ. Exp. Bot. 176, 104085. https://doi.org/10.1016/j.envexpbot.2020.104085

Assis, C.O. De, 2013. Níveis de fertilização e seus efeitos no crescimento, nas características da madeira e do carvão em clones de híbrido de Eucalyptus grandis x Eucalyptus urophylla. Universidade de Lavras.

Barbosa, B.M., Colodette, J.L., Cabral, C.P.T., 2014. Efeito da fertilização na qualidade da madeira de Eucalyptus spp. Sci. For. 42, 29–39.

Battie-Laclau, P., Delgado-Rojas, J.S., Christina, M., Nouvellon, Y., Bouillet, J.-P., Piccolo, M. de C., Moreira, M.Z., Gonçalves, J.L. de M., Roupsard, O., Laclau, J.-P., 2016. Potassium fertilization increases water-use efficiency for stem biomass production without affecting intrinsic water-use efficiency in Eucalyptus grandis plantations. For. Ecol. Manage. 364, 77–89. https://doi.org/10.1016/j.foreco.2016.01.004

Battie-Laclau, P., Laclau, J.P., Domec, J.C., Christina, M., Bouillet, J.P., de Cassia Piccolo, M., de Moraes Gonçalves, J.L., Moreira, R.M., Krusche, A.V., Bouvet, J.M., Nouvellon, Y., 2014. Effects of potassium and sodium supply on drought-adaptive mechanisms in Eucalyptus grandis plantations. New Phytol. 203, 401–413. https://doi.org/10.1111/nph.12810

Battie-Laclau, P., Laclau, J.P., Piccolo, M. de C., Arenque, B.C., Beri, C., Mietton, L., Muniz, M.R.A., Jordan-Meille, L., Buckeridge, M.S., Nouvellon, Y., Ranger, J., Bouillet, J.P., 2013. Influence of potassium and sodium nutrition on leaf area components in Eucalyptus grandis trees. Plant Soil 371, 19–35. https://doi.org/10.1007/s11104-013-1663-7

Bowyer, J.L., Shmulsky, R., Haygreen, J.G., 2007. Forest Products and Wood Science: An Introduction. Wiley.

Câmara, A.P., Vidaurre, G.B., Oliveira, J.C.L., de Toledo Picoli, E.A., Almeida, M.N.F., Roque, R.M., Tomazello Filho, M., Souza, H.J.P., Oliveira, T.R., Campoe, O.C., 2020. Changes in hydraulic architecture across a water availability gradient for two contrasting commercial Eucalyptus clones. For. Ecol. Manage. 474, 118380. https://doi.org/10.1016/j.foreco.2020.118380

Campelo, F., Mayer, K., Grabner, M., 2019. xRing—An R package to identify and measure tree-ring features using X-ray microdensity profiles. Dendrochronologia 53, 17–21. https://doi.org/10.1016/j.dendro.2018.11.002

Castro, V.R., Chambi-Legoas, R., Filho, M.T., Surdi, P.G., Zanuncio, J.C., Zanuncio, A.J.V., 2020. The effect of soil nutrients and moisture during ontogeny on apparent wood density of Eucalyptus grandis. Sci. Rep. 10, 2530. https://doi.org/10.1038/s41598-020-59559-2

Castro, V.R., Surdi, P.G., Tomazello Filho, M., Chaix, G., Laclau, J.P., 2017. Efeito da disponibilidade hídrica e da aplicação de potássio e sódio no crescimento em diâmetro do tronco de árvores de Eucalyptus grandis. Sci. For. 45, 89–99. https://doi.org/10.18671/scifor.v45n113.08

Chambi-Legoas, R., Chaix, G., Tomazello-Filho, M., 2020. Effects of potassium/sodium fertilization and throughfall exclusion on growth patterns of Eucalyptus grandis W. Hill ex Maiden during extreme drought periods. New For. 51. https://doi.org/10.1007/s11056-019-09716-x

Christina, M., Le Maire, G., Battie-Laclau, P., Nouvellon, Y., Bouillet, J.P., Jourdan, C., de Moraes Gon??alves, J., Laclau, J.P., 2015. Measured and modeled interactive effects of potassium deficiency and water deficit on gross primary productivity and light-use efficiency in Eucalyptus grandis plantations. Glob. Chang. Biol. 21, 2022–2039. https://doi.org/10.1111/gcb.12817

Christina, M., le Maire, G., Nouvellon, Y., Vezy, R., Bordon, B., Battie-Laclau, P., Gonçalves, J.L.M., Delgado-Rojas, J.S., Bouillet, J.P., Laclau, J.P., 2018. Simulating the effects of different potassium and water supply regimes on soil water content and water table depth over a rotation of a tropical Eucalyptus grandis plantation. For. Ecol. Manage. 418, 4–14. https://doi.org/10.1016/j.foreco.2017.12.048

Debell, D.S., Keyes, C.R., Gartner, B.L., 2001. Wood density of Eucalyptus saligna grown in Hawaiian plantations : effects of silvicultural practices and relation to growth rate. Aust. For. 64, 106–110. https://doi.org/10.1080/00049158.2001.10676173

Drew, D.M., Downes, G.M., Evans, R., 2011. Short-term growth responses and associated wood density fluctuations in variously irrigated Eucalyptus globulus. Trees 25, 153–161. https://doi.org/10.1007/s00468-010-0494-x

Drew, D.M., Downes, G.M., O'Grady, A.P., Read, J., Worledge, D., 2009. High resolution temporal variation in wood properties in irrigated and nonirrigated Eucalyptus globulus. Ann. For. Sci. 66, 406–406. https://doi.org/10.1051/forest/2009017

Epron, D., Cabral, O.M.R., Laclau, J.P., Dannoura, M., Packer, A.P., Plain, C., Battie-Laclau, P., Moreira, M.Z., Trivelin, P.C.O., Bouillet, J.P., Grant, D., Nouvellon, Y., 2015. In situ 13CO2 pulse labelling of field-grown eucalypt trees revealed the effects of potassium nutrition and throughfall exclusion on phloem transport of photosynthetic carbon. Tree Physiol. 36, 6–21. https://doi.org/10.1093/treephys/tpv090

February, E.C., Stock, W.D., Bond, W.J., Le Roux, D.J., 1995. Relationships between water availability and selected vessel characteristics in Eucalyptus grandis and two hybrids. IAWA J. 16, 269–276. https://doi.org/10.1163/22941932-90001410

Franco, M.P., 2014. Efeito da substituição do potássio pelo sódio em árvores de Eucalyptus grandis W. Hill ex Maiden, visando a expansão das plantações florestais sob condições de estresse hídrico. Universidade de São Paulo, Piracicaba. https://doi.org/10.11606/D.11.2014.tde-28072014-145056

Franklin, G.L., 1945. Preparation of thin sections of synthetic resins and wood-resin composites, and a new macerating method for wood. Nature 155, 51. https://doi.org/10.1038/155051a0

Freitas, P.D.C. e, Sette Jr, C.R., Castro, V.R. De, Chaix, G., Laclau, J.P., Tomazello Filho, M., 2015. Efeito da disponibilidade hídrica e da aplicação de potássio e sodio nas característica anatômicas do lenho juvenil de Eucalyptus grandis. Árvore 39, 405–416. https://doi.org/10.1590/0100-67622015000200020

Gominho, J., Figueira, J., Rodrigues, J.C., 2001. Within-tree variation of heartwood, extractives and wood density in the eucalypt hybrid Urograndis (Eucalyptus grandis × E. urophylla). Wood fiber Sci. 33, 3–8.

Gominho, J., Pereira, H., 2005. The influence of tree spacing in heartwood content in Eucalyptus globulus Labill. Wood fiber Sci. 4, 582–590.

Gominho, J., Pereira, H., 2000. Variability of heartwood content in plantation-grown Eucalyptus globulus Labill. Wood Fiber Sci.

Gonçalves, J.L. de M., Alvares, C.A., Higa, A.R., Silva, L.D., Alfenas, A.C., Stahl, J., Ferraz, S.F. de B., Lima, W. de P., Brancalion, P.H.S., Hubner, A., Bouillet, J.-P.D., Nouvellon, Y., Epron, D., 2013. Integrating genetic and silvicultural strategies to minimize abiotic and biotic constraints in Brazilian eucalypt plantations. For. Ecol. Manage. 301, 6–27. https://doi.org/10.1016/j.foreco.2012.12.030

Gonçalves, J.L. de M., Stape, J.L., Laclau, J.-P., Smethurst, P., Gava, J.L., 2004. Silvicultural effects on the productivity and wood quality of eucalypt plantations. For. Ecol. Manage. 193, 45–61. https://doi.org/10.1016/j.foreco.2004.01.022

Johansen, D.A., 1940. Plant microtechnique. McGraw-Hill Publishing Company, Ltd., London.

Júnior, C.R.S., Filho, M.T., Dias, C.T.D.S., Chagas, M.P., Laclau, J.P., 2009. Efeito da aplicação de potássio e sódio nas características do lenho de árvores de Eucalyptus grandis W.Hill, aos 24 meses de idade. Floresta 39, 535–546.

Lachenbruch, B., Moore, J.R., Evans, R., 2011. Radial Variation in Wood Structure and Function in Woody Plants, and Hypotheses for Its Occurrence, in: Meinzer, F.C., Lachenbruch, B., Dawson, T.E. (Eds.), Size- and Age-Related Changes in Tree Structure and Function. Springer Netherlands, Dordrecht, pp. 121–164. https://doi.org/10.1007/978-94-007-1242-3_5

Laclau, J.P., Almeida, J.C.R., Gonalves, J.L.M., Saint-Andr, L., Ventura, M., Ranger, J., Moreira, R.M., Nouvellon, Y., 2009. Influence of nitrogen and potassium fertilization on leaf lifespan and allocation of above-ground growth in Eucalyptus plantations. Tree Physiol. 29, 111–124. https://doi.org/10.1093/treephys/tpn010

Laclau, J.P., Ranger, J., de Moraes Gonçalves, J.L., Maquère, V., Krusche, A. V., M'Bou, A.T., Nouvellon, Y., Saint-André, L., Bouillet, J.P., de Cassia Piccolo, M., Deleporte, P., 2010. Biogeochemical cycles of nutrients in tropical Eucalyptus plantations. Main features shown by intensive monitoring in Congo and Brazil. For. Ecol. Manage. 259, 1771–1785. https://doi.org/10.1016/j.foreco.2009.06.010

Lourenço, A., Gominho, J., Pereira, H., 2011. Modeling of sapwood and heartwood delignification kinetics of Eucalyptus globulus using consecutive and simultaneous approaches. J. Wood Sci. 57, 20–26. https://doi.org/10.1007/s10086-010-1137-y

Miranda, I., Almeida, M.H., Pereira, H., 2001. Provenance and site variation of wood density in Eucalyptus globulus Labill. at harvest age and its relation to a non-destructive early assessment. For. Ecol. Manage. 149, 235–240. https://doi.org/10.1016/S0378-1127(00)00560-0

Miranda, I., Gominho, J., Lourenço, A., Pereira, H., 2006. The influence of irrigation and fertilization on heartwood and sapwood contents in 18-year-old Eucalyptus globulus trees. Can. J. For. Res. 36, 2675–2683. https://doi.org/10.1139/X06-130

Morais, M., Pereira, H., 2007. Heartwood and sapwood variation in Eucalyptus globulus Labill. trees at the end of rotation for pulp wood production. Ann. For. Sci. 64, 665–671. https://doi.org/10.1051/forest:2007045

Naidoo, S., Zboňák, A., Pammenter, N.W., Ahmed, F., 2007. Assessing the effects of water availability and soil characteristics on selected wood properties of E . grandis in South Africa. IUFRO Durban 1–11.

Pfautsch, S., Harbusch, M., Wesolowski, A., Smith, R., Macfarlane, C., Tjoelker, M.G., Reich, P.B., Adams, M.A., 2016. Climate determines vascular traits in the ecologically diverse genus Eucalyptus. Ecol. Lett. 19, 240–248. https://doi.org/10.1111/ele.12559

Pillai, P.K.C., Pandalai, R.C., Dhamodaran, T.K., Sankaran, K. V., 2013. Effect of silvicultural practices on fibre properties of Eucalyptus wood from short-rotation plantations. New For. 44, 521–532. https://doi.org/10.1007/s11056-012-9360-6

Rana, V., Singh, S.P., Gupta, P.K., 2011. Eucalypts in Pulp and Paper Industry, in: Bhojvaid, P.P., Kaushik, S., Singh, Y.P., Kumar, D., Thapliyal, M., Barthwal, S. (Eds.), Eucalypts in India. ENVIS Centre on Forestry, Indian Council of Forestry Research and Education, Dehradun, pp. 470–506.

Raymond, C.A., Muneri, A., 2000. Effect of fertilizer on wood properties of Eucalyptus globulus. Can. J. For. Res. Can. Rech. For. 30, 136–144.

Schneider, C.A., Rasband, W.S., Eliceiri, K.W., 2012. NIH Image to ImageJ: 25 years of image analysis. Nat. Methods 9, 671–675. https://doi.org/10.1038/nmeth.2089

Searson, M.J., Thomas, D.S., Montagu, K.D., Conroy, J.P., 2004. Wood density and anatomy of water-limited eucalypts. Tree Physiol. 24, 1295–1302.

Sette Jr, C.R., Deus Jr, J.C. De, Tomazello Filho, M., Pádua, F.A. De, Calil, F.N., Laclau, J.P., 2014. Alterações na qualidade da madeira de Eucalyptus grandis causadas pela adubação mineral. Rev. Cern. 20, 251–258. https://doi.org/10.1590/01047760.201420021499

Sette Jr, C.R., Oliveira, I.R. De, Tomazello Filho, M., Minoru, F., Laclau, J.P., 2012. Efeito da idade e posição de amostragem na densidade e caracteristicas anatômicas da madeira de Eucalyptus grandis. Rev. Árvore 36, 1183–1190. https://doi.org/10.1590/S0100-67622012000600019

Shmulsky, R., Jones, P.D., 2011. Forest Products and Wood Science An Introduction: Sixth Edition, Sixth Edit. ed, Forest Products and Wood Science An Introduction: Sixth Edition. Wiley-Blackwell. https://doi.org/10.1002/9780470960035

Silva, C., Filho, T., Oliveira, S., 2007. Influência da idade e da posição radial nas dimensões das fibras e dos vasos da madeira de Eucalyptus grandis Hill ex . Maiden. Rev. Árvore 31, 1081–1090. https://doi.org/10.1590/S0100-67622007000600013

Tariq, A., Pan, K., Olatunji, O.A., Graciano, C., Li, Z., Li, N., Song, D., Sun, F., Wu, X., Dakhil, M.A., Sun, X., Zhang, L., 2019. Impact of phosphorus application on drought resistant responses of <scp> Eucalyptus grandis </scp> seedlings. Physiol. Plant. 166, 894–908. https://doi.org/10.1111/ppl.12868

Thomas, D.S., Montagu, K.D., Conroy, J.P., 2007. Temperature effects on wood anatomy, wood density, photosynthesis and biomass partitioning of Eucalyptus grandis seedlings. Tree Physiol. 27, 251–260. https://doi.org/10.1093/treephys/27.2.251

Tomazello Filho, M., 2006. Efeito da irrigação e fertilização nas propiedades do lenho de árvores de Eucalyptus grandis x urophylla. Escola Superior de Agricultura Luiz de Queiroz, Universidade de São Paulo.

Tomazello, M., Brazolin, S., Chagas, M.P., Oliveira, J.T.S., Ballarin, a. W., Benjamin, C. a, 2008. Application of X-Ray Technique in Nondestructive Evaluation of Eucalypt Wood. Maderas. Cienc. y Tecnol. 10, 139–149. https://doi.org/10.4067/S0718-221X2008000200006

Wang, Z., Du, A., Xu, Y., Zhu, W., Zhang, J., 2019. Factors limiting the growth of eucalyptus and the characteristics of growth and water use under water and fertilizer management in the dry season of Leizhou Peninsula, China. Agronomy 9, 590. https://doi.org/10.3390/agronomy9100590

Wilkins, A.P., 1990. Influence of silvicultural treatment on growth and wood density of Eucalyptus grandis grown on a previous pasture site. Aust. For. 53, 168–172. https://doi.org/10.1080/00049158.1990.10676074

Zobel, B.J., van Buijtenen, J.P., 1989. Variation Within and Among Trees, in: Zobel, B.J., Buijtenen, J.P. van (Eds.), Wood Variation: Its Causes and Control. Springer-Verlag, pp. 72–131. https://doi.org/10.1007/978-3-642-74069-5_3

5. WOOD DENSITY PREDICTION USING NEAR-INFRARED HYPERSPECTRAL IMAGING: AN APPLICATION TO EARLY SELECTION OF *Eucalyptus grandis* TREES

Abstract

Because its biological nature wood is a heterogeny material, which properties vary across time. It makes difficult to know the wood properties at a given future age of trees. In addition, the site and climate are strong factor that can increase or decrease wood heterogeneity. In this study, we will know if it is possible to make an early selection of *Eucalyptus grandis* trees for wood density and if a drier site can influence early selection. For this, we assessed inter-annual wood density using near-infrared hyperspectral imaging (NIR-HSI), a technique not yet widely tested in Eucalyptus but that has demonstrated good performance to predict wood density and chemical properties in other species. We sample 38 trees of 6 years of age growing under two different water regimes: (i) 37% throughfall reduction (–W), which simulate a dry site, and (ii) undisturbed throughfall (+W). Near-infrared hyperspectral images (NIR-HSI) were used to build high-resolution maps of wood density of the whole cross-section. After delimitation of annual growth rings, average wood density at each age and growth ring was extracted to evaluate juvenile-mature wood correlations. The NIR-HSI calibrated with a weighted partial least square regression (LWPLSR) model demonstrates good performance to predict wood density of whole cross-section (R^2 = 0.73, RMSECV = 0.48 g cm^{-3}). Correlations between ages 1-3 and ages 5-6 were strong (r = 0.85 to 0.94), similarly correlation between rings 1-3 and rings 4-5 were moderate to strong (r = 0.51 to 0.87). In –W plots, juvenile-mature correlations were slightly lower than in +W plots. Our results suggest that juvenile tree selection for wood density, even at 1 year of age, is feasible to predict wood density at 6 years of age. In drier sites, tree selection should be at 3 years of age.

Keywords: NIRS; wood densitometry; water deficit; wood quality; juvenile selection.

5.1. Introduction

Wood density is one of the most important variables for measuring wood quality since it is highly related to many other properties such as strength, stiffness, durability, workability, dimensional stability (Shelly, 2001). In pulp and paper, wood density is related to pulp and paper quality (Rana et al., 2011). Genotypes with the fastest growth rate are the main objective in many breeding programs of Eucalyptus, which could lead to a decrease in wood density with future fast-growing varieties since higher growth rates are moderately related to lower wood densities (Chambi-Legoas et al., 2021; Wilkins and Horne, 1991). Therefore, although improving wood density of Eucalyptus trees is not yet in demand in breeding programs, it is important to anticipate future needs to select varieties not only for high growth rates but also for lower growth/wood density ratios. For other uses such as furniture and construction, the selection of varieties for wood density is crucial. The strong correlations between wood densities at juvenile and mature stages assure the suitable selection of the best varieties at juvenile stage.

However, due to its biological nature, wood properties can vary greatly over time, making the wood density prediction difficult at mature stages and, therefore, affecting the suitability of early selection for wood density. Factors such as site, climate variability, and genotype can affect the wood density variation across tree age (Miranda et al., 2001; Wilkins and Horne, 1991; Zobel and van Buijtenen, 1989). Particularly, soil water availability has been shown to affect the density of the wood (Chambi-Legoas et al., 2021), trees growing in drier sites were shown to be able to produce wood with a higher density (Naidoo et al., 2007; Pfautsch et al., 2016). This suggests that long-term drier conditions could increase/decrease wood density heterogeneity due to impacts on growth rate and wood anatomy (Chambi-Legoas et al., 2021, in publication). Then it would be possible a marked difference in juvenile-mature correlation in wood density between trees growing in drier sites and trees growing in wet sites.

Nevertheless, the determination of inter-annual (between tree rings) variation must represent the whole tree for wood density predictions. Thus, since lateral growth reflects most of the growth responses to environmental variability, mapping wood density over the whole cross-section is an efficient method for evaluating juvenile-mature correlations.

Commonly, density variation in annual rings is performed using X-ray microdensitometry (XRD). Although this technique provides high spatial resolution and accuracy in wood density estimation, it is time-consuming. It only allows analyzing a small region from wood disks because of the difficulty of obtaining a thin and uniform cut of entire discs (Fernandes et al., 2013a). Therefore, it appears that XRD alone is not a reliable tool to analyze the whole discs samples.

Near-infrared hyperspectral imaging (NIR-HSI) is a technique that integrates the near-infrared spectroscopy (NIRS) and digital imaging. The NIR-HSI measures the interaction of near-infrared radiation (780 to 2500 nm wavelengths) with the matter at several points simultaneously. This interaction is quantified by reflectance or transmittance and collected as a hyperspectral image, a reflectance spectra record for each pixel of the target surface over hundreds of wavelengths (Bhargave, 2013; Geladi et al., 2004). As a result, a hyperspectral cube, composed of a series of images at each wavelength, is generated (Yin et al., 2017). NIR-HSI allows the simultaneous obtention of spectral and spatial information of the entire samples (Yin et al., 2017). Time-consuming is low because the spectral collection does not require sample preparation, and it allows for the analysis of the whole cross-section of discs. Thus, NIR-HIS can be a valuable and practical tool if appropriate models can be developed to calibrate spectral information to estimate the target variables. Density profiles from XRD can be used as reference values to develop calibration models for NIR-HIS.

NIR-HIS images have already been used to measure wood density of loblolly pine (*Pinus taeda* L.) log disks (Mora et al., 2011), subalpine fir (*Abies lasiocarpa* Hook) boards (Haddadi et al., 2015), quaking aspen (*Populus tremuloides* Michx), balsam poplar (*Populus balsamifera* L.), and black spruce (*Picea mariana* Mill.) logs (Haddadi et al., 2016), resulting in calibration and validation models with high accuracies. However, all these studies have measured the average densities of the whole cross-section of disks because reference data were measured in large or whole sections of disks. Mapping the wood density variation along radial or cross-sections at high spatial resolution using the NIR-HSI technique needs reference data of wood density at a high spatial resolution for spectral calibration information of NIR-HIS images, such as those provided by micro X-ray densitometry. The only studies of this type were developed in stone pine (*Pinus pinea* L.) samples, resulting in robust prediction models (Fernandes et al., 2013a, 2013b).

Particularly, in Eucalyptus species, there are no studies reporting predictions models of wood density using NIR-HIS. However, many available studies are using NIRS, such as for *Eucalyptus globulus* radial increment cores (Downes et al., 2014, 2011), *Eucalyptus urophylla* disks (Hein et al., 2009a), *Eucalyptus grandis* logs (Rosso et al., 2013), *E. grandis* disks (Hein et al., 2009b) and *Eucalyptus camaldulensis* log disks (Inagaki et al., 2012), all with robust calibration models for wood density predictions.

In this framework, we investigated the use of NIR-HSI in combination with XRD to indirectly estimate wood density from relating XRD density values with NIR-HSI spectra, and thus, evaluate the juvenile-mature correlations on wood density for early selection of *E. grandis* trees. The objective of this study was (i) to evaluate the performance of using NIR-HSI to estimate wood density variation across age, (ii) to estimate the juvenile-mature correlations on wood density, and (iii) to examine the effects of water deficit on these correlations. The results of this

study should provide helpful insights to evaluate the reliability to select for wood density at early growth stages in *E. grandis* trees growing in different soil water availability conditions using NIR-HSI.

5.2. Material and Methods

5.2.1. Sampling description

The samples used in this study come from an experimental plantation of a highly productive *E. grandis* clone, installed in June 2010 at the Itatinga Experimental Station of the University of São Paulo, São Paulo State, Brazil (23°02'S, 48°38'W, 850 m a.s.l.). The experimental plantation consisted of two levels of water regime: 37% throughfall reduction and non-throughfall reduction, and three levels of fertilization: potassium supply, sodium addition, and control (no potassium nor sodium supply), distributed in three blocks, arranged in a split-plot design. More information about the experiment can be found in Battie-Laclau et al. (2016) and Chambi-Legoas et al. (2019).

Fifty-four trees (9 trees by treatment) were sampled randomly at 6 years after planting. A cross-sectional disk (3 cm height) at breast height was cut from each tree.

One face of the disks was polished (120 sandpaper, 120 grains $inch^{-2}$) to remove surface imperfections and burrs, obtaining a clean and perfect surface. In the sequence, to reduce and homogenize the wood moisture content of samples, discs were conditioned in a climatic chamber (20 °C, 60% HR) for 48 hours, reaching 12- 15% moisture content of the wood.

5.2.2. Acquisition and pre-processing of near-infrared hyperspectral images

The near-infrared hyperspectral images (NIR- HSI) were obtained using a stationary chemical imaging camera (SisuCHEMA, SWIR, Specim®). According to Franco (2018), the equipment has a 30 mm front lens (50-100 mm field of view) and a line scanning system, operating in a wavelength range of 928 to 2524 nm with intervals of 6 nm. The sample scanning speed is 40 mm/sec. This wavelength range was segmented into 256 spectral channels, resulting in a NIR-HSI image cube with 256 images. Image acquisition was carried out on the transversal polished face of disks, with a spatial resolution of 625 μm/pixel. The HI-NIR data were transformed into pseudo-absorbance values using a white reference standard and dark internal reference. For this, a logarithmic function was applied for relating total reflectance and sample spectrum, and both were corrected for the dark reference (Franco, 2018).

The first 20 and the last 10 wavelength channels were removed because it was too noisy. The retained 226 channels comprising between 1048 nm to 2456 nm wavelength were used to process NIR-HSI images (Figure 1).

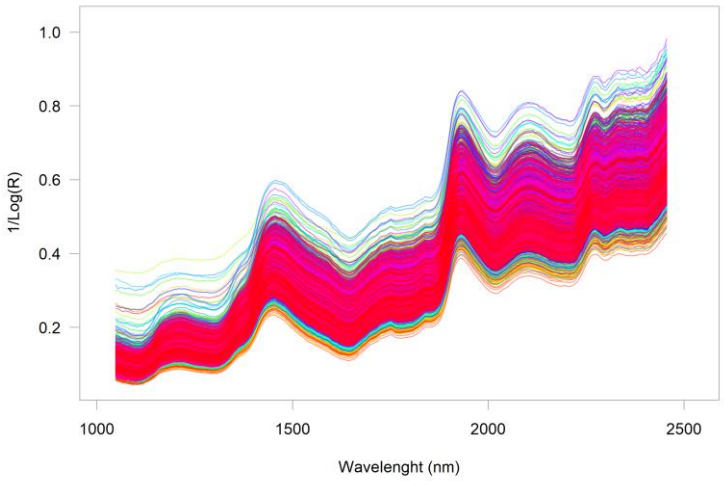

Figure 1. Reflectance spectra 1048 - 2456 nm of the *E. grandis* wood samples.

5.2.3. Wood density data by X-ray densitometer and matching to NIR-HSI images

Rectangular prism sections bark-to-bark (2 cm width and 3 cm height, pith centered) were cut from the cross-sectional discs at breast height, and in the sequence, the sections were glued to wooden supports. Then, a thin diametrical slice (1.7 to 2.0 mm thickness) was cut (perpendicular to the fibers) from the same face of NIR-HIS image acquisition (polished face) of each disk, using a parallel double circular sawing equipment.

The samples were conditioned in a climatic chamber (20 ° C, 60% HR) for 48 hours, reaching 12- 15% wood moisture content. Subsequently, radiographic images of wood samples were obtained using the Faxitron MX-20 Cabinet X-Ray Imaging System (Faxitron X-Ray Corporation, Lincolnshire, IL, USA) of the Laboratory LAIM of University of São Paulo (USP). The X-ray images were produced with 10 kV and 30 mA and an exposure time of 10 seconds at a resolution of 27 μm per pixel and saved in TIF format.

Matching the entire X-ray images with NIR-HIS images is complex and can produce pixel misallocation errors. To deal with this, we defined a region of interest (ROI) of ≈1.9 mm wide (passing through the pith and excluding bark), which comprises 70 pixels for X-ray images and 3 pixels for NIR-HSI images (Figure 2).

For each NIR-HIS image, the pixels delimited by the ROI were extracted and averaged at each row. In X-ray images, using the X-ring package (Campelo et al., 2019) in R software, a calibration curve was fitted from known values of density and thicknesses of a step-wedge recorded in each image. Then, based on the grayscale value of pixels and sample thickness, the wood density profile values were calculated at 1-pixel intervals (27 μm) along with the ROI. Finally, we divided and averaged the profile into as many values as pixels rows had the NIR-HIS image to assign a density value to each pixel row of NIR-HIS images (Figure 2).

As a result, 8000 measurements (42 disks, between 112-221 measurement by disk) of hyperspectral reflectance and corresponding density value were created for the PLS-based calibrations.

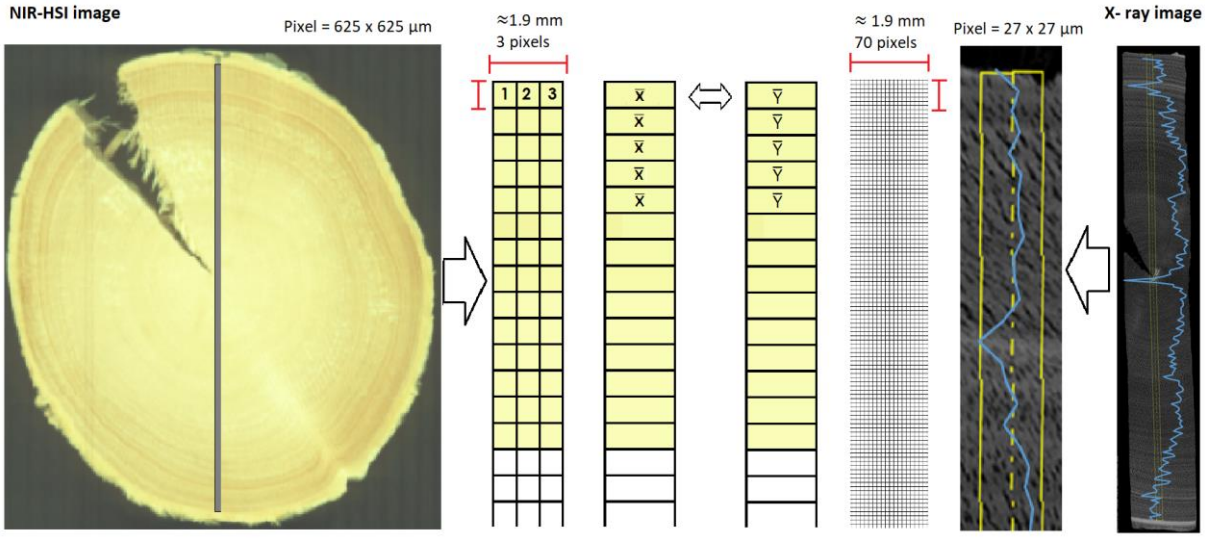

Figure 2. Schematic representation of the pre-processing of NIR-HSI. The NIR-HSI images were analyzed into a region of interest of three pixels width (≈1.9 mm). Then, the spectra of three pixels were averaged at each row and matched to pixels of X-ray images.

5.2.4. Sampling and distribution of spectra and wood density values

The pith region has an unusually high density due to its chemical composition, producing abnormal spectra compared to spectra of normal wood (Rodrigues et al., 2013). Due to this reason, the pith region spectra were removed.

We divided the data into a group for model calibration (calibration group) and model-independent validation (validation group). One row out of every 6 rows was extracted from data ordered by ascending density value for the validation group. Thus calibration and validation group had 2065 (83%) and 413 (17%) observations, respectively.

In order to identify other abnormal spectra (outliers), a principal component analysis (PCA) was applied to the first derivatives of spectra (1st der). PCA reduced the high dimensionality of data (226 variables) to two principal components (PCs), which explained the 92% of data variability. From the PCA, no outliers were detected (Figure 3). In addition, PCA showed a high representative sampling for the validation group. Spectra extraction of NIRS-HSI images was performed in MATLAB R2015a software (The Mathworks Inc., Natick, MA, USA).

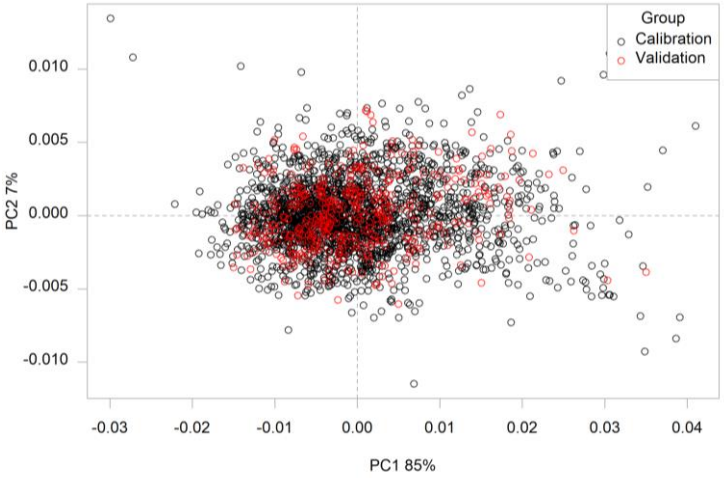

Figure 3. Principal component analysis (PCA) score plots (PC1 and PC2) of the preprocessed spectra for calibration and validation data sets.

Boxplots and histograms of wood density values showed that the validation group was a highly representative sample of data. Wood density values of both groups followed a normal distribution (Figure 4 and Figure 5).

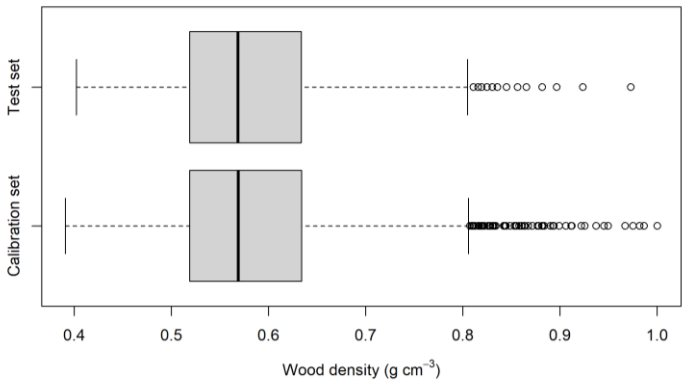

Figure 4. Boxplots of wood density values for calibration and validation data sets.

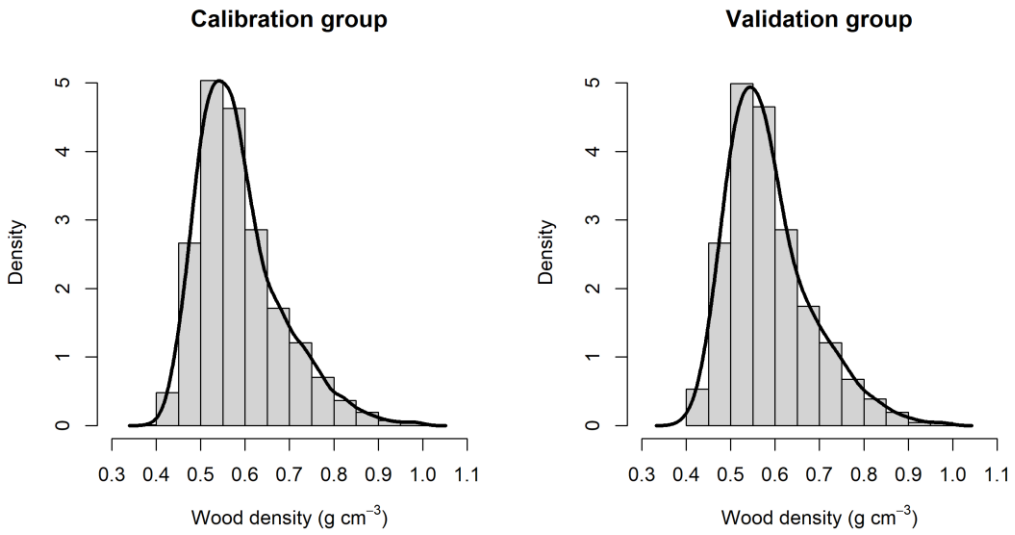

Figure 5. Density curve and histogram of wood density values for calibration and validation data sets.

5.2.5. Calibration model selection

Two models, PLSR (partial least squares regression) and LWPLSR (locally weighted partial least squared regression), were tested for calibration using the cross-validation (CV) method.

PLS is a multivariate statistical method that projects the independent and dependent variables to a new space so that the relationship between the new variables is as strong as possible (Geladi et al., 2004; Geladi and Kowalski, 1986). In our case, the independent variable consisted of the reflectance values for various spectral channels and at various positions of the sample (pixels), while the dependent variable consisted of wood density values calculated from X-ray microdensitometry. From both variables, the PLS produces a new set of uncorrelated variables called latent variables (LVs). The first few LVs account for most of the variability of the set of independent variables. In a regression step, the PLS uses the firsts LVs to predict the dependent variable, generating a calibration model (Forina et al., 2007).

According to Lesnoff (2021), in LWPLSR, different to standard PLSR, a priori weights are defined from dissimilarities (e.g., distances) between the new observation to predict and the training observations, are given to the n training observations. These weights are used for calculating the PLS scores and loadings and the regression model of the response over the scores (weighted least squares). For each observation to predict, all the n training observations should be used. However, this can be very time-consuming for large n. To avoid this, a k nearest neighbors to the observation to predict is defined in the training set, and then applied to LWPLSR only to this pre-selected neighborhood. We defined k=50 after preliminary trials.

For calibration in CV, the samples are arranged randomly in *k-fold* segments; one segment is removed from the calibration sample set to be used as a sample set for validation. In a new round, the segment returns to the calibration set, and a new segment is selected as validation set. The process is repeated until all the segments have been tested in the validation procedure. The repeated CV can be randomly replicated a desired number of times (nrep). The CV results of each repetition and replication are combined to estimate the model's predictive performance.

In our study, CV were run in five data segments randomly built (*k-fold* = 5) and replicated 20 times (nrep = 20). The numbers of LVs in PLSR and LWPLSR were set at 20. Several pre-treatments of spectra data were tested:

raw : non-pretreatment
snv : Standard normal variate transformation:
detrend : Detrend transformation:
savgol : Savitzky-Golay smoothing
savgol(snv) : savgol of snv
savgol1 : First derivative of Savitzky-Golay smoothing
savgol1(snv) : savgol1 of snv
snv (savgol1) : snv of savgol1
savgol2 : Second derivative of Savitzky-Golay smoothing
savgol2(snv) : savgol2 of snv
snv (savgol2) : snv of savgol2

The models with the minimum root mean square error of cross-validation (RMSECV) provided the optimal number of latent variables (LV's) and best pretreatment to perform independent validation of PLS and LWPLSR models in the validation group data set. The validation procedure consists of evaluating the efficiency of the calibration model in the prediction of new data set (Salzer, 2008). PLS and LWPLSR were performed in Rstudio software.

5.2.6. Juvenil-mature correlations of wood density.

The best calibration model was applied in NIR-HIS images to create images of wood density map of whole discs (Figure 6A). Annual growth rings were delimitated in discs from increments on diameter at breast height (DBH) measured by dendrometer bands at 14-day intervals in the trees over 6 years. The onset of the growth period was defined in October. Juvenil-mature correlations of wood density were evaluated using two approaches: correlation between individual growth rings (ring-ring correlations) (Figure 6B) and correlation between aggregated growth rings, i.e., area of all the rings from pith up to a given age (age-age correlations) (Figure 6C). Delimitations of growth rings and extraction of mean wood density from growth rings were performed in ImageJ using a personalized macro.

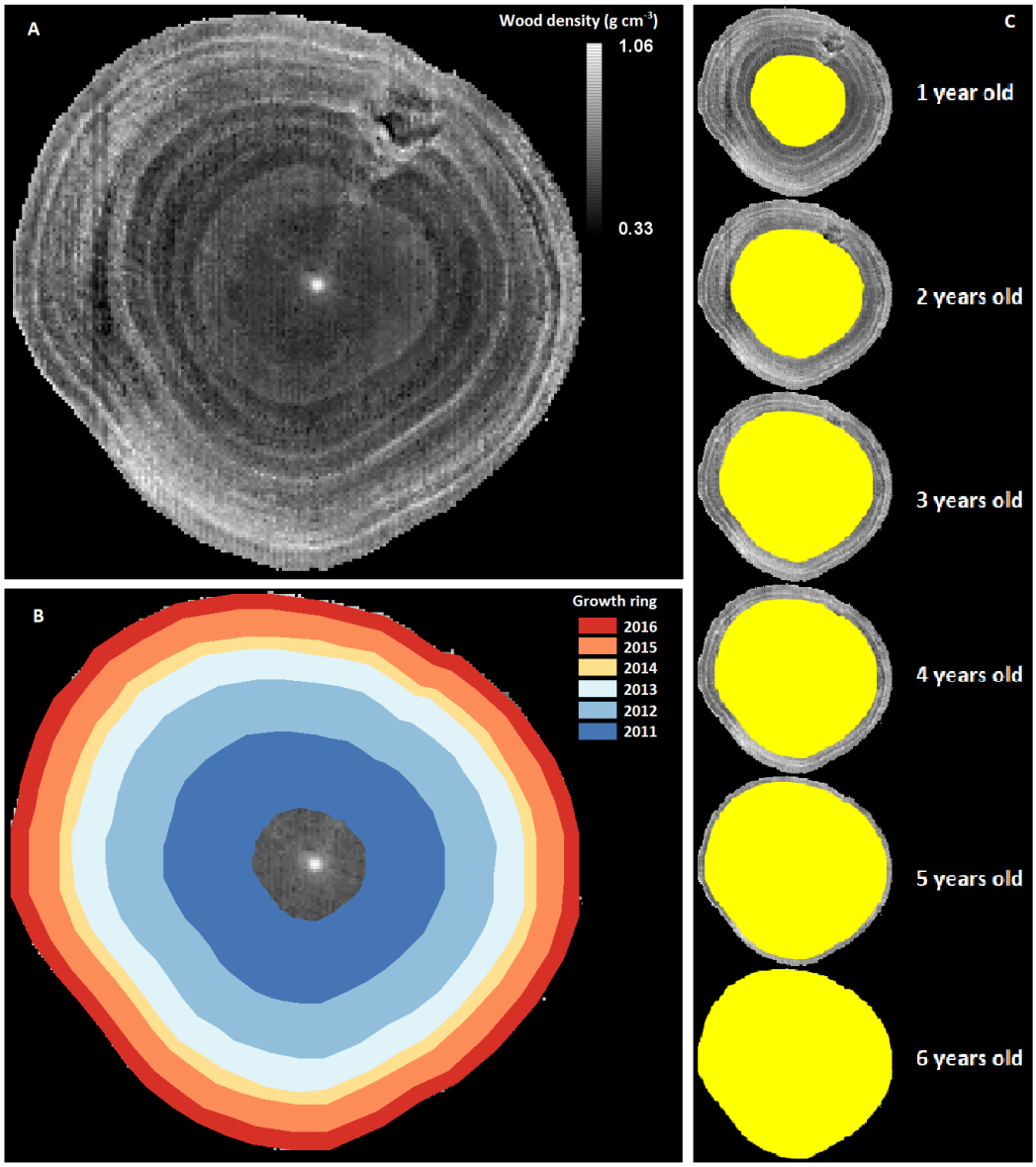

Figure 6. Wood density map of a disc predicted with the best calibration model (A), it annual growth rings (B), and transversal area delimitation at each year old (C).

5.3. Results

The PLSR calibration models in CV with raw spectra and 9 LVs, and with savgol spectra pretreatment and 17 LVs, showed the lowest RMSECV about 0.053 g cm^{-3} and 0.052 g cm^{-3}, respectively. Based on the number of LVs, the model with raw spectra was the best PLSR calibration model in CV (Table 1). However, the LWPLSR calibration models showed higher performance than the PLSR models (Table 2). The LWPLSR model with raw spectra and 3 LVs had the lowest RMSEP (0.047 g cm^{-3}).

Table 1. Parameters of best PLSR calibration models in CV for each pretreatment, based in the minimum RMSECV.

Spectra pretreatments	LVs	RMSECV	R^2_{CV}
raw	9	0.053	0.695
snv	9	0.054	0.679
detrend	9	0.055	0.665
savgol	17	0.052	0.698
savgol(snv)	16	0.054	0.685
savgol1	11	0.053	0.694
savgol1(snv)	11	0.054	0.676
snv(savgol1)	10	0.055	0.672
savgol2	16	0.055	0.662
savgol2(snv)	18	0.056	0.654
snv(savgol2)	16	0.056	0.656

Table 2. Parameters of best LWPLSR calibration models for each pretreatment, based on the minimum RMSEP.

Spectra pretreatments	Number of PC for dissimilarities	*h*	*k*	LVs	RMSEP	R^2
raw	10	2	50	3	0.047	0.753
snv	10	1	300	2	0.048	0.740
detrend	10	1	2065	7	0.051	0.714
savgol	20	2	500	9	0.048	0.747
savgolsnv	20	4	500	13	0.049	0.731
savgol1	10	2	500	8	0.049	0.735
savgol1(snv)	10	2	500	8	0.050	0.728
snv(savgol1)	20	1	500	3	0.051	0.715

The best performance of PLSR models with raw spectra is reached with 9 LVs (Figure 7A), whereas in LWPLSR models, it is with only 3 LVs (Figure 7B).

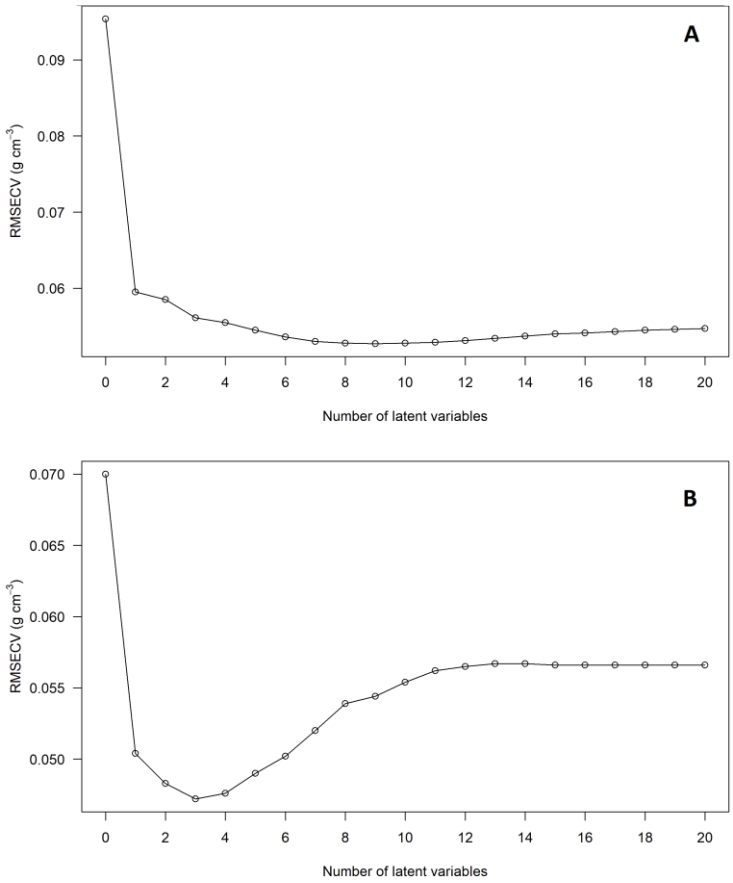

Figure 7. Variation of RMSECV according number of latent variables (LVs) in PLSR calibration model (A) and LWPLSR calibration model, with raw spectra.

In CV, the LWPLSR with 4 LV showed better performance (R^2 = 0.73 and RMSECV = 0.048 g cm^{-3}) than PLSR (R^2 = 0.69 and RMSECV = 0.053 g cm^{-3}) (Figure 8). In independent validation in test set, similar results were found, LWPLSR showed a high performance (R^2 = 0.74 and RMSEP = 0.048 g cm^{-3}) better than PLSR (R^2 = 0.68 and RMSECV = 0.053 g cm^{-3}) (Figure 9).

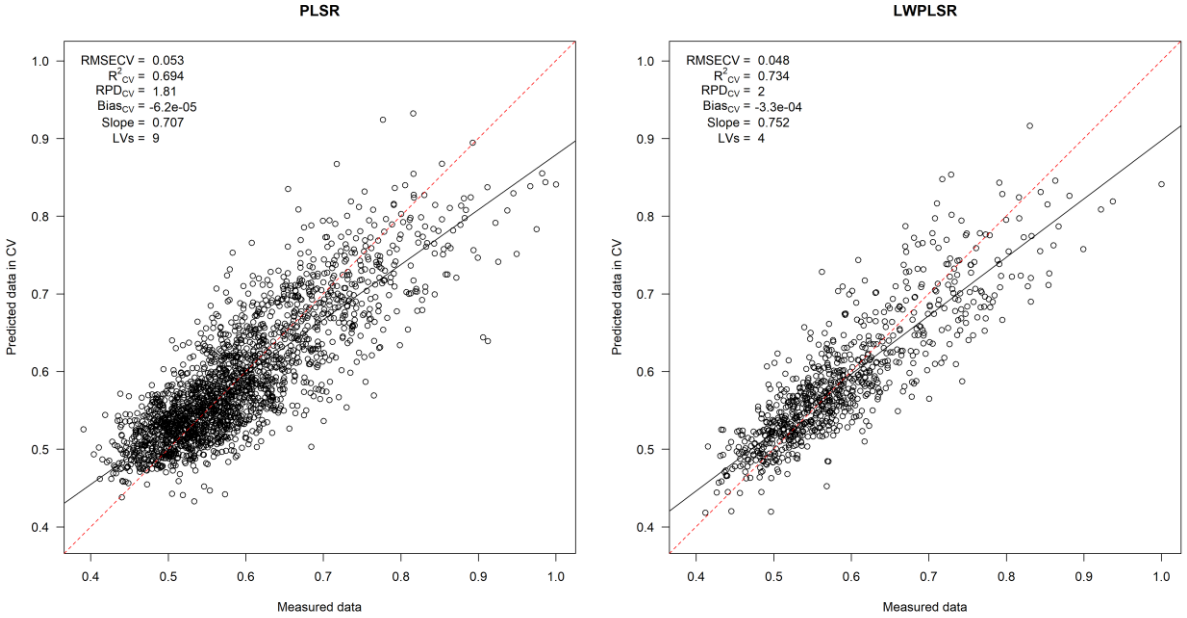

Figure 8. Results of the cross-validation of the PLS calibration model. R^2 is the coefficient of determination; RMSE is the Root quadratic square error. The PLS model was constructed with 6 latent variables (LV).

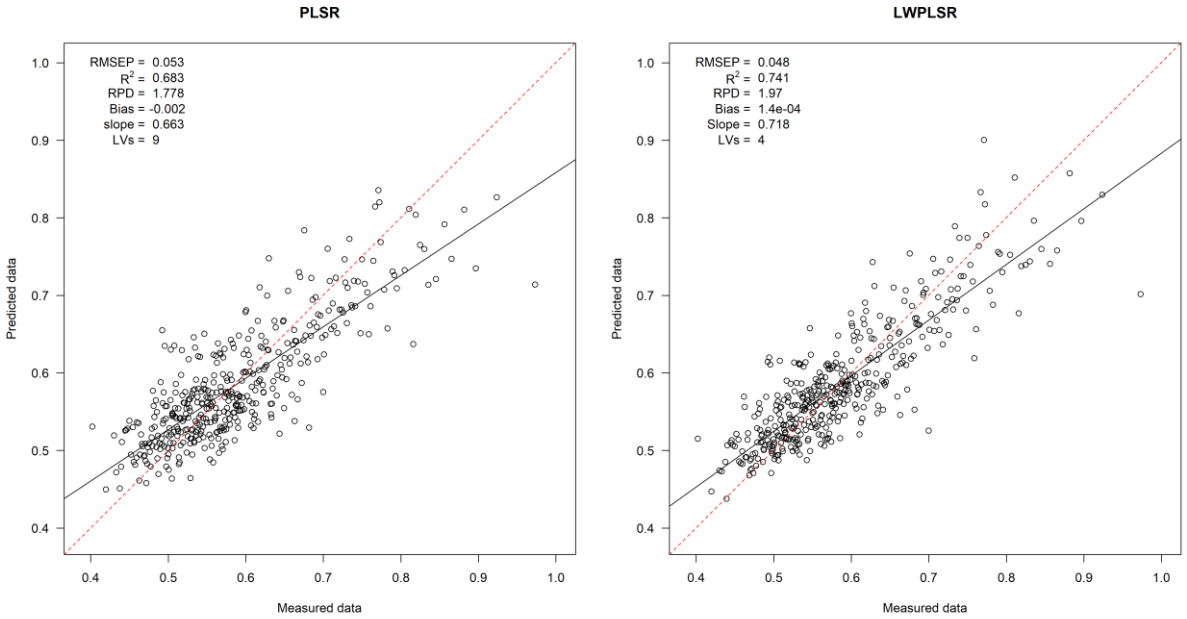

Figure 9. Results of the independent validation (with one sample) of the PLS calibration model. R^2 is the coefficient of determination; RMSE is the Root quadratic square error.

We observed moderate ring-ring correlations between the first and lasts growth rings (r = 0.54 to 0.7) (Figure 10A). Separate analysis for +W and –W trees showed a higher correlation in +W than in –W (Figure 10B).

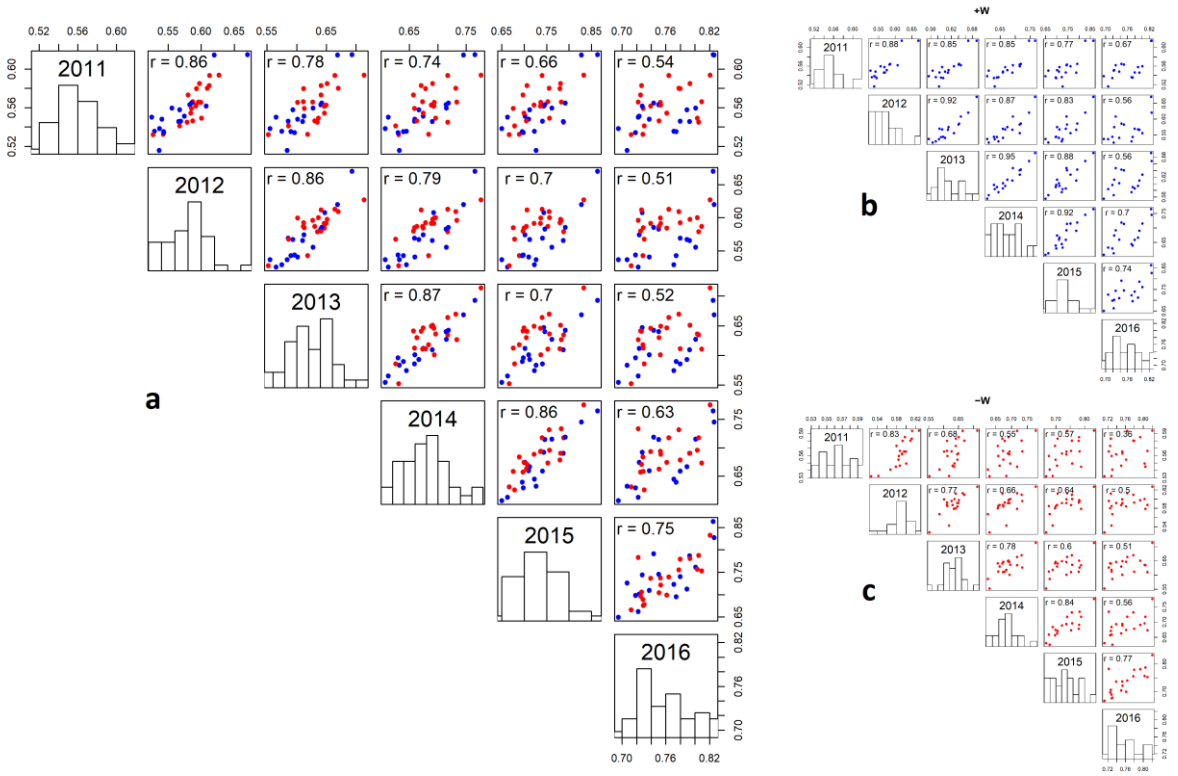

Figure 10. Ring-ring correlation matrix plot for all trees (A), trees under undisturbed throughfall (+W) (b), and trees under 37% throughfall reduction (−W) (c).

Unlike ring-ring correlations, age-age correlations were strong over 6 years. Wood density at 6 years old was highly correlated with wood density at 1 year old (r = 0.85), and correlation increased until 0.9 when correlated with wood density at 3 years old (Figure 11A). Age-age correlations were higher in +W plots than in –W plots (Figure 11B).

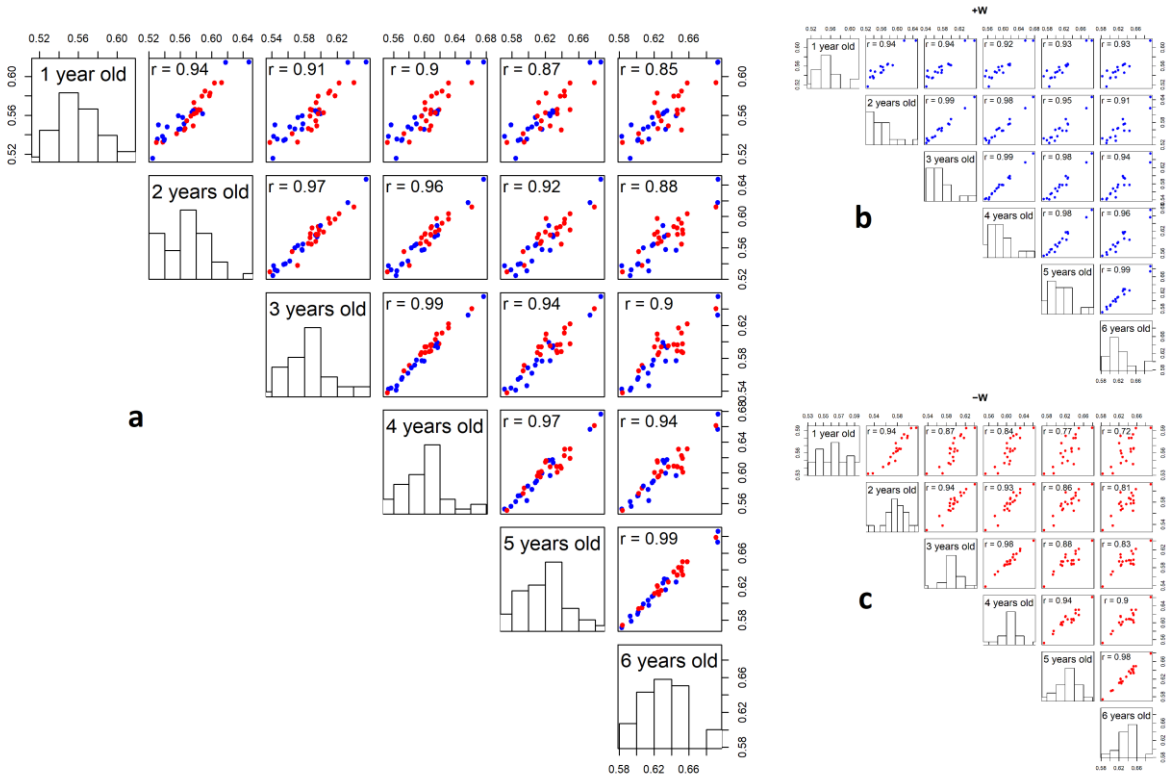

Figure 11. Age-age correlation matrix plot for all trees (a), trees under undisturbed throughfall (+W) (b), and trees under 37% throughfall reduction (−W) (c).

Boxplots showed that inter-annual wood density variation was similar between +W and –W (Figure 12 and Figure 13).

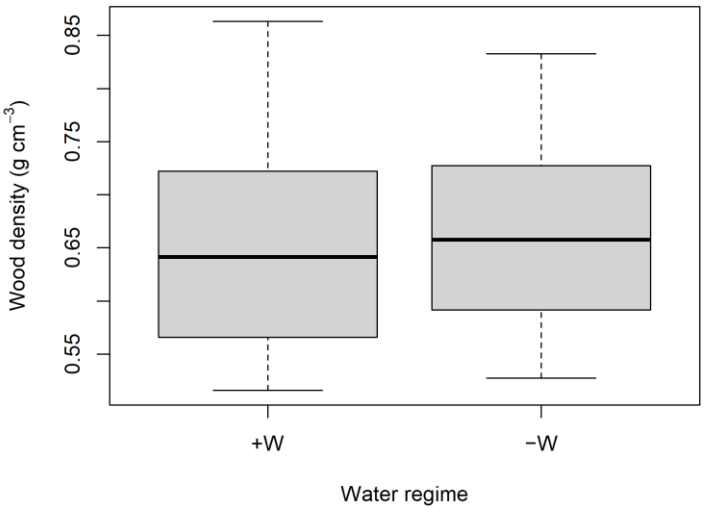

Figure 12. Boxplot of wood density by water regime.

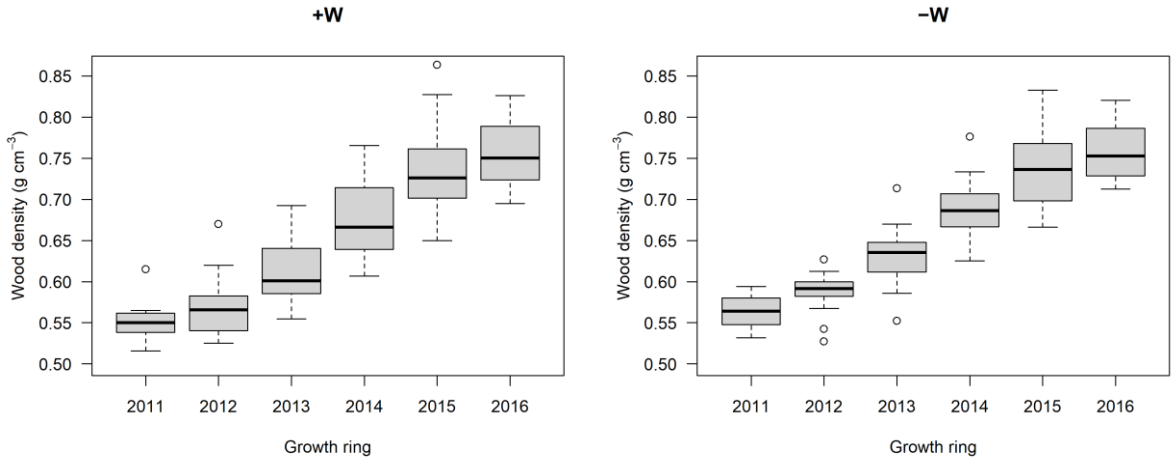

Figure 13. Boxplot of wood density by growth rings and water regime.

5.4. Discussion

Calibration with LWPLS model demonstrated better performance than with PLS model for wood density prediction on *E. grandis* trees. In addition, our LWPLS model produced lower RMSECV = 0.048 g cm-3 that PLS model in *Pinus pinea* which reported a RMSECV= 0.065 g cm-3 (Fernandes et al., 2013a). Other studies focused on estimating the mean density of the whole sample, reported better or worse performance of PLS models. For example, Haddadi et al. (2016) reported an R^2 of 0.49 - 0.91 and RMSECV of 0.01 - 0.043 on cross-validation, and R^2 of 0.48 - 0.70, RMSEP of 0.021 - 0.049 on independent validation, for *Populus tremuloides*, *Populus balsamifera,* and *Picea mariana*. In *Pinus pinea*, the PLS model calibration had an R^2= 0.81 and RMSE=0.024 g cm^{-3} on cross-validation, and R^2=0.71 and RMSEP=0.024 g cm^{-3} on independent validation (Mora et al., 2011).

Applying the LWPLS calibration model on new NIR-HSI images of tree discs provided wood density maps at high resolution (625 µm x 625 µm) valid to explore wood density variations across tree age. As observed, the PLS model calibration of NIR-HSI improves inspection of cross-sectional variation of wood density, compared to X-ray images that are limited to a narrow radial section.

Age-age correlations of wood density were high. At 3 years of age, which is the common selection age for growth (Bouvet, 1992; Bouvet et al., 2003), the wood density was strongly correlated with wood density at 6 years of age (r=0.9). Also, the correlation between age 1 and 6 was 0.85, indicating that selection under 3 years old is also feasible. These results agree with breeding improvement studies in Eucalyptus species. For example, the selection at 3 years of age was efficient to predict wood density at 6 years of age (r = 0.9) for *E. grandis* in Colombia (Osorio et al., 2003). Similarly, correlations for wood density between age 3 and 6 (r = 0.93) were reported for *Eucalyptus nitens* in Australia (Greaves et al., 1997). Even wood density at 16-17 years of age can be efficiently predicted from 4-5 years of age (r = 0.77 to 0.96) in *Eucalyptus globulus* in Australia (Stackpole et al., 2010).

Ring-ring correlations were not as large as the age-age correlations over 6 years. It was expected because annual rings in a younger core make up part of the same core at an older age (i.e., they have rings in common). Thus, age-age correlations for average core values can exist even when the wood properties of different aged rings are uncorrelated (Vargas-Hernandez and Adams, 1992). However, in our study, ring-ring correlations remained high to moderate. Correlation between rings 1-2 and rings 5-6 were moderate-high, varying from 0.51 to 0.7, indicating that

trees with high densities at young ages tended to form denser wood in subsequent years. Then the high age-age correlations were accompanied by significant ring-ring correlations, which is desirable for juvenile selection. It is important for short-cycle plantations where high growth rates in basal area are maintained throughout the cycle, and therefore each growth ring strongly affects the overall density. Similar relations between ring-ring and age-age approaches were also observed for wood density in Douglas-Fir (Vargas-Hernandez and Adams, 1992) and growth in Loblolly pine (Lambeth et al., 1983).

Selection studies in different water regimes are important to know if increasing tree stress affects juvenile-mature correlations for tree selection. In trees subjected to 37% throughfall exclusion (–W) the correlations between 1-2 and 5-6 years old were lower than in trees with normal water availability (+W). However, even under water stress conditions, the selection at 3 years old is efficient (r=081). This point is critical to consider in the framework of tree breeding programs when tests are made in water deficit regions. This study provides new experimental data on the effects of water deficit for tree selection on wood density. When considering only +W trees, the correlation between age 1 and age 6 is robust (r = 0.93), suggesting the feasibility of making a proper tree selection even at 1 year of age. Furthermore, our results showed no significant differences between +W and –W trees on wood density heterogeneity. Thus, the significant decreases in juvenile-mature correlations of wood density on water-stressed trees cannot be explained by changes in wood heterogeneity.

5.5. Conclusions

The use of NIR-HSI demonstrates good performance to predict wood density using LWPLSR model calibration and be helpful to build wood density maps of the whole cross-section. The age-age and ring-ring correlations showed that juvenile selection of trees under 3 years is feasible to predict wood density at 6 years in *E. grandis* trees. In non-water limited sites, tree selection can be highly accurate even at 1 year of age. Juvenile-mature correlations are slightly reduced in drier sites.

References

Battie-Laclau, P., Delgado-Rojas, J.S., Christina, M., Nouvellon, Y., Bouillet, J.-P., Piccolo, M. de C., Moreira, M.Z., Gonçalves, J.L. de M., Roupsard, O., Laclau, J.-P., 2016. Potassium fertilization increases water-use efficiency for stem biomass production without affecting intrinsic water-use efficiency in Eucalyptus grandis plantations. For. Ecol. Manage. 364, 77–89. https://doi.org/10.1016/j.foreco.2016.01.004

Bhargave, R., 2013. Infrared and Raman spectroscopic imaging for histopathology. Wiley-VCH, p. SMD2. https://doi.org/10.1364/sensors.2011.smd2

Bouvet, J.M., 1992. Geno-Phenotypic Regression and Juvenile-Mature Correlations: Methodological Tools for Clonal Selection of Eucalyptus Hybrids in Congo. South African For. J. 160, 13–18.

Bouvet, J.M., Vigneron, P., Gouma, R., Saya, A., 2003. Trends in Variances and Heritabilities with Age. Silvae Genet. 52, 121–133.

Campelo, F., Mayer, K., Grabner, M., 2019. xRing—An R package to identify and measure tree-ring features using X-ray microdensity profiles. Dendrochronologia 53, 17–21. https://doi.org/10.1016/j.dendro.2018.11.002

Chambi-Legoas, R., Chaix, G., Castro, V.R., Franco, M.P., Tomazello-Filho, M., 2021. Inter-annual effects of potassium/sodium fertilization and water deficit on wood quality of Eucalyptus grandis trees over a full rotation. For. Ecol. Manage. 496, 119415. https://doi.org/10.1016/j.foreco.2021.119415

Chambi-Legoas, R., Chaix, G., Tomazello-Filho, M., 2020. Effects of potassium/sodium fertilization and throughfall exclusion on growth patterns of Eucalyptus grandis W. Hill ex Maiden during extreme drought periods. New For. 51, 21–40. https://doi.org/10.1007/s11056-019-09716-x

Downes, G., Harwood, C., Washusen, R., Ebdon, N., Evans, R., White, D., Dumbrell, I., 2014. Wood properties of Eucalyptus globulus at three sites in Western Australia: effects of fertiliser and plantation stocking. Aust. For. 77, 179–188. https://doi.org/10.1080/00049158.2014.970742

Downes, G.M., Meder, R., Bond, H., Ebdon, N., Hicks, C., Harwood, C., 2011. Measurement of cellulose content, Kraft pulp yield and basic density in eucalypt woodmeal using multisite and multispecies near infra-red spectroscopic calibrations. South. For. a J. For. Sci. 73, 181–186. https://doi.org/10.2989/20702620.2011.639489

Fernandes, A., Lousada, J., Morais, J., Xavier, J., Pereira, J., Melo-Pinto, P., 2013a. Measurement of intra-ring wood density by means of imaging VIS/NIR spectroscopy (hyperspectral imaging). Holzforschung 67, 59–65. https://doi.org/10.1515/hf-2011-0258

Fernandes, A., Lousada, J., Morais, J., Xavier, J., Pereira, J., Melo-Pinto, P., 2013b. Comparison between neural networks and partial least squares for intra-growth ring wood density measurement with hyperspectral imaging. Comput. Electron. Agric. 94, 71–81. https://doi.org/10.1016/j.compag.2013.03.010

Forina, M., Lanteri, S., Casale, M., 2007. Multivariate calibration. J. Chromatogr. A. https://doi.org/10.1016/j.chroma.2007.03.082

Franco, M.P., 2018. Plasticidade de árvores de Eucalyptus grandis no contexto das mudanças climáticas : interação do déficit hídrico e da fertilização no crescimento e qualidade do lenho das árvores de árvores de Eucalyptus grandis. Universidade de São Paulo.

Geladi, P., Burger, J., Lestander, T., 2004. Hyperspectral imaging: calibration problems and solutions. Chemom. Intell. Lab. Syst. 72, 209–217. https://doi.org/10.1016/J.CHEMOLAB.2004.01.023

Geladi, P., Kowalski, B.R., 1986. Partial least-squares regression: a tutorial. Anal. Chim. Acta 185, 1–17. https://doi.org/10.1016/0003-2670(86)80028-9

Greaves, B.L., Borralho, N.M.G., Raymond, C.A., Evans, R., Whiteman, P., 1997. Age-age correlations in, and relationships between basic density and growth in Eucalyptus nitens. Silvae Genet. 46, 264–270.

Haddadi, A., Leblon, B., Burger, J., Pirouz, Z., Groves, K., Nader, J., 2015. Using near-infrared hyperspectral images on subalpine fir board. Part 2: Density and basic specific gravity estimation. Wood Mater. Sci. Eng. 10, 41–56. https://doi.org/10.1080/17480272.2015.1011231

Haddadi, A., Leblon, B., Pirouz, Z., Nader, J., Groves, K., 2016. Prediction of wood properties for thawed and frozen logs of quaking aspen, balsam poplar, and black spruce from near-infrared hyperspectral images. Wood Sci. Technol. 50, 221–243. https://doi.org/10.1007/s00226-015-0767-z

Hein, P.R.G., Lima, J.T., Chaix, G., 2009a. Robustness of models based on near infrared spectra to predict the basic density in Eucalyptus urophylla wood. J. Near Infrared Spectrosc. 17, 141–150. https://doi.org/10.1255/jnirs.833

Hein, P.R.G., Maioli Campos, A.C., Trugilho, P.F., Lima, J.T., Chaix, G., 2009b. Near infrared spectroscopy for estimating wood basic density in Eucalyptus urophylla and Eucalyptus grandis. Cerne 15, 133–141.

Inagaki, T., Schwanninger, M., Kato, R., Kurata, Y., Thanapase, W., Puthson, P., Tsuchikawa, S., 2012. Eucalyptus camaldulensis density and fiber length estimated by near-infrared spectroscopy. Wood Sci. Technol. 46, 143–155. https://doi.org/10.1007/s00226-010-0379-6

Lambeth, C.C., van Buijtenen, J.P., Duke, S.D., McCullough, R.B., 1983. Early selection is effective in 20-year-old genetic tests of Loblolly pine. Silvae Genet.

Lesnoff, M., 2021. R package rnirs: Dimension reduction, Regression and Discrimination for Chemometrics.

Miranda, I., Almeida, M.H., Pereira, H., 2001. Provenance and site variation of wood density in Eucalyptus globulus Labill. at harvest age and its relation to a non-destructive early assessment. For. Ecol. Manage. 149, 235–240. https://doi.org/10.1016/S0378-1127(00)00560-0

Mora, C.R., Schimleck, L.R., Yoon, S.C., Thai, C.N., 2011. Determination of basic density and moisture content of loblolly pine wood disks using a near infrared hyperspectral imaging system. J. Near Infrared Spectrosc. 19, 401–409. https://doi.org/10.1255/jnirs.948

Naidoo, S., Zboňák, A., Pammenter, N.W., Ahmed, F., 2007. Assessing the effects of water availability and soil characteristics on selected wood properties of E . grandis in South Africa. IUFRO Durban 1–11.

Osorio, L.F., White, T.L., Huber, D.A., 2003. Age-age and trait-trait correlations for Eucalyptus grandis Hill ex Maiden and their implications for optimal selection age and design of clonal trials. Theor. Appl. Genet. 106, 735–743. https://doi.org/10.1007/s00122-002-1124-9

Pfautsch, S., Harbusch, M., Wesolowski, A., Smith, R., Macfarlane, C., Tjoelker, M.G., Reich, P.B., Adams, M.A., 2016. Climate determines vascular traits in the ecologically diverse genus Eucalyptus. Ecol. Lett. 19, 240–248. https://doi.org/10.1111/ele.12559

Rana, V., Singh, S.P., Gupta, P.K., 2011. Eucalypts in Pulp and Paper Industry, in: Bhojvaid, P.P., Kaushik, S., Singh, Y.P., Kumar, D., Thapliyal, M., Barthwal, S. (Eds.), Eucalypts in India. ENVIS Centre on Forestry, Indian Council of Forestry Research and Education, Dehradun, pp. 470–506.

Rodrigues, J., Fujimoto, T., Schwanninger, M., Tsuchikawa, S., 2013. Prediction of wood density using near infrared-based partial least squares regression models calibrated with X-ray microdensity. NIR news 24, 4. https://doi.org/10.1255/nirn.1352

Rosso, S., de Muniz, G.I.B., de Matos, J.L.M., Haselein, C.R., Hein, P.R.G., Lopes, M. de C., 2013. Predição da massa específica de Eucalyptus grandis W. Hill ex Maiden por espectroscopia no infravermelho próximo. Cerne 19, 647–652. https://doi.org/10.1590/S0104-77602013000400015

Salzer, R., 2008. Practical Guide to Interpretive Near-Infrared Spectroscopy. By Jerry Workman, Jr. and Lois Weyer. Angew. Chemie Int. Ed. 47, 4628–4629. https://doi.org/10.1002/anie.200885575

Searson, M.J., Thomas, D.S., Montagu, K.D., Conroy, J.P., 2004. Wood density and anatomy of water-limited eucalypts. Tree Physiol. 24, 1295–1302.

Shelly, J.R., 2001. Wood: Materials for Furniture, in: Encyclopedia of Materials: Science and Technology. Elsevier, pp. 9658–9662. https://doi.org/10.1016/b0-08-043152-6/01750-2

Stackpole, D.J., Vaillancourt, R.E., de Aguigar, M., Potts, B.M., 2010. Age trends in genetic parameters for growth and wood density in Eucalyptus globulus. Tree Genet. Genomes 6, 179–193. https://doi.org/10.1007/s11295-009-0239-4

Vargas-Hernandez, J., Adams, W.T., 1992. Age-Age Correlations and Early Selection for Wood Density in Young Coastal Douglas-Fir. For. Sci. 38, 467–478.

Wilkins, A.P., Horne, R., 1991. Wood-density variation of young plantation-grown Eucalyptus grandis in response to silvicultural treatments. For. Ecol. Manage. 40, 39–50. https://doi.org/10.1016/0378-1127(91)90090-I

Yin, W., Zhang, C., Zhu, H., Zhao, Y., He, Y., 2017. Application of near-infrared hyperspectral imaging to discriminate different geographical origins of Chinese wolfberries. PLoS One 12, e0180534. https://doi.org/10.1371/journal.pone.0180534

Zobel, B.J., van Buijtenen, J.P., 1989. Variation Within and Among Trees, in: Zobel, B.J., Buijtenen, J.P. van (Eds.), Wood Variation: Its Causes and Control. Springer-Verlag, pp. 72–131. https://doi.org/10.1007/978-3-642-74069-5_3

6. FINAL CONSIDERATIONS

For the sustainability of the forestry sector, the increase in forest productivity must consider the effect of risks associated with unfavorable climate scenarios, such as the occurrence of severe droughts. One of the great challenges is the adaptation of silvicultural practices to climate change and longer water stress conditions, not only to achieve greater water use efficiency, but also to increase tree resilience.

Although potassium fertilization significantly increased water use, the trees showed high plasticity in response to changes in rainfall and soil water availability and a great ability to recover their growth after extreme and prolonged drought. Excluding the effect of anomalous droughts, the positive effect of K fertilization was observed in each year of growth, the effect in the last stage being similar to the early stage of trees. Under normal water availability conditions, K fertilization increased the tree basal area by up to 3 times. Even during dry seasons, K fertilization increased the growth rate by 1.5 times compared to K-deficient trees. Under 37% throughfall reduction, the increases with K were about 2 times higher than K-deficient trees.

Growth arrest was only observed for severe water stress, either due to 6 extremely dry months (during the 2014 dry season) or by 80% throughfall reduction. However, even in these conditions, there were no mortality events. Our findings suggest high conservation of the xylem vascular system under extreme drought conditions and high plasticity of hydraulic conductivity closely related to changes in water availability. In addition, fertilized trees showed increased xylem plasticity, mainly related to vessel size changes, to cope with severe drought. The results suggest an additive effect of K to increase resilience during long-term drought periods and recovery ability for growth following drought.

These positive effects of K addition on stem volume do not involve significant losses on wood quality, even under water stress. Na as a substitute for K should consider the negative impacts on the wood density of *E. grandis* trees and their lower productivity.

Field observations worldwide have shown that tree height is the strongest predictor of tree mortality during intense drought, with large trees becoming twice more vulnerable to die than small trees (Bennett et al., 2015; McIntyre et al., 2015; Stovall et al., 2019). Therefore, further studies should evaluate long-cycle Eucalyptus plantations and test if the effects of severe drought on more mature trees (large trees) may differ greatly from what was found in this study evaluating short-cycle plantations.

In perspective, the project has considered evaluating wood properties to know if *E. grandis* trees maintain good wood quality during the recovery period. On the other hand, since the evaluation of wood quality in this thesis has been limited to anatomical and physical properties, future studies should address the chemical properties of wood, as there is likely to be an effect on chemical properties (lignin and cellulose content), and the benefits or detriment of K and Na on wood quality could be enhanced or balanced by chemical effects on wood.

References

Bennett, A.C., Mcdowell, N.G., Allen, C.D., Anderson-Teixeira, K.J., 2015. Larger trees suffer most during drought in forests worldwide. Nat. Plants 1. https://doi.org/10.1038/nplants.2015.139

McIntyre, P.J., Thorne, J.H., Dolanc, C.R., Flint, A.L., Flint, L.E., Kelly, M., Ackerly, D.D., 2015. Twentieth-century shifts in forest structure in California: Denser forests, smaller trees, and increased dominance of oaks. Proc. Natl. Acad. Sci. U. S. A. 112, 1458–1463. https://doi.org/10.1073/pnas.1410186112

Stovall, A.E.L., Shugart, H., Yang, X., 2019. Tree height explains mortality risk during an intense drought. Nat. Commun. 10, 1–6. https://doi.org/10.1038/s41467-019-12380-6